UNIVERSITÀ DEGLI STUDI DEL MOLISE

PhD School in Translational and Clinical Medicine

XXX Cycle

Department of Medicine and Health Science

S.S.D. MED/50

Final Dissertation

A cholinergic-sympathetic pathway mediates the activation of immune system in hypertension

Tutor: Chiar.ma Prof.
Daniela Carnevale
Dept. of Angio-Cardio-Neurology
IRCCS Neuromed
"Sapienza" University of Rome

Coordinator: Chiar.mo Prof.
Ciro Costagliola
Dept. of Medicine and Health Sciences "V.Tiberio"
University of Molise

PhD Student:
Dr. Marialuisa Perrotta
Matricola: 153743

Academic Year 2016/2017

Table of contents

Introduction

1. The sympathetic control of hypertension……..……*page 2*
2. Neurogenic hypertension……..…..*page 4*
3. The role of the immune system in hypertension.....*page 7*

3.1 Inflammatory “Priming” in hypertension……..……..*page 9*

4. The neural-inflammatory reflex……..*page 12*

4.1 The α7nAChR in the inflammatory reflex……..……...*page 13*

5. The involvement of the splenic PlGF in hypertension……...……..*page 15*
6. References……...*page 19*

Experimental section

7. A cholinergic-sympathetic pathway primes immunity in hypertension and mediates brain-to-spleen communication……*page 27*
8. Deoxycorticosterone acetate-salt hypertension activates placental growth factor in the spleen to couple sympathetic drive and immune system activation……*page 64*

Conclusions……*page 90*

Acknowledgment……..…….....*page 92*

1. The sympathetic control of hypertension

The autonomic nervous system includes afferent and efferent neurons connecting the central nervous system (CNS) and the visceral organs (Saper, 2002). The sympathetic and parasympathetic neurons represent the two major branches of the autonomic nervous system having the pivotal role to control organ functions and to maintain homeostasis by two serial neurons interconnected: the first is located in the CNS and the second in the peripheral ganglia. The parasympathetic neurons originate in the brain and in the sacral section of the spinal cord: ganglia are in or close to the innervated organs; the sympathetic neurons originate in the thoracic and lumbar sites of the spinal cord: ganglia are located in proximity of the spinal cord.

This specific organization of the two systems allows to control physiological functions in peripheral districts in response to internal and external environmental stimuli (Saper, 2002). In the control of cardiovascular functions, the sympathetic nervous system (SNS) has been historically presented as opposing to the parasympathetic nervous system (PNS). The decrease in baroreceptor reflex activity and increase in chemoreceptor activity enhance the exaggerated sympathetic nerve activity (SNA) and reduce the parasympathetic nerve activity (PSNA) in cardiovascular diseases such as hypertension, atherosclerosis, myocardial infarction, heart failure and diabetes, as described in **Figure 1** (Abboud, 2012).

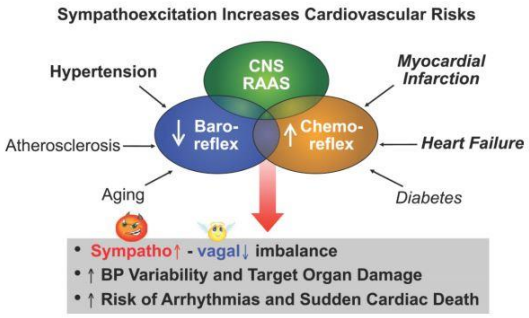

Figure 1. Involved mechanisms in exaggerated sympathetic activity in cardiovascular disease and in hypertension.
By Abboud et al., 2012.

Moreover, several experimental evidences show to date a new aspect of the SNS as a key regulator of the cardiovascular system under physiological and pathological conditions. The sympathetic drive is implicated in the regulation of some functions in peripheral organs involved in the homeostasis of the cardiovascular system, such as the heart, vasculature and kidneys. A common feature of many cardiovascular diseases, like hypertension, is an increase of the SNA. In the past decades, the researches in this field invested many resources to develop experimental models of cardiovascular diseases and many techniques to analyze the dysregulation of SNS. The evaluation of the nervous trafficking in typical cardiovascular organs was a field of great interest allowing to important information on the mechanisms underlying the nerve reflexes involved in the regulation of blood pressure, in renal and cardiac function and in vascular contractility (Abboud, 1982; Guyenet, 2006; Malpas, 2010).

Hypertension is a chronic elevation of blood pressure and although it is one of the most important human health problem (Lawes et al., 2008), the principal causes of the disease remain undefined. The etiology of hypertension cannot be often determined in the majority of patients with “essential” hypertension (Coffman, 2011) and the understanding of molecular mechanisms underlying the disease is crucial for basic and translational researchers in this field.

Despite these advances, it has been difficult to treat hypertensive patients because the majority of these are unresponsive to ongoing treatment showing an increased SNA related to neural pathway in neurogenic hypertension (Mann et al., 2003). Furthermore, an increase of SNA is evident in the early stages of hypertension and it does not occur equally in all tissues, but a larger effect on occurs in key organs as the kidneys (Osborn et al., 2007). The sympathetic innervation of the kidney is considered the principal district in the regulation of blood pressure and the denervation of renal sympathetic fibers is a novel approach to treat uncontrolled hypertension (Esler, 2011; Coffman, 2011; Victor, 2015; **see Figure 2**). Decades of studies supported the efficacy of this approach and the neurogenic origin of hemodynamic variations in hypertension have been well investigated (Victor, 2015; **see Figure 2**).

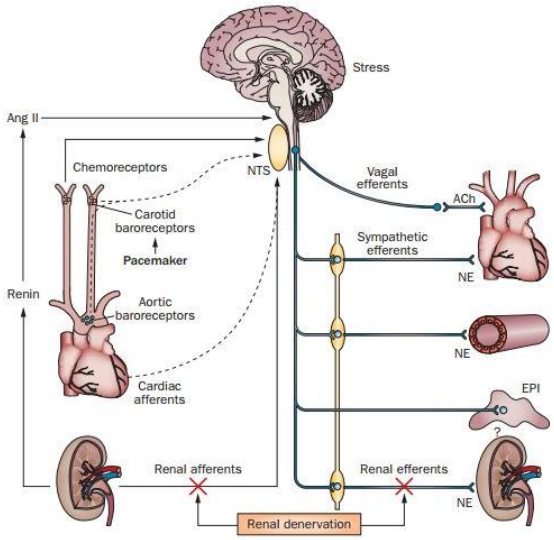

Figure 2. Sympathetic neural mechanisms of blood pressure regulation and renal denervation. The scheme represents principal neural influences on sympathetic outflow to the heart, peripheral vasculature, and kidneys. Furthermore, three major components of the arterial baroreflex arc are shown: the afferent arm, the central integration and the efferent arm.
By Victor, 2015.

Although therapeutic strategies have been developed against the main components involved in blood pressure regulation, many patients are resistant to antihypertensive treatments, suggesting that there are still unidentified mechanisms underlying blood pressure control (Lawes, 2008). The Mosaic Theory of hypertension supports that many factors, including genetic, environmental, adaptive, neural and many others, can contribute to increase blood pressure (Page, 1967) highlighting that the disease is not predominantly caused by the perturbation of only one district as the renal one. Among these, some milestone papers suggest the role of inflammation in the development of hypertension (Guzik et al., 2007; Vinh et al., 2010; Harrison, 2013). In this new point of view, the Theory by Dr. Page's Mosaic (Page, 1967) represents a suggestion for further studies in the context of hypertension, in order to dissect the complexity of the disease.

2. Neurogenic hypertension

Hypertension is known as a neurogenic disease and the most probable cause is ascribable to an abnormality of the autonomic nervous system activity rather than a vascular or renal damage (Abboud et al., 2012; Victor, 2015). An alteration of neural control mechanisms

(vagal and sympathetic drive) of cardiovascular system is the principal feature of neurogenic hypertension (Zubcevic et al., 2011). As previously discussed, borderline hypertensive patients show an increased vasomotor and cardiac sympathetic drive and a reduction of parasympathetic one (Anderson et al., 1989; Grassi, 2009). Furthermore, hypertensive patients show a higher plasma norepinephrine level and norepinephrine spillover in both the peripheral circulation and blood draining from the brain and a raised sympathetic postganglionic activity in the skeletal muscle vascular bed (Anderson et al., 1989; Grassi, 2009). In animal models of the disease, the mineralocorticoid excess, which depends on salt absorption from the kidney, have also been associated to an elevated sympathetic drive indicating a strong association between renal dysfunction and sympathetic overdrive (Krum et al., 2009). An evidence from spontaneously hypertensive rats demonstrates that the sympathetic over activity occurs before the onset of hypertension (Simms et al., 2009).

The background level of the sympathetic tone is crucial for long-term blood pressure control and it is finely regulated by specific regions of central nervous system, as the rostral ventrolateral medulla (RVLM), the spinal cord, the hypothalamus and the nucleus of the solitary tract (NTS) (Guyenet, 2006; Victor, 2015). The renin-angiotensin system (RAS) is active in brain regions that regulate the sympathetic outflow and it is activated in different forms of hypertension. In particular, it is known that RAS maintains a state of sympathetic over activity acting on central neurons in the SFO (subfornical organ) (Coble et al., 2015) that is one of several circumventricular organs (CVOs) that lie outside the blood brain barrier (BBB) and thus have access to circulating AngiotensinII (AngII). A hypothesis by Osborn and colleagues on the neurogenic hypertension asserts that circulating AngII combined with high salt intake increases SNA in the disease (Osborn et al., 2007; **see Figure 3**). The brain targets for circulating AngII are neurons in the area postrema (AP), SFO and possibly other circumventricular organs. AngII signaling is integrated with sodium-sensitive neurons in the SFO and/or organum vasculosum of the lamina terminalis (OVLT) and drives sympathetic premotor neurons in the RVLM via the paraventricular nucleus (PVN) (Osborn et al., 2007). AngII has potent effects on blood pressure and cardiovascular function through its activation in these brain specific areas (Simpson, 1981) that are unprotected by the BBB coupling AngII signals with neural circuits that activated peripheral systems as the sympathetic drive involved in maintaining blood pressure homeostasis. The SFO is a region particularly populated by AngII receptors and more interestingly, studies have shown that the lesioning in this region markedly attenuated hypertension caused by an increase of circulating AngII (Mangiapane and Simpson, 1980; Hendel and Collister, 2004).

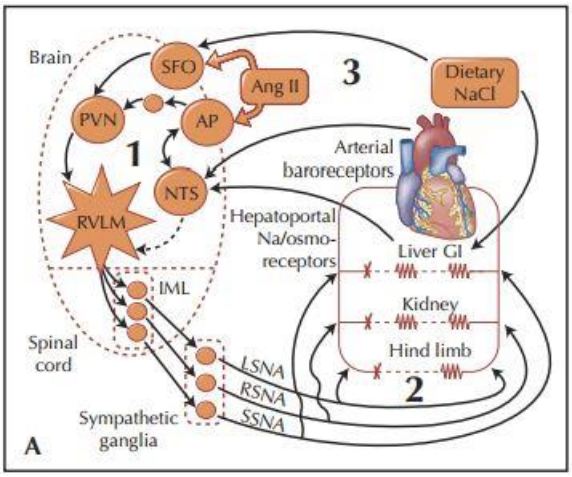

Figure 3. Representation of the central hypothesis proposed by Osborn and colleagues. Central nervous system pathways involved in AngII–salt-dependent hypertension and schematic interface between neural pathways and cardiovascular target organs are shown. Furthermore, probable neural pathways from AngII and salt that influence neural control mechanisms of the cardiovascular system are illustrated.
By Osborn et al, 2007.

AngII is the principal molecule of the RAS raising blood pressure primarily through the activation of type 1 angiotensin (AT1) receptors (Crowley et al., 2004) and this signaling is well demonstrated by clinical trials showing the strong efficacy of AT1 receptor blockers (ARBs) in improving the complications of hypertension as well as the chronic kidney diseases (Lewis et al., 2001).

The deoxycorticosterone acetate (DOCA)-salt provokes a different form of hypertension dependent on the altered regulation of central pressor mechanisms including the brain renin-angiotensin system (Nishimura et al., 1999). AT1aR in the SFO, and possibly other nuclei, such as the PVN, contribute to the effects of DOCA-salt on arterial pressure and fluid and sodium intake, supporting the hypothesis that AT1aR signaling in the SFO is important for DOCA-salt hypertension (Grobe et al., 2011; Hilzendeger et al., 2013). In fact, the effect of SFO-targeted ablation of endogenous AT1aR is evaluated in $AT1aR^{flox}$ mice with deletion of AT1aR in SFO that exhibit a blunted increase in arterial pressure. Increased sympathetic cardiac modulation is significantly reduced in DOCA-salt mice when AT1aR is deleted in the SFO (Hilzendeger et al., 2013). These data highlight the contribution of AT1aR in the SFO to arterial blood pressure regulation by changes on sympathetic cardiac modulation in the DOCA-salt model of hypertension. It is known that chronic DOCA-salt treatment suppresses the peripheral RAS, but has different effects on the brain RAS as compared to chronic AngII. Chronic DOCA-salt causes a reduction in renal angiotensin converting enzyme (ACE) and

this treatment has no effect on the brain ACE (Nishimura et al., 1999). Conversely, Angiotensinogen is down regulated by DOCA-salt treatment in both kidney and brain (Nishimura et al., 1999). The majory of studies have indicated that DOCA-salt hypertension is principally mediated by the activation of the brain RAS (Schenk and McNeill, 1992). In fact, DOCA-salt treatment results in increased angiotensin receptor density specifically in cardiovascular control regions of the brain, including the subfornical organ, median preoptic nucleus, paraventricular nucleus, and area postrema (Palkovits and Záborszky, 1977; Mangiapane and Simpson, 1980; Gutkind et al., 1988; Nishimura et al., 1999).

More interestingly, neurons from these same forebrain regions extend to sites critical to the emotional stress response, including the bed nucleus of the stria terminalis (Sunn et al., 2003). Psychological stress can contribute to the development of hypertension and has been correlated with an excessive rise in blood pressure in patients with unstable hypertension (Matthews et al., 2004). In animal model, a repeated exposure or chronic stress elicits changes in baseline blood pressure (Alkadh et al., 2005). It has been observed that emotional stress can also activate the RAS and thus increase endogenous production of AngII (Krause et al., 2011). Indeed, a study conducted by Harrison group demonstrates that the AngII infusion increases blood pressure reactivity to acute stress, vascular inflammation and corticotrophin releasing hormone (CRH) gene expression in the PVN, showing for the first time that psychological stress enhanced both the central neurohormonal stress response and the peripheral vascular inflammation after chronic low-dose AngII infusion (Marvar et al., 2012).

3. The role of the immune system in hypertension

Simultaneously with the recognition that CNS and SNS play a crucial role in hypertension, it has been recognized that chronic functional and structural alterations observed in hypertension are determined by the inflammatory system that causes damage in target organs as kidney and vasculature (Abboud et al., 2012; **see Figure 4**).

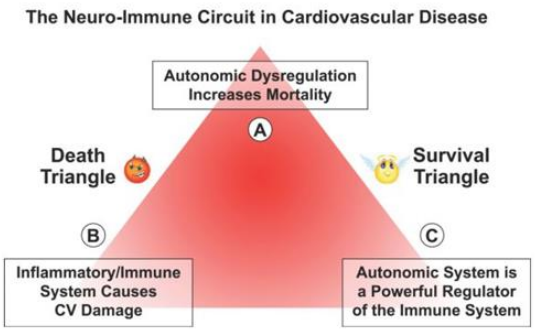

Figure 4. Sympathetic and immune system interplay in cardiovascular disease. The triangle reflects the convergence of the neural and immune mechanisms in cardiovascular disease.
By Abboud et al., 2012.

Immune organs are densely innervated by the SNS and in particular, the spleen is a reservoir of immune cells of both the innate and the adaptive immune systems (Lori et al., 2017; Nance and Sanders, 2007). Many evidence suggest that the immune system contributes to the development of the hypertension (Guzik et al., 2007; Wenzel et al., 2011). An old study demonstrated that mice with genetic aplasia of the thymus are protected from the onset of the disease, suggesting that the adaptive immunity could have a key role in the hypertension (Svendsen, 1976). Additionally, the transfer of splenic cells from hypertensive rats promoted an elevation of blood pressure in control recipient rats (Olsen, 1980). After, the idea is corroborate by experiments in which it was found that the immunosuppression attenuated hypertension in Okamoto spontaneously hypertensive rats and reduced the renal damage in Sprague-Dawley rats (Khraibi et al., 1984). Moreover, the most significant studies highlighting the importance of immune cells in hypertension came from the David Harrison laboratory. They showed that immune cells are crucial players in hypertension in mice chronically treated with AngII and that mice deprived of lymphocytes are protected from AngII-induced hypertension (Guzik et al., 2007). Additionally, by the same group, it was found that CD8 KO mice, but not CD4 KO mice, are protected from hypertension, leading to a further knowledge of the immune mechanisms involved in the onset of the disease (Vinh et al., 2010). In particular, chronic AngII causes an increase of cells expressing CD86 in the splenic marginal zone. The CD86 is a marker of co-stimulation, a pathway elicited by antigen presenting cells (APCs). This research demonstrated a dealing between innate and adaptive immunity during the development of hypertensive disease (Vinh et al., 2010). These investigators also showed that T cells were essential for other forms of hypertension, as induced by DOCA-salt and norepinephrine (Guzik et al., 2007; Marvar et al., 2010),

suggesting that the inflammatory component participates to a mechanism crucial for the development of the disease.

Another work, more important in this field, has been described by Wenzel and colleagues that reported that mice with deletion of Lysozyme M (LysM) positive macrophages, obtained by a selective deletion of monocyte/macrophages, were protected from vascular dysfunction and hypertension in murine model of AngII (Wenzel et al., 2011). Furthermore, Crowley and colleagues showed that immune system is essential for developing of hypertension and mice with immune deficiency are protected from the blood pressure increase (Zhang and Crowley, 2015). This group found that mice unable to support a Th1 response due to deficiency of the transcription factor, T-bet, had preserved hypertensive responses but were protected from renal damage during chronic AngII administration, suggesting that Th1 cells increase the damage of hypertensive target organs as kidney through mechanisms independents from blood pressure regulation (Zhang et al., 2012). T cells are involved in the development of other forms of hypertension as Dahl-sensitive rats in which are crucial for the increase of blood pressure levels (De Miguel et al., 2010; Mattson, 2014).

More recently, Tracey and colleagues showed that mice lacking ChAT expression in CD4+ T cells have an elevation of arterial blood pressure levels as compared to control mice and conversely, Jurkat T cells overexpressing ChAT (JTChAT) decreased blood pressure when infused into mice (Olofsson et al., 2016).

3.1 Inflammatory "Priming" in hypertension

Macrophages and neutrophils of the innate immunity are the first line of defense against pathogens, while lymphocytes of the adaptive immunity provide increased protection against reinfection by the same pathogen. Conversely, to innate immunity, the adaptive immune system is highly specific. In the adaptive immunity, the APCs capture and process proteins of pathogen into small peptides that then are presented as major histocompatibility complex (MHC). T lymphocytes activation is mediated by dendritic cells (DC) that process antigens and present the peptides within MHC II. Dendritic cells then migrate to secondary lymphoid organs, including the spleen and lymph nodes, where they activate a T cell with a T cell receptor able to recognize the antigenic peptide. This interaction is termed "immunologic synapse." An important interaction in this site is the costimulation that involves B7 ligands on the APCs (CD80 and CD86) with CD28 on the T cell (Harrison et al., 2011). After the costimulation, T cells start to proliferate and produce cytokines altering the expression of

receptors that lead to their egression from the secondary lymphoid organs towards sites of peripheral inflammation. The classical cellular adaptive immune response is described in **Figure 5**.

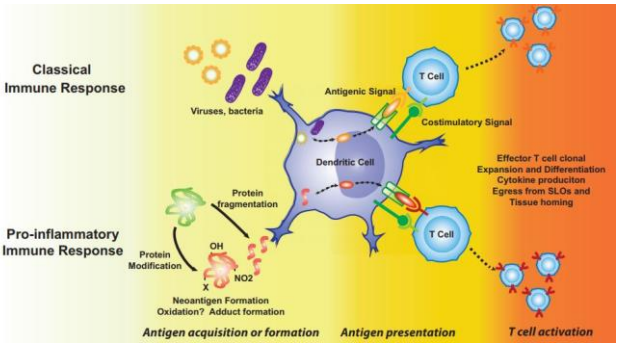

Figure 5. Priming of the immune response. In the classical immune response, foreign proteins are processed in dendritic cell and are presented on surface within an MHC. In hypertension, it is hypothesized that endogenous proteins are modified, by oxidation, fragmentation, or other modifications and they are not recognized as self. T cells are activated by costimulation pathway and egress from secondary lymphoid organs towards target organs of inflammation, typical of hypertensive disease, as kidney and vessels.
By Harrison et al., 2011.

Activated T cells enter the kidney and vasculature where the cytokine IL-17 promotes the entry of other inflammatory cells such as macrophages. These inflammatory cells release cytokines that cause vasoconstriction promoting sodium and water absorption and causing hypertension. IL-17 is implicated in a variety of diseases including rheumatoid arthritis (Witowski et al., 2004). It is produced by TH17 cells, a subset of CD4+ cells (Witowski et al., 2004), and also by CD8+ cells (Kondo et al., 2009). Very interesting, the increase of blood pressure levels in mice lacking IL-17 was comparable to that observed in wild-type mice, resulting protected from hypertension. It was demonstrated that IL-17 promoted the chemotaxis of other inflammatory cells, stimulating the release of other chemokines (Hartupee et al., 2007). Indeed, the vascular accumulation of leukocytes (including T cells) caused by angiotensin II is reduced in IL-17$^{-/-}$ mice, contributing to the vascular pathophysiology of hypertension, demonstrating the importance of the adaptive immune response in the onset of hypertensive disease.

A very old work showing the role of the central nervous system in peripheral vascular inflammation demonstrated that lesions in the anteroventral 3rd ventricular (AV3V) prevented hypertension and the activation of circulating T cells and the infiltration of leukocytes caused

by AngII. This finding showed that the direct actions of AngII on T cells and peripheral tissues are not responsible for the inflammation but that it was required a central action of AngII to establish the inflammation in AngII-induced hypertension (Brody et al., 1978).

Several studies have linked the central nervous system to inflammation. The sympathetic fibers terminate in definite areas of the spleen reached of T cell (Lori et al., 2017) where they release norepinephrine as the principal neurotransmitter, which can both inhibit and stimulate T cell activation and proliferation (Madden et al., 1995). Norepinephrine stimulates naïve CD4 lymphocytes cultured under TH1-promoting conditions to produce more IFNγ than in non-stimulated cells (Swanson et al., 2001). Very intriguingly, Ganta and colleagues demonstrated that intracerebroventricular administration of AngII increased splenic sympathetic nerve activity (SSNA), which in turn stimulated mRNA expression of several cytokines in splenocytes. Splenic sympathectomy abrogated these effects suggesting a clear link between the central action of AngII and the immune responses in the spleen (Ganta et al., 2005; **see Figure 6**).

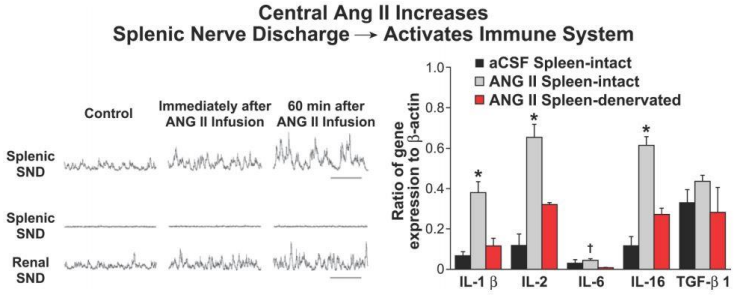

Figure 6. Central AngII increases splenic nerve discharge and activates immune system. The sympathetic innervation of the spleen provides a direct link between central sympathetic neural circuits and immunocompetent cells in the spleen.
By Ganta et al., 2005.

The sympathetic innervation of the spleen provides a direct link between central sympathetic neural circuits and immune responses in this lymphoid organ (Felten, 1985; Felten and Olschowka, 1987), and changes in the level of efferent splenic sympathetic nerve discharge (SND) can alter immune responses in the spleen (Ganta et al., 2005). These data introduce the concept of the anti-inflammatory neural reflex in hypertensive disease in which the spleen represents a hub between the nervous and immune system.

4. The neural-inflammatory reflex

The inflammatory reflex describes that the CNS responds to inflammatory stimuli acting to limit peripheral or systemic inflammation (Tracey, 2002; Rosas-Ballina and Tracey, 2009; Rosas-Ballina et al., 2011). Considerable works demonstrate that the 'cholinergic anti-inflammatory pathway' constitutes the efferent neural arm of the inflammatory reflex (Huston et al., 2009; Rosas-Ballina et al., 2011). Tracey and colleagues have focused on the role of vagus nerve dependent circuits to control innate immunity (Borovikova et al., 2000; Huston et al., 2009; Pavlov et al., 2009; Rosas-Ballina et al., 2011; Reardon et al., 2013). The vagus nerve is the mediator of both the afferent and efferent signals of the neural reflex (Rosas-Ballina and Tracey, 2009; **see Figure 7**). Vagal afferents are widely distributed in most visceral organs and it can be activated by the release of cytokines from tissue injury or inflammation (Rosas-Ballina and Tracey, 2009; **see Figure 7**). The reflex is then centrally mediated through the NTS and the dorsal motor nucleus of the vagus and activates the vagal efferent. When activated, the vagal efferent suppresses the cytokine release from macrophages in the spleen. The circuit requires acetylcholine (ACh) signaling through α7 nicotinic receptors (**see Figure 7**) (Rosas-Ballina et al., 2011; Reardon et al., 2013). Memory T-lymphocytes are components of the peripheral neural control of innate immunity in the spleen and are able to produce ACh (Rosas-Ballina et al., 2011).

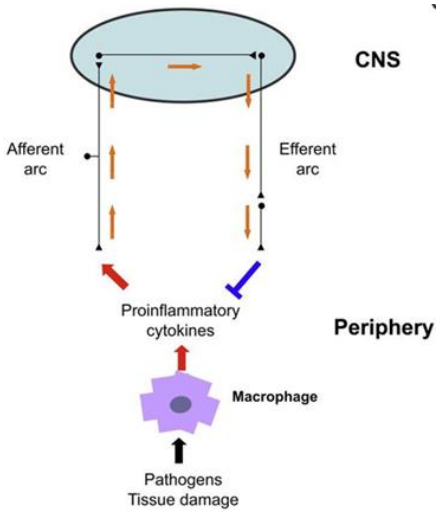

Figure 7. The Inflammatory Reflex. Control systems orchestrated by the autonomic nervous system integrate input signals and deliver responses. Cytokines produced by immune cells in response to endogenous and exogenous stimuli activate afferent neurons of the vagus nerve that conveys this information to the brain where signal integration occurs. A response is elicited through the cholinergic anti-inflammatory pathway, the efferent arc of this inflammatory reflex, which modifies immune function and maintains homeostasis.
By Rosas- Ballina and Tracey, 2009.

Borovikova and colleagues found that cutting the vagus nerve in anaesthetized rats caused a 40% increase in their inflammatory response (measured by TNF plasma levels) to a high dose of intravenous lipopolysaccharide (LPS) (Borovikova et al., 2000). Conversely, Martelli and colleagues measured plasma TNF responses to intravenous LPS in anaesthetized rats finding that cutting the vagus nerve had no effect on this measure of inflammation (Martelli et al., 2014). Moreover, sectioning of the splanchnic sympathetic nerves increased the TNF response to LPS five-fold, concluding that the efferent arm of the inflammatory reflex is mediated by the splanchnic sympathetic nerves but not by the vagus nerve (Martelli et al., 2014; McAllen et al., 2015).

4.1 α7nAChR in the inflammatory reflex

Substantial literature from Tracey research group confirms that the cholinergic anti-inflammatory pathway conveys signals from the brain to the spleen via the vagus nerve and the splenic nerve and it is dependent on the α7 subunit of the nicotinic acetylcholine receptor. In fact, activation of cholinergic anti-inflammatory pathway by electrical stimulation of the vagus nerve (VNS) or administration of α7 selective drugs is effective in ameliorating inflammation and improving survival in experimental models of sepsis (Borovikova et al., 2000).

α7 is the subunity of nicotinic acetylcholine receptor. Nicotinic receptors nAChRs are ligand-gated ion channels comprising a family of hetero- or homopentameric structures derived from the products of 17 genes. They are excitatory receptors for the neurotransmitter acetylcholine playing a crucial role in the central and peripheral nervous system (Chatzidaki and Millar, 2015). In brain neurons, α7 is a homo pentameric calcium channel expressed predominantly in presynaptic nerve terminals where it modulates neurotransmitter release and in postsynaptic neurons where it induces excitatory signals. Sixteen human nAChR subunits (α1- α7, α9, α10, β1-β4, γ, δ and ε) have been identified. The α7 subunit is more widely referred as neuronal subunit (Millar and Gotti, 2009) and it forms functional homomeric [(α7)5] nAChRs. It is considered atypical and it has a relatively low sensitivity to acetylcholine, high calcium permeability and exhibits very fast desensitization (Couturier et al., 1990). Each nAChR subunit contains an amino-terminal extracellular domain and four transmembrane helices (TM1-TM4). The pore of the channel is lined by the second transmembrane domain (TM2) from five co-assembled subunits (Millar and Gotti, 2009; **see Figure 8**).

In the central nervous system, α7 is associated with neuronal plasticity (Berg and Conroy, 2002). In macrophages, signaling through α7 attenuates TNF production through a mechanism dependent upon inhibition of NF-κB nuclear translocation and activation of Jak-STAT pathways (Borovikova et al., 2000). Furthermore, these receptors are expressed in both sympathetic and parasympathetic ganglia where they mediate the synaptic transmission.

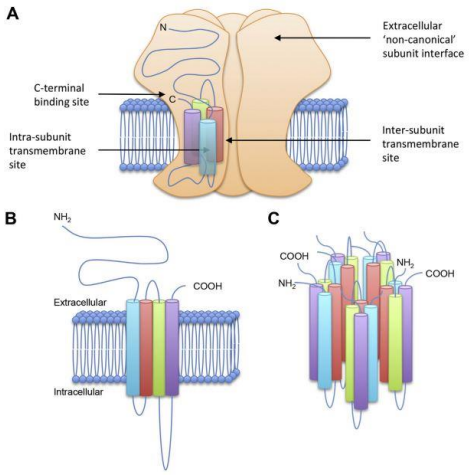

Figure 8. Cartoon representation of nAChR structure and subunit topology.
By Chatzidaki and Millar, 2015.

Interestingly, α7nAChR actively participates to the cholinergic anti-inflammatory reflex and, though initially discovered as a modulator of macrophage function, has been shown to couple the vagus-splenic connection at the neuronal level (Rosas-Ballina et al., 2008; Vida et al., 2011). Yet α7nAChR is not required for the parasympathetic modulations exerted by the vagus nerve in typical cardiovascular parameters such as heart rate (Deck et al., 2005).

The spleen contains acetylcholine and a direct electrical stimulation of the splenic nerve mediates the release of acetylcholine in the lymphoid organ (Leaders and Dayrit, 1965). Since the spleen lacks cholinergic nerve fibers (Bellinger et al., 1993), acetylcholine in this lymphoid organ may be derived from lymphocytes and other immune cells that synthesize and release acetylcholine close to nerve endings (Kawashima and Fujii, 2004). This may explain how electrical stimulation of the vagus nerve can induce acetylcholine release in the spleen, which in turn regulates cytokine release through α7 expressed on responding cells (Rosas-Ballina et al., 2008). Vida and colleagues show that vagus nerve modulates systemic norepinephrine via the splenic nerve throught α7nAChR and the spleen and furthermore that the vagotomy prevents afferent vagus nerve towards the central nervous system. Both vagus

nerve stimulation and α7nAChR agonists in mice activate the splenic nerve to produce norepinephrine via the α7nAChR. These results demonstrates that acetylcholine released by the vagus nerve in the celiac mesenteric ganglia is able to activate postsynaptic α7nAChR of the splenic nerve, leading to the release of norepinephrine in the spleen. The anti-inflammatory potential of the vagus nerve and α7nAChR agonists is inhibited by splenectomy or splenic neurectomy. Splenic nerve stimulation, performed via an abdominal flank incision, mimics the anti-inflammatory mechanism of the vagus nerve and α7nAChR agonists to induce norepinephrine and to prevent LPS-induced serum TNF levels (Vida et al., 2011; **see Figure 9**). More interestingly, the vagus nerve stimulation is recently shown to mediate protection from kidney ischemia-reperfusion injury through α7nAChR in splenocytes (Inoue et al., 2016).

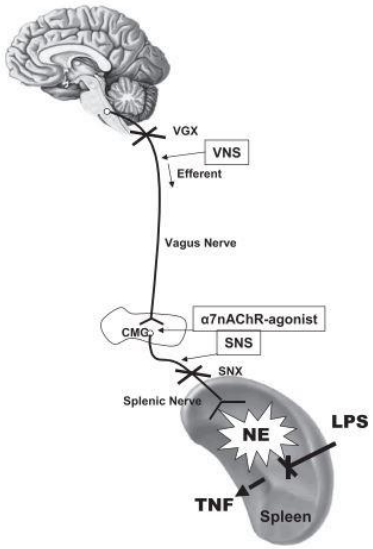

Figure 9. α7nAChR represents a unique molecular link between the parasympathetic and sympathetic system to control inflammation. Splenic nerve stimulation (SNS) mimics vagal and cholinergic induction of norepinephrine (NE) and re-establishes neuromodulation in α7 nicotinic acetylcholine receptor (α7nAChR)-deficient mice. Vagus nerve and cholinergic agonists inhibit systemic inflammation by activating the noradrenergic splenic nerve via the α7nAChR nicotinic receptors.
By Vida et al., 2011.

5. The involvement of the splenic PlGF in hypertension

The Placental growth factor (PlGF) is a member of the vascular endothelial growth factor (VEGF) family. Besides to PlGF, VEGF family includes VEGF-A, -B, -C, and –D. These

growth factors were identified as promoters of proliferation, migration and survival of endothelial cells (Leung et al., 1989) and they have been implicated in inflammatory processes, including rheumatoid arthritis, cancer and inflammatory bowel disease (Kuenen et al., 2002). In fact, increased levels of VEGF in animal and human models of sepsis (Yano et al., 2006; Yano et al., 2008) and the inhibition of their signaling with soluble fms-like tyrosine kinase-1 (sFlt-1) or antibodies against flt-related receptor tyrosine kinase-a (Flk-1) improved morbidity and mortality in sepsi (Yano et al., 2006). Furthermore, circulating levels of PlGF are normally undetectable but an increase of PlGF levels have been described in several conditions, including cancer (Chen et al., 2004) and sepsi (Yano et al., 2008).

Originally, PlGF was identified in the placenta (Khaliq et al., 1996) but it has subsequently been shown to be expressed in other tissues, including the heart, lung, thyroid gland and skeletal muscle (Autiero et al., 2003). PlGF is also found to be expressed in cardiac tissue. In this tissue, PlGF increases in hypoxic/ischemic myocardium (Torry et al., 2009), contributes to pathological angiogenesis (Carmeliet et al., 2001; Lutton et al., 2002) and atherosclerosis (Khurana et al., 2005) and may have both positive and negative effects on tumor growth (Fischer et al., 2007; Van de Veire et al., 2010). These aspects show how the environment can influence its effects.

Furthermore, it was found that PlGF acts as a chemotactic agent for monocytes (Pipp et al., 2003) that participate in the cardiac inflammatory response to pressure overload and support adaptive cardiac remodeling (Endo et al., 2007). PlGF is considered a regulator of the tissue inhibitor of metalloproteinases-3/tumor necrosis factor-α-converting enzyme axis and the consequent TNF-α activation in response to transverse aortic constriction, thus allowing the establishment of an inflammatory response necessary for adaptive cardiac remodeling (Carnevale et al., 2011).

A consistent and increasing amount of reports associates the use of anti-angiogenic therapies based on inhibitors of the VEGF, with an increase of cardiovascular risk and in particular, the development of hypertensive disease (Small et al., 2014). There are important papers reporting the protective effects of PlGF inhibition in various models of cancers, where the main results were obtained in terms of inhibition of tumor growth through immuno-modulating functions (Snuderl et al., 2013). Indeed, the inhibition of PlGF in cancer seems to have a dual positive role: on the one hand, it would protect from tumor growth (Van de Veire et al., 2010; Snuderl et al., 2013; Incio et al., 2016) and at same time hamper hypertension (Carnevale et al., 2014).

Carnevale and colleagues demonstrated that PlGF inhibition was associated with a protection from blood pressure increase and target organ damage in the experimental model

of hypertension induced by chronic infusion of AngII (Carnevale et al., 2014). To define unambiguously the role of PlGF in the onset of hypertension through modulation of the immune system in the splenic reservoir, Carnevale and colleagues studied chimeric mice, generated by spleen transplantation among WT mice and PlGF-deficient mice. Chimeric mice were then subjected to chronic AngII infusion. In WT mice that received PlGF-deficient spleens, AngII failed to raise blood pressure and to mobilize T cells towards target organs of hypertension as aorta and kidney (Carnevale et al., 2014; **see Figure 10**). With these findings, they concluded that splenic PlGF was crucial for the onset of hypertension.

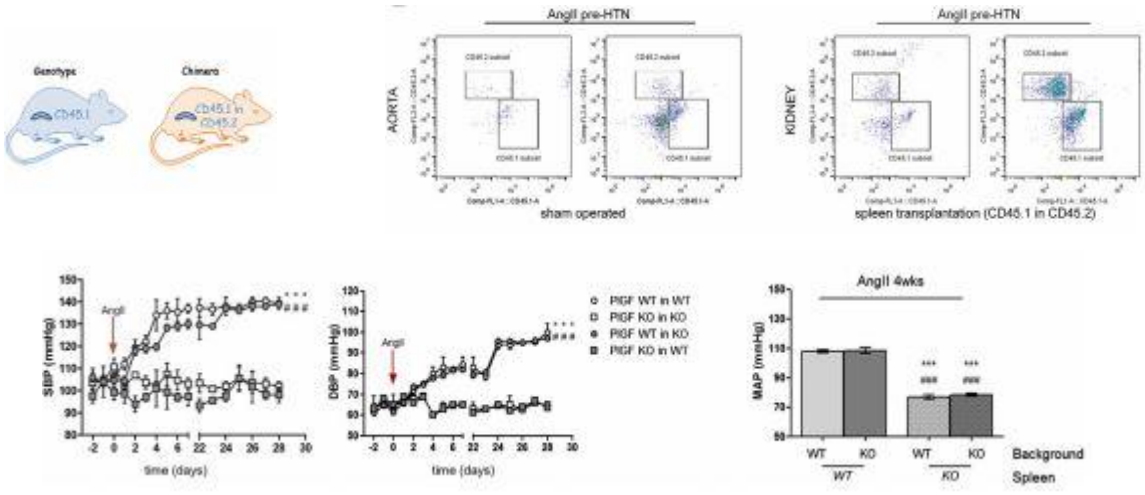

Figure 10. Splenic PlGF in hypertension. Blood pressure (BP) responses to chronic AngII, in different groups of chimeric mice, obtained by spleen transplantation among PlGF-deficient (PlGF KO) mice and WT mice. In this figure, it is represented a cartoon with chimeric mice obtained after spleen transplantation (up and left panel); the accumulation of T cells from the donor spleen (CD45.1) measured by flow cytometry (up and right panel); BP response to chronic AngII, in splenectomized WT versus sham mice (down and left panel); BP response to chronic AngII, in different groups of chimeric mice, obtained by spleen transplantation among PlGF-deficient (PlGF KO) mice and WT mice.
By Carnevale et al. 2014.

Furthermore, Carnevale and colleagues also identified an epigenetic modulation in which PlGF was able to mediate the mechanism of T cells costimulation (Carnevale et al., 2014). PlGF is expressed in the marginal zone of the spleen, in a network of fibroblastic reticular cells (FRCs), identified by ER-TR7 and CD169 antigens. In this zone, the spleen is particularly enriched of macrophages and DCs, acting as APCs, and directly or indirectly activating T cells. In the Harrison lab, it has been demonstrated that the AngII hypertensive

challenge is able to increase the percentage of the co-stimulatory molecule CD86 (Vinh et al., 2010). Carnevale and colleagues found that after AngII, the absence of PlGF significantly protected from CD86 increase in the marginal zone of the spleen, promoting PlGF as a crucial regulator of neuroimmune dealing in hypertensive condition (Carnevale et al., 2014; Carnevale and Lembo, 2015).

6. References

Abboud FM, Harwani SC and Chapleau MW. Autonomic neural regulation of the immune system: implications for hypertension and cardiovascular disease. Hypertension. **2012**; 59.4: 755-62.

Abboud FM. The sympathetic system in hypertension. State-of-the-art review. Hypertension. **1982**; 4: 208-25.

Alkadhi KA et al. Psychosocial stress-induced hypertension results from in vivo expression of long-term potentiation in rat sympathetic ganglia. Neurobiol Dis. **2005**; 20: 849-57.

Anderson EA, Sinkey CA, Lawton WJ and Mark AL. Elevated sympathetic nerve activity in borderline hypertensive humans: Evidence from direct intraneural recordings. Hypertension. **1989**; 14: 177-83.

Autiero M, Luttun A, Tjwa M and. Carmeliet P. Placental growth factor and its receptor, vascular endothelial growth factor receptor-1: novel targets for stimulation of ischemic tissue revascularization and inhibition of angiogenic and inflammatory disorders. J Thromb Haemost. **2003**; 1: 1356-70.

Bellinger DL et al. Acetylcholinesterase staining and choline acetyltransferase activity in the young adult rat spleen: lack of evidence for cholinergic innervation. Brain Behav Immun. **1993**; 7: 191-204.

Berg DK and Conroy WG. Nicotinic alpha 7 receptors: synaptic options and downstream signaling in neurons. J Neurobiol. **2002**; 53: 512-23.

Borovikova LV et al. Vagus nerve stimulation attenuates the systemic inflammatory response to endotoxin. Nature. **2000**; 405: 458-62.

Brody M et al. Critical role of the AV3V region in development and maintenance of experimental hypertension. In: Schmitt H, Meyers P, eds. Perspectives in Nephrology and Hypertension. New York, NY: Wiley and Flammarion. **1978**: 76-84.

Carmeliet P et al. Synergism between vascular endothelial growth factor and placental growth factor contributes to angiogenesis and plasma extravasation in pathological conditions. Nat Med. **2001**; 7: 575-83.

Carnevale D and Lembo G. PlGF, immune system and hypertension. Oncotarget. **2015**; 6: 18246-7.

Carnevale D et al. Placental growth factor regulates cardiac inflammation through the tissue inhibitor of metalloproteinases-3/tumor necrosis factor-α-converting enzyme axis:

crucial role for adaptive cardiac remodeling during cardiac pressure overload. Circulation. **2011**; 124: 1337-50.

Carnevale D et al. The angiogenic factor PlGF mediates a neuroimmune interaction in the spleen to allow the onset of hypertension. Immunity. **2014**; 41: 737-52.

Casto R and Phillips MI. Mechanism of pressor effects by angiotensin in the nucleus tractus solitaries of rats. Am J Physiol. **1984**; 247:R575-81.

Chatzidaki A and Millar NS. Allosteric modulation of nicotinic acetylcholine receptors. Biochem Pharmacol. **2015**; 97: 40817.

Chen CN et al. The significance of placenta growth factor in angiogenesis and clinical outcome of human gastric cancer. Cancer Lett. **2004**; 213: 73-82.

Coble JP et al. Mechanisms of brain renin angiotensin system-induced drinking and blood pressure: importance of the subfornical organ. American journal of physiology. Regulatory, integrative and comparative physiology. **2015**; 308.4: R238-49.

Coffman TM. Under pressure: the search for the essential mechanisms of hypertension. Nat Med. **2011**; 17:1402-9.

Couturier S et al. A neuronal nicotinic acetylcholine receptor subunit (a7) is developmentally regulated and forms a homo-oligomeric channel blocked by a-BTX. Neuron. **1990**; 5: 847-56.

Crowley SD, Tharaux PL, Audoly LP and Coffman TM. Exploring type I angiotensin (AT1) receptor functions through gene targeting. Acta Physiol Scand. **2004**; 181: 561-70.

De Miguel C, Das S, Lund H and Mattson DL. T-lymphocytes mediate hypertension and kidney damage in Dahl salt-sensitive rats. Am J Physiol Regul Integr Comp Physiol. **2010**; 298: R1136-42.

Deck J. et al. α7-Nicotinic acetylcholine receptor subunit is not required for parasympathetic control of the heart in the mouse. Physiol Genomics. **2005**; 22: 86-92.

Endo J et al. Bone marrow derived cells are involved in the pathogenesis of cardiac hypertrophy in response to TAC. Circulation. **2007**; 116: 1176-84.

Esler MD et al. Renal sympathetic denervation for treatment of drug-resistant hypertension: one-year results from the Symplicity HTN-2 randomized, controlled trial. Circulation. **2012**; 126: 2976-82.

Esler MD. The sympathetic nervous system through the ages: from Thomas Willis to resistant hypertension. Experimental Physiology. **2011**; 96.7: 611-22.

Felten DL et al. Noradrenergic and peptidergic innervation of lymphoid tissue. J Immunol. **1985**; 135: 755S–765S.

Felten SY and Olschowka JA. Noradrenergic sympathetic innervation of the spleen. II. Tyrosine hydroxylase (TH)-positive nerve terminals form synaptic like contacts on lymphocytes in the splenic white pulp. J Neurosci Res. **1987**; 18: 37-48.

Fischer C. et al. Anti-PlGF inhibits growth of VEGF(R)-inhibitor-resistant tumors without affecting healthy vessels. Cell. **2007**; 131: 463 -75.

Ganta CK et al. Central angiotensin II-enhanced splenic cytokine gene expression is mediated by the sympathetic nervous system. American Journal of Physiology: Heart and Circulatory Physiology. **2005**; 289.4: 1683-91.

Grassi G. Assessment of sympathetic cardiovascular drive in human hypertension: achievements and perspectives. Hypertension. **2009**; 54: 690-7.

Grobe JL et al. CHBPR–Angiotensinergic Signaling in the Brain Mediates Metabolic Effects of Deoxycorticosterone (DOCA)-Salt in C57 Mice. Hypertension. **2011**; 57: 600-7.

Gutkind JS, Kurihara M and Saavedra JM. Increased angiotensin II receptors in brain nuclei of DOCA-salt hypertensive rats. Am J Physiol. **1988**; 255: H646-50.

Guyenet PG. The sympathetic control of blood pressure. Nat Rev Neurosci. **2006**; 7: 335-46.

Guzik TJ et al. Role of the T cell in the genesis of angiotensin II induced hypertension and vascular dysfunction. J Exp Med. **2007**; 204.10: 2449-60.

Harrison DG et al. Inflammation, Immunity and Hypertension. Hypertension. **2011**; 57: 132-40.

Hartupee J, Liu C, Novotny M, Li X and Hamilton T. IL-17 enhances chemokine gene expression through mRNA stabilization. J Immunol. **2007**; 179: 4135-41

Hendel MD and Collister JP. Role of the subfornical organ in chronic Ang II induced hypertension. FASEB J. **2004**; 18: A672.

Huston et al. Cholinergic Neural Signals to the Spleen Down-Regulate Leukocyte Trafficking via CD11b. J Immunol. **2009**; 183: 552-9.

Incio J et al. PlGF/VEGFR-1 Signaling Promotes Macrophage Polarization and Accelerated Tumor Progression in Obesity. Clin Cancer Res. **2016**; 22: 2993-3004.

Inoue T. et al. Vagus nerve stimulation mediates protection from kidney ischemia-reperfusion injury through α7nAChR+ splenocytes. J Clin Invest. **2016**; 126: 1939-52.

Jacob F, Clark LA, Guzman PA and Osborn JW. Role of renal nerves in development of hypertension in DOCA-salt model in rats: a telemetric approach. Am J Physiol Heart Circ Physiol. **2005**; 289: H1519-29.

Kawashima K and Fujii T. Expression of non-neuronal acetylcholine in lymphocytes and its contribution to the regulation of immune function. Front Biosci. **2004**; 9:2063-85.

Khaliq A et al. Localisation of placenta growth factor (PIGF) in human term placenta. Growth Factors. **1996**; 13: 243-50.

Khraibi AA, Norman RA and Dzielak DJ. Chronic immunosuppression attenuates hypertension in Okamoto spontaneously hypertensive rats. Am J Physiol Heart Circ Physiol. **1984**; 247: H722-6.

Khurana R et al. Placental growth factor promotes atherosclerotic intimal thickening and macrophage accumulation. Circulation. **2005**; 111: 2828 -36.

Kondo T, Takata H, Matsuki F and Takiguchi M. Cutting edge: Phenotypic characterization and differentiation of human CD8+ T cells producing IL-17. J Immunol. **2009**; 182: 1794-8.

Krause EG et al. Blood-borne angiotensin ii acts in the brain to influence behavioral and endocrine responses to psychogenic stress. J Neurosci. **2011**; 31:15009-15.

Krum H et al. Catheter-based renal sympathetic denervation for resistant hypertension: a multicentre safety and proof-of-principle cohort study. Lancet. **2009**; 373: 1275-81.

Kuenen BC et al. Analysis of coagulation cascade and endothelial cell activation during inhibition of vascular endothelial growth factor/vascular endothelial growth factor receptor pathway in cancer patients. Arterioscler Thromb Vasc Biol. **2002**; 22: 1500-5.

Lawes, CM, Vander Hoorn S and Rodgers A. Global burden of blood-pressure related disease. Lancet. **2008**; 371: 1513-8.

Leaders FE and Dayrit CJ. THE CHOLINERGIC COMPONENT IN THE SYMPATHETIC INNERVATION TO THE SPLEEN. Pharmacol Exp Ther. **1965**; 147: 145-52.

Leung DW et al. Vascular endothelial growth factor is a secreted angiogenic mitogen. Science. **1989**; 246: 1306-9.

Lewis EJ et al. Renoprotective effect of the angiotensin-receptor antagonist irbesartan in patients with nephropathy due to type 2 diabetes. N Engl J Med. **2001**; 345: 851-60.

Lori A, Perrotta M, Lembo G and Carnevale D. The Spleen: A Hub Connecting Nervous and Immune Systems in Cardiovascular and Metabolic Diseases. Int J Mol Sci. **2017**; 18: 1-12.

Luttun A et al. Revascularization of ischemic tissues by PlGF treatment, and inhibition of tumor angiogenesis, arthritis and atherosclerosis by anti-Flt1. Nat Med. **2002**; 8: 831-40.

Madden KS, Sanders VM and Felten DL. Catecholamine influences and sympathetic neural modulation of immune responsiveness. Annu Rev Pharmacol Toxicol. **1995**; 35: 417-48.

Malpas SC. Sympathetic nervous system overactivity and its role in the development of cardiovascular disease. Physiol Rev. **2010**; 90: 513-57.

Mangiapane ML and Simpson JB. Subfornical organ lesions reduce the pressor effect of systemic angiotensin II. Neuroendocrinology. **1980**; 31: 380-4.

Mann SJ. Neurogenic essential hypertension revisited the case for increased clinical and research attention. Am J Hypertens. **2003**; 16: 881-8.

Martelli D, Yao ST, McKinley MJ and McAllen RM. Reflex control of inflammation by sympathetic nerves, not the vagus. J Physiol. **2014**; 592: 1677-8.

Marvar PJ et al. Central and peripheral mechanisms of T-lymphocyte activation and vascular inflammation produced by angiotensin II-induced hypertension. Circ Res. **2010**; 107: 263-70.

Marvar PJ et al. T lymphocytes and vascular inflammation contribute to stress-dependent hypertension. Biol Psychiatry. **2012**; 71: 774-82.

Matthews KA et al. Blood pressure reactivity to psychological stress predicts hypertension in the cardia study. Circulation. **2004**; 110:74-78.

Mattson DL. Infiltrating immune cells in the kidney in salt-sensitive hypertension and renal injury. American Journal of Physiology - Renal Physiology. **2014**; 307: F499-508.

McAllen RM et al. The interface between cholinergic pathways and the immune system and its relevance to arthritis. Arthritis Res Ther. **2015**; 17: 87.

McBryde FD et al. Angiotensin II-based hypertension and the sympathetic nervous system: the role of dose and increased dietary salt in rabbits. Exp Physiol. **2007**; 92: 831-40.

Millar NS and Gotti C. Diversity of vertebrate nicotinic acetylcholine receptors. Neuropharmacol. **2009**; 56: 237-46.

Nance DM and Sanders VM. Autonomic innervation and regulation of the immune system. Brain, Behavior and Immunity. **2007**; 21.6: 736-45.

Nataraj C et al. Angiotensin II regulates cellular immune responses through a calcineurin-dependent pathway. J Clin Invest. **1999**; 104: 1693-701.

Nishimura M et al. Regulation of brain renin angiotensin system by benzamil-blockable sodium channels. Am J Physiol. **1999**; 276:R1416-24.

Olofsson PS et al. Blood pressure regulation by CD4+ lymphocytes expressing choline acetyltransferase. Nat Biotechnol. **2016**; 34: 1066-71.

Olsen F. Transfer of arterial hypertension by splenic cells from DOCA-salt hypertensive and renal hypertensive rats to normotensive recipients. Acta Pathol Microbiol Scand C. **1980**; 88: 1-5.

Osborn JW et al. Circulating angiotensin II and dietary salt: converging signals for neurogenic hypertension. Curr Hypertens Rep. **2007**; 9: 228-35.

Page IH. The mosaic theory of arterial hypertension--its interpretation. Perspect Biol Med. **1967**; 10: 325-33.

Palkovits M and Záborszky L. Neuroanatomy of central cardiovascular control. Nucleus tractus solitarius afferent and efferent neuronal connections in relation to the baroreceptor reflex arc. Prog Brain Res. **1977**; 47: 9-34.

Pavlov VA et al. Brain acetylcholinesterase activity controls systemic cytokine levels through the cholinergic anti-inflammatory pathway. Brain Behav Immun. **2009**; 23: 41-5.

Pipp F et al. VEGFR-1-selective VEGF homologue PlGF is arteriogenic: evidence for a monocyte-mediated mechanism. Circ Res. **2003**; 92: 378-85.

Reardon C et al. Lymphocyte-derived ACh regulates local innate but not adaptive immunity. Proc Natl Acad Sci U S A. **2013**; 110: 1410-5.

Rosas-Ballina M and Tracey KJ. The neurology of the immune system: neural reflexes regulate immunity. Neuron. **2009**; 64: 28-32.

Rosas-Ballina M et al. Acetylcholine-synthesizing T cells relay neural signals in a vagus nerve circuit. Science. **2011**; 334: 98-101.

Rosas-Ballina M et al. Splenic nerve is required for cholinergic anti inflammatory pathway control of TNF in endotoxemia. Proc Natl Acad Sci U S A. **2008**; 105: 11008-13.

Saper CB. The central autonomic nervous system: conscious visceral perception and autonomic pattern generation. Annu Rev Neurosci. **2002**; 25: 433-69.

Schenk J and McNeill JH. The pathogenesis of DOCA-salt hypertension. J Pharmacol Toxicol Methods. **1992**; 27:161-70.

Simms AE, Paton JF, Pickering AE, Allen AM. Amplified respiratory-sympathetic coupling in the spontaneously hypertensive rat: does it contribute to hypertension? J Physiol. **2009**; 587: 597-610.

Simpson JB. The circumventricular organs and the central actions of angiotensin. Neuroendocrinology. **1981**; 32: 248-56.

Small HY et al. Hypertension due to antiangiogenic cancer therapy with vascular endothelial growth factor inhibitors: understanding and managing a new syndrome. Can J Cardiol. **2014**; 30: 534-43.

Snuderl M et al. Targeting placental growth factor/neuropilin 1 pathway inhibits growth and spread of medulloblastoma. Cell. **2013**; 152: 1065-76.

Sunn N, McKinley MJ and Oldfield BJ. Circulating angiotensin ii activates neurones in circumventricular organs of the lamina terminalis that project to the bed nucleus of the stria terminalis. J Neuroendocrinol. **2003**; 15: 725-31.

Svendsen UG. Evidence for an initial, thymus independent and a chronic, thymus dependent phase of DOCA and salt hypertension in mice. Acta Pathologica et Microbiologica Scandinavica. Section A, Pathology. **1976**; 84.6: 523-8.

Swanson MA, Lee WT and Sanders VM. IFN-gamma production by Th1 cells generated from naive CD4+ T cells exposed to norepinephrine. J Immunol. **2001**; 166: 232-40.

Torry RJ et al. Hypoxia increases placenta growth factor expression in human myocardium and cultured neonatal rat cardiomyocytes. J Heart Lung Transplant. **2009**; 28: 183-90.

Tracey KJ. The inflammatory reflex. Nature. **2002**; 420: 853-9.

Van de Veire S et al. Further pharmacological and genetic evidence for the efficacy of PlGF inhibition in cancer and eye disease. Cell. **2010**; 141: 178-90.

Victor RG. Carotid baroreflex activation therapy for resistant hypertension. Nat Rev. Cardiol. **2015**; 12: 451-63.

Vida G, Peña G, Deitch EA and Ulloa L. α7-cholinergic receptor mediates vagal induction of splenic norepinephrine. J Immunol. **2011**; 186: 4340-6.

Vinh A et al. Inhibition and genetic ablation of the B7/CD28 T-cell costimulation axis prevents experimental hypertension. Circulation. **2010**; 122.24: 2529-37.

Wenzel P et al. Lysozyme M-positive monocytes mediate angiotensin II-induced arterial hypertension and vascular dysfunction. Circulation. **2011**; 124.12: 1370-81.

Witowski J, Ksiazek K and Jorres A. Interleukin-17: a mediator of inflammatory responses. Cell Mol Life Sci. **2004**; 61:567-79.

Yano et al. Elevated levels of placental growth factor represent an adaptive host response in sepsis. J Exp Med. **2008**; 205: 2623-31.

Yano K et al. Vascular endothelial growth factor is an important determinant of sepsis morbidity and mortality. J Exp Med. **2006**; 203: 1447-58.

Zubcevic J et al. Autonomic-immune-vascular interaction: an emerging concept for neurogenic hypertension. Hypertension. **2011**; 57.6: 1026-33.

7. A cholinergic-sympathetic pathway primes immunity in hypertension and mediates brain-to-spleen communication.

Carnevale D, Perrotta M, Pallante F, Fardella V, Iacobucci R, Fardella S, Carnevale L, Carnevale R, De Lucia M, Cifelli G, Lembo G.

This work was published in Nat Commun. 2016 Sep 27;7:13035.

Abstract

The crucial role of the immune system in hypertension is now widely recognized. We previously reported that hypertensive challenges couple the nervous drive with immune system activation, but the physiological and molecular mechanisms of this connection are unknown. Here, we show that hypertensive challenges activate splenic sympathetic nerve discharge to prime immune response. More specifically, a vagus-splenic nerve drive, mediated by nicotinic cholinergic receptors, links the brain and spleen. The sympathetic discharge induced by hypertensive stimuli was absent in both coeliac vagotomized mice and in mice lacking α7nAChR, a receptor typically expressed by peripheral ganglionic neurons. This cholinergic-sympathetic pathway is necessary for T cell activation and egression on hypertensive challenges. In addition, we show that selectively thermoablating the splenic nerve prevents T cell egression and protects against hypertension. This novel experimental procedure for selective splenic denervation suggests new clinical strategies for resistant hypertension.

Introduction

Despite the wide spectrum of antihypertensive medications currently available, a significant proportion of patients still have poorly controlled blood pressure and, consequently, resistant hypertension[1,2,3]. In the first half of the past century, the Mosaic Theory of Hypertension proposed that many factors, including genetics and environment as well as nervous, mechanical and hormonal perturbations, interplay to raise blood pressure[4]. Because the

aetiology of hypertension is multifaceted, its solution must involve more than a single anatomical organ.

In the last decade, immunity emerged as a crucial player in hypertension: immune cells infiltrate the vessel walls and kidneys of hypertensive animals, and mice without lymphocytes are protected from angiotensinII (AngII)-induced hypertension[5,6,7,8,9]. Despite growing awareness of immune cells' role in hypertension, blood pressure control has been considered primarily the work of the autonomic nervous system[10]. The sympathetic nervous system, by contrast, has historically been thought to influence blood pressure control via regulation of key physiological parameters including heart rate, vascular tone and renal sodium excretion[3]. Clinically, sympathetic innervation of the kidney has been seen as the cause of hypertension, and renal denervation has been regarded as an intriguing new approach to treating uncontrolled high blood pressure[11,12,13].

The autonomic nervous system also regulates of immunity[14,15,16,17], though its role is often overlooked. Previously, we have found that placental growth factor (PlGF), an angiogenic growth factor belonging to the vascular endothelial growth factor (VEGF) family, links the nervous drive to immune system activation[7]. We performed a coeliac ganglionectomy to selectively disrupt sympathetic innervation of splanchnic circulation and found that PlGF activation, immune system recruitment and increased blood pressure depend on this pathway[7]. Interestingly, preliminary studies indicated that splanchnic innervation would impact hypertension[18]. However, two main questions remain unanswered: (i) which splanchnic nervous compartment is responsible for these effects on immunity and blood pressure regulation and (ii) how is the brain-to-splanchnic compartment connection established at the onset of hypertension.

Hypertensive stimuli activate splenic nerve discharge

Although chronic AngII has been shown to be a potent driver of splanchnic circulation[18], we do not yet know which downstream nervous district is engaged by hypertensive stimuli to increase blood pressure. The chronic effects of AngII are mediated by brain signals transmitted via the peripheral networks[19]. Indeed, lesions in central nervous system organs, which are able to sense peripheral challenges, prevent AngII infusion from raising blood pressure[19]. Taken together, these connections suggest that peripherally-delivered hypertensive stimuli activate a nervous drive in the brain that is conveyed through splanchnic circulation. Given that immune system activation in hypertension depends on the same

pathway, we hypothesized that the splenic nerve could be the splanchnic innervation connecting the brain and immune cells.

To test this idea, we established a procedure for recording sympathetic nerve activity (SNA) in mice. First, we validated splenic nerve SNA (SSNA) recording by inducing reflex responses to blood pressure changes. We pharmacologically manipulated blood pressure with sodium nitroprusside and phenylephrine to evaluate typical SNA reflex responses (Supplementary Figs 1 and 2). We found that SSNA increased quickly in response to lowered blood pressure, as expected for sympathetic activity (Supplementary Fig. 1a–c). To further assess nerve activity, we evaluated synchronous sympathetic bursts. Analysis of SSNA showed that most nerve bursts synchronized with raw blood pressure signal (Supplementary Fig. 1d,e), a result that is consistent with the semirhythmic SNA observed in nerves in nearby compartments, including the splanchnic[10,20,21,22]. Ganglionic blockade with hexamethonium abolished SSNA activity (Supplementary Fig. 1f), which overlapped the residual postmortem recording (Supplementary Fig. 1g) that was used thereafter as the positive action potential threshold. As expected, the opposite response was observed when mice were challenged with phenylephrine to acutely increase blood pressure. Indeed, the SSNA, although similarly pulse synchronous, was markedly reduced (Supplementary Fig. 2a–g).

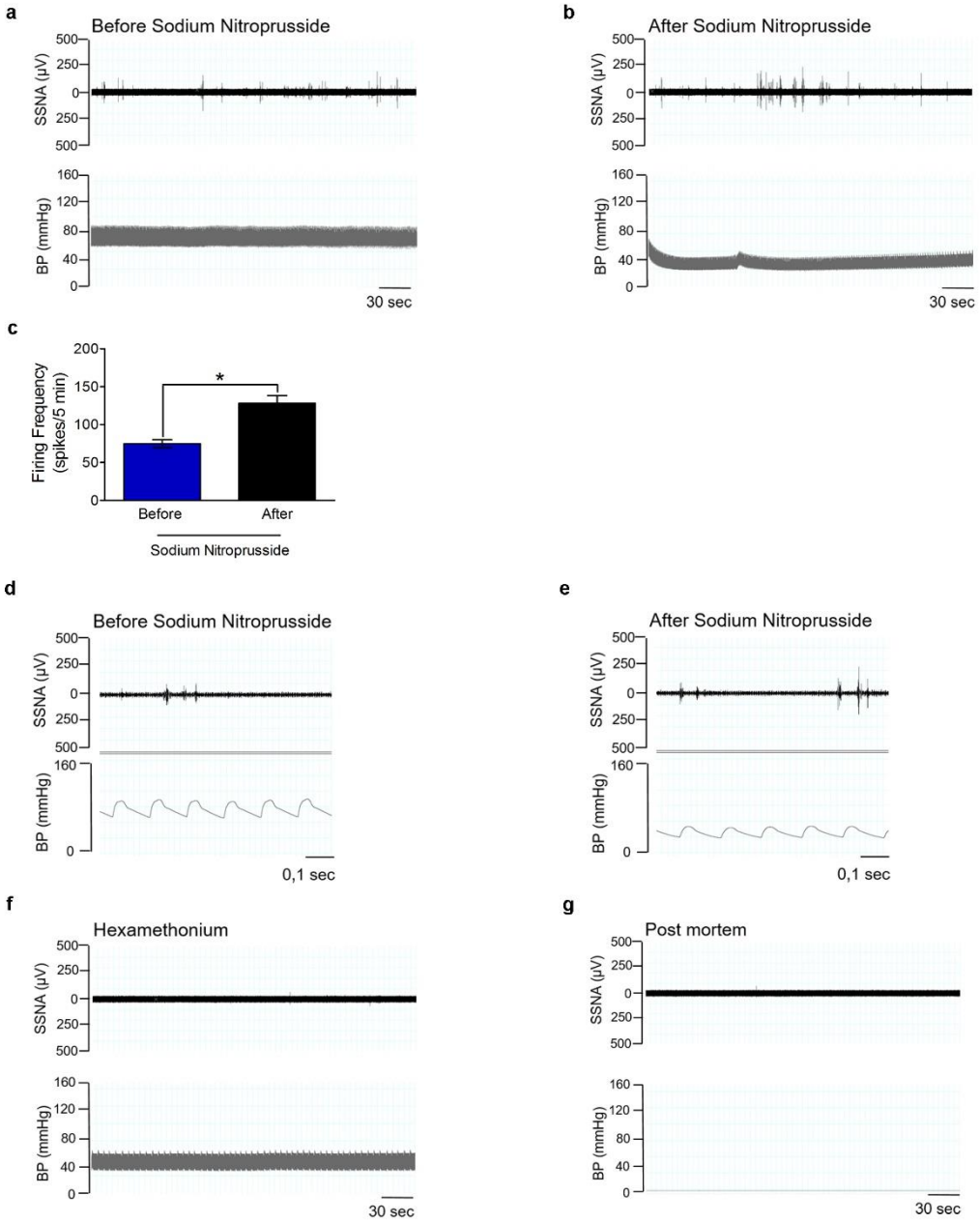

Supplementary Figure 1. Acute fall in blood pressure determines activation of sympathetic nerve activity in splenic nerve. (**a**) Representative recording of splenic sympathetic nerve activity (SSNA) during baseline (upper panel) and corresponding raw blood pressure signal (lower panel). (**b**) Effect of Sodium Nitroprusside (SNP) administration on SSNA activity (upper panel) and blood pressure (lower panel). (**c**) Quantitative analysis of firing frequency indicating a significant increase in SSNA after SNP-induced fall in blood pressure (n_{mice}=4; Paired Samples Student's t-test, t(3) = 5.442, *p<0.05). (**d,e**) Representative details of recordings showing that sympathetic burst are pulse synchronous, after the peak of Systolic Blood Pressure. (**f,g**) Representative recording of SSNA activity (upper panel) and blood pressure (lower panel) obtained after ganglionic blockade with Hexamethonium (**f**) and postmortem (**g**).

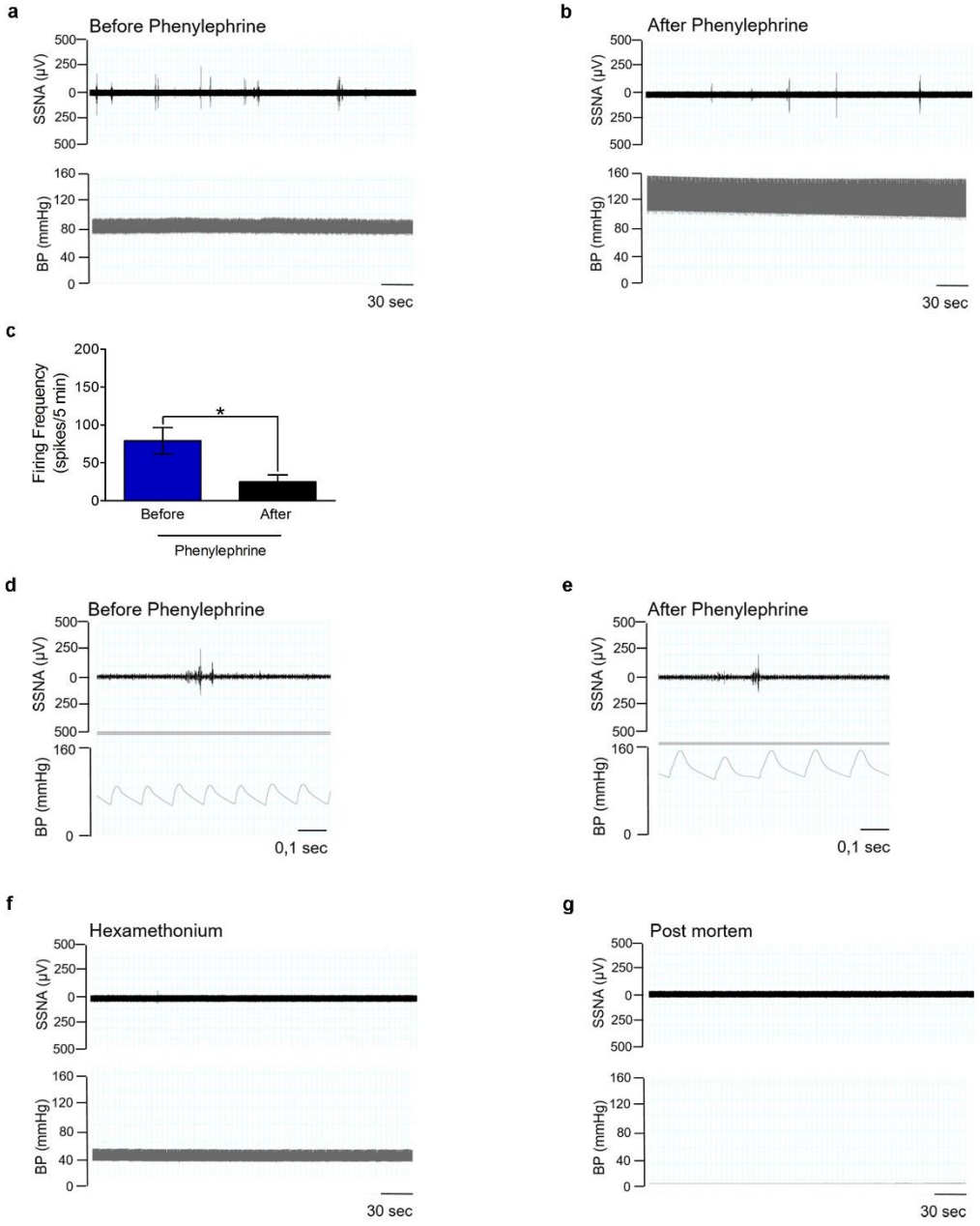

Supplementary Figure 2. Acute increase in blood pressure inhibits activation of sympathetic nerve activity in splenic nerve. (**a**) Representative recording of splenic sympathetic nerve activity (SSNA) during baseline (upper panel) and corresponding raw blood pressure signal (lower panel). (**b**) Effect of Phenylephrine (Phe) administration on SSNA activity (upper panel) and blood pressure (lower panel). (**c**) Quantitative analysis of firing frequency confirming the significant inhibitory effect of blood pressure increase on SSNA (n_{mice}=4;Paired Samples Student's t-test, t(3) = 4.035, *p<0.05). (**d,e**) Representative details of recordings showing that sympathetic burst are pulse synchronous, after the peak of Systolic Blood Pressure. (**f,g**) Representative recording of SSNA activity (upper panel) and blood pressure (lower panel) obtained after ganglionic blockade with Hexamethonium (**f**) and postmortem (**g**).

After validating the direct SSNA recording method, we tested whether chronic AngII infusion activates SSNA to modulate subsequent T cell activation. To avoid the potentially confounding effects of increased blood pressure itself, we analyzed mice 3 days after starting AngII infusion, when blood pressure has not yet significantly changed (Supplementary Fig. 3). To find the appropriate time point for examining the connection between nervous drive and immune activation, we performed a time course analysis of T cell recruitment in target organs. After 3 days, we could detect T cells in the aortas (Supplementary Fig. 4a,b) and kidneys (Supplementary Fig. 4c,d) of AngII-infused mice.

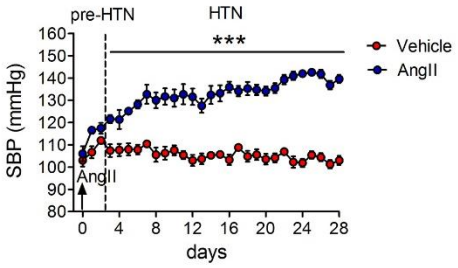

Supplementary Figure 3. Three days of AngII infusion is the earliest time point for blood pressure increase. Blood pressure measurement in mice infused with AngII or Vehicle for 28 days indicates that three days is not yet significantly different from that of control mice (Veh and AngII n_{mice}=7 for; Two-way ANOVA for repeated measures; Systolic Blood Pressure SBP, $F_{(interaction)}$= 10.96, ***p<0.001).

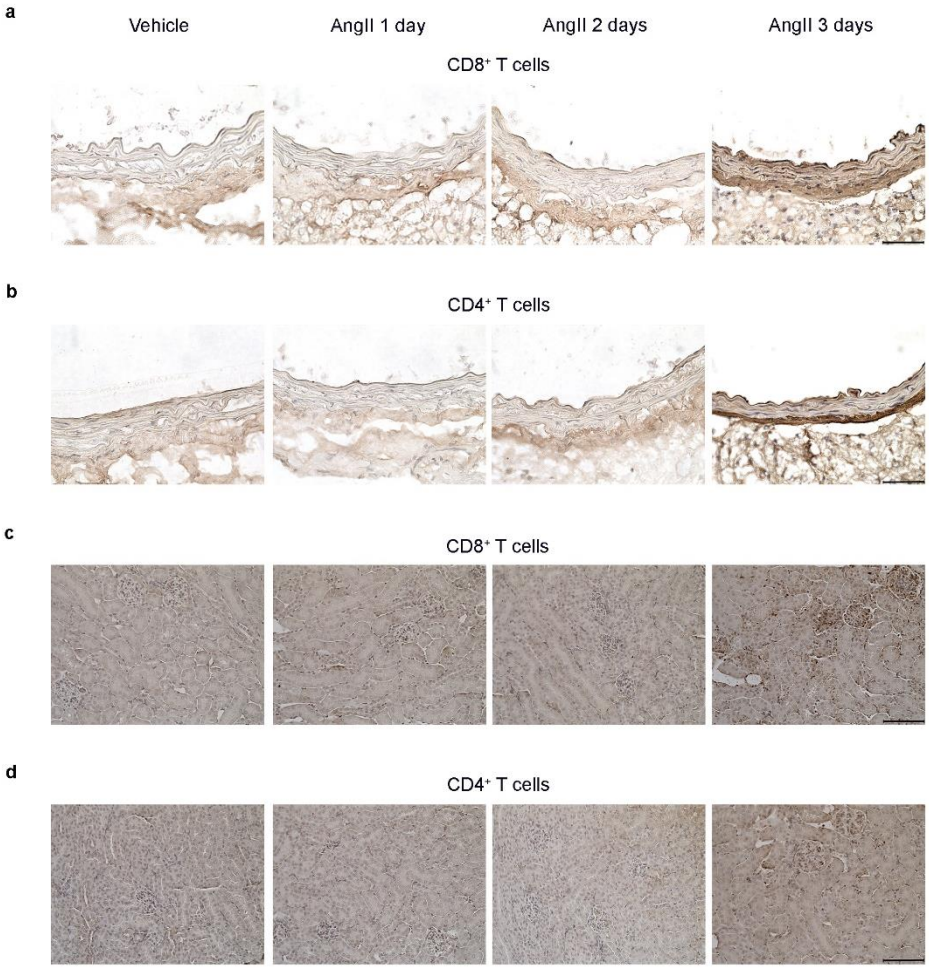

Supplementary Figure 4. Three days of AngII infusion is the earliest time point for immune system activation. (**a-d**) Analysis of $CD8^+$ and $CD4^+$ T cells in aortas (**a,b**) and kidneys (**c,d**) of mouse infused with Vehicle or AngII for 1, 2 and 3 days shows that the early infiltration is visible at 3 days (n_{mice}=6 for each group; scale bar (**a,b**), 50 μm and (**c,d**) 100 μm).

Next, we used a bipolar electrode to record SSNA in splenic nerve bundles in mice infused with either AngII or Vehicle (Fig. 1). A representative recording of splenic nerve discharge clearly shows increased rhythmic SSNA bursts above the background noise, as defined by the postmortem recording (Fig. 1a,b). Simultaneous blood pressure recording demonstrated animal stability during the procedure (Fig. 1c). Changes in SSNA included increases in either the number of sympathetic bursts or the amplitude of individual bursts. We found that AngII-infused mice had significantly higher SSNA, measured both as firing frequency (Fig. 1d) and as mean amplitude gain (Fig. 1e), than controls.

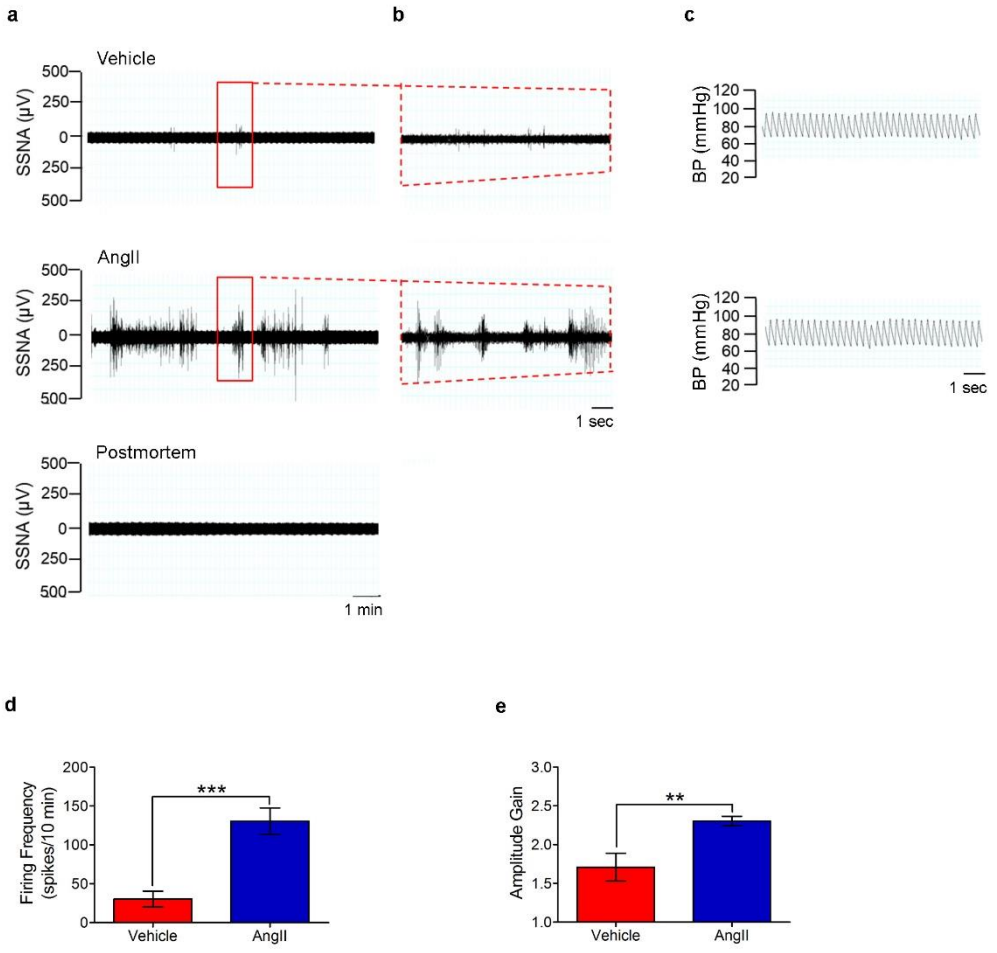

Figure 1. AngII activates discharge of the splenic nerve. a,b) Representative raw signals of SSNA in a time bin of 10 min in (a) show a significantly increased nerve discharge in AngII-infused mice as compared with vehicle. Raw signal of residual SSNA during postmortem was used to identify the signal threshold level for each recording. In (b) it is represented an enlarged view of 10 s of SSNA raw signal from the red window in a. (c) Blood pressure (BP) monitoring during SSNA recording excluded hemodynamic effects. (d) Firing frequency, represented by the mean number of spikes in a time bin, was significantly higher in AngII-infused mice as compared with vehicle (vehicle n_{mice}=8 and AngII n_{mice}=10; independent samples Student's t-test, t(16)=−4.697, ***P<0.001). (e) Analysis of mean amplitude gain of spikes showed that AngII-infused mice had also increased SSNA in the pattern of burst amplitude as compared with vehicle (vehicle n_{mice}=8 and AngII n_{mice}=10; independent samples Student's t-test, t(9)=−3.120, **P<0.01).

To determine if the increased SSNA was a selective response to AngII, we also performed experiments with deoxycorticosterone acetate (DOCA)-salt hypertensive mice, a model characterized by increased AngII levels in the brain and reduced peripheral renin–angiotensin system (RAS) activation[23]. As in the experiments detailed above, in this model we studied mice at the beginning of blood pressure increase (Supplementary Fig. 5) and

again found elevated SSNA (Fig. 2a–c). Quantitative analysis confirmed that SSNA activation is similar in DOCA-salt-treated mice and AngII-hypertensive mice (Fig. 2d,e), thereby suggesting the brain-to-splenic nerve drive is a common pathway for hypertensive challenges that are sensed by the brain and consequently lead to elevated blood pressure.

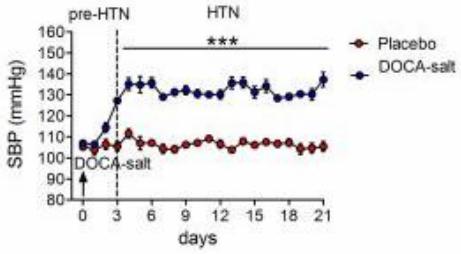

Supplementary Figure 5. DOCA-salt challenge induces hypertension in WT mice. DOCA-salt rises blood pressure in a time-dependent way, with a significant steady-state increase starting at 3 days after pellet implantation (Placebo and DOCA-salt n_{mice}=7; Two-way ANOVA for repeated measures; Systolic Blood Pressure SBP, $F_{(interaction)}$ = 7.784, ***p<0.001).

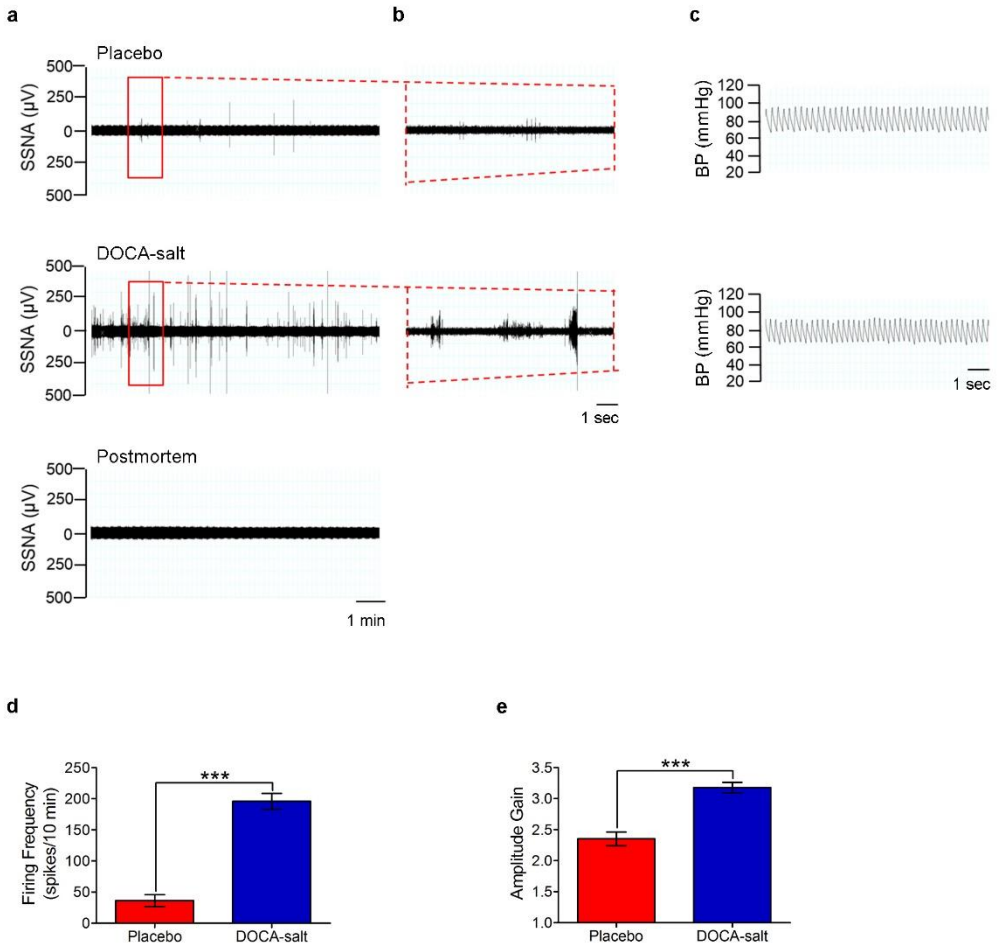

Figure 2. Activation of splenic nerve activity is a common response to hypertensive stimuli. a–c) DOCA-salt hypertensive challenge significantly increased splenic nerve discharge, in a similar way to that observed in AngII-infused mice, as shown by the representative raw signals of SSNA in a time bin of 10 min (a) and a particular of 10 s from the red window in b. Residual SSNA during postmortem (lower panel in a) and BP monitoring (c) are shown as well. (d) DOCA-salt induced a significant increase in firing frequency, expressed as the mean number of spikes in a time bin, as compared with mice receiving placebo (Placebo n_{mice}=6 and DOCA-salt n_{mice}=7; independent samples Student's t-test, t(11)=−9.654, ***P<0.001). (e) DOCA-salt-treated mice display a significant higher mean amplitude gain of spikes, as compared with mice receiving placebo alone (Placebo n_{mice}=6 and DOCA-salt n_{mice}=7; independent samples Student's t-test, t(11)=−5.977, ***P<0.001).

The vagal-coeliac-splenic connection mediates hypertension

Sympathetic innervation of the spleen has been recognized as a crucial mechanism for modulating immune cell functions[24,25,26]. For many years, autonomic innervation of immune organs did not seem relevant to cardiology, but current evidence for immunity's vital role in

blood pressure regulation necessitates investigating neuro-immune reflexes in hypertension. Sympathetic and parasympathetic innervations of the splanchnic organs have been traditionally regarded as anatomically separate along their peripheral routes. If the innervations are indeed separate, the splenic nerve should be activated by a pre-ganglionic neuron in the paravertebral ganglia chain that connects to the intermediolateral grey column in the spinal cord. However, immunologists have identified a cholinergic anti-inflammatory reflex that is mediated by the vagus nerve's coeliac branch and specifically targets splenic innervation during septic challenges[24,25,26,27].

To investigate whether and how vagal signals could affect splenic nerve activity during hypertensive challenges, we performed cervical vagotomy while recording SSNA (Fig. 3a–c). Cervical vagotomy completely prevented AngII from activating the splenic nerve (Fig. 3a,b). These results indicate that AngII-induced splenic nerve activation is mediated by the cervical vagus nerve. Unexpectedly, we found no reduction in residual SSNA gain amplitude after both cervical and coeliac vagotomy (Fig. 3c), a result that suggests hypertensive stimuli use different sympathetic pathways for SSNA firing frequency and individual burst amplitude. As previously reported concerning the regulation of other organs[10], our results indicate that a specific brain cell network produces rhythmical discharges in the splenic nerve through the vagus connection. Conversely, other central nervous system cell groups regulate splenic nerve gain amplitude independently from the vagus nerve. To further uncover the relative contributions of the vagus nerve's afferent versus efferent arms, we performed a coeliac vagotomy that also completely inhibited AngII-induced SSNA (Fig. 3d,e), still with no effect on the gain amplitude of splenic nerve activity (Fig. 3f). In addition, we analyzed the chronic response to AngII in mice with left coeliac vagotomy. Inhibiting vagus nerve efferents hampered the blood pressure increase typically induced by AngII (Fig. 4a,b) as well as the T cell egression (Fig. 4c,d).

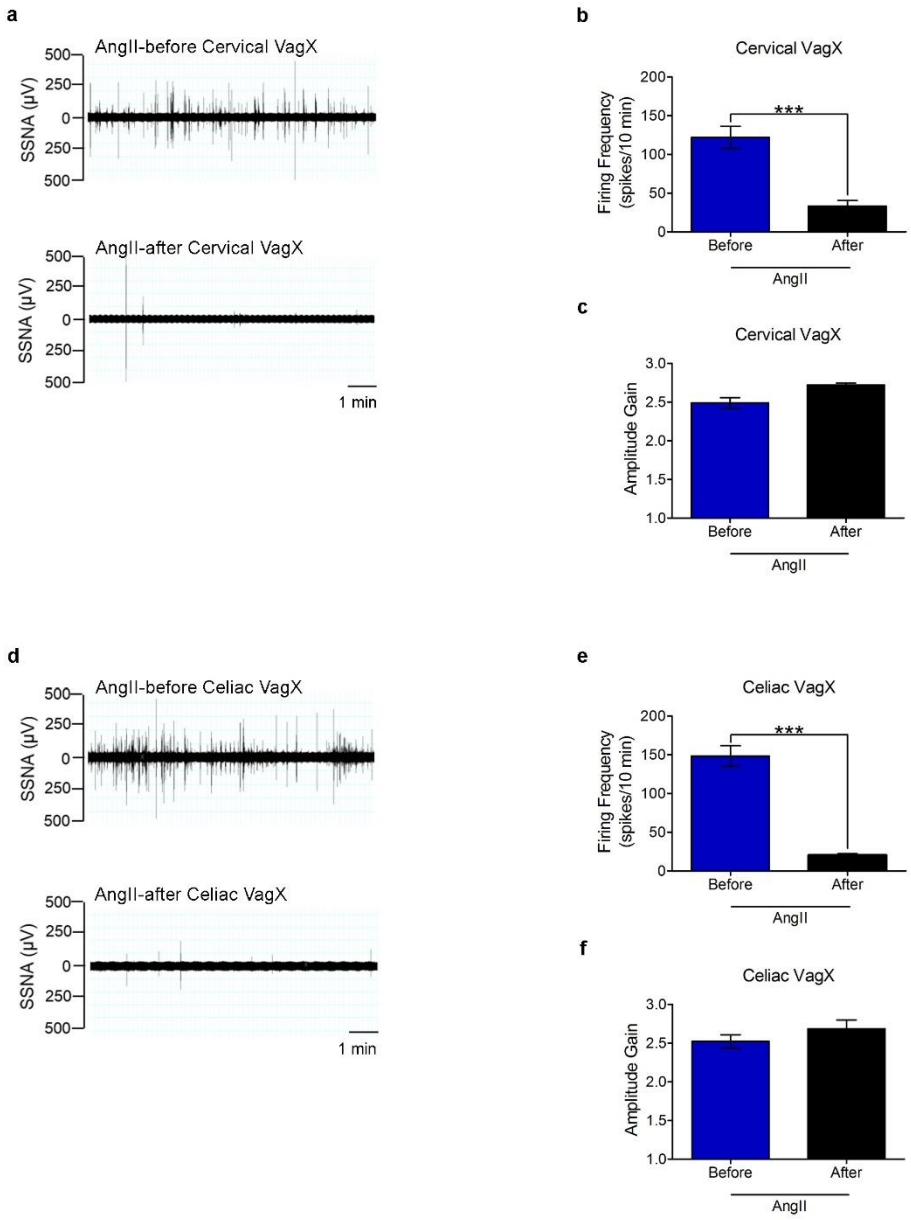

Figure 3. Efferent vagus nerve resection blocks the SSNA induced by hypertensive stimuli. (a) Mice infused with AngII were subjected to cervical vagotomy (VagX) while recording SSNA. As shown by the representative raw signals of SSNA, cervical VagX completely abolishes splenic nerve activity. (b) Analysis of firing frequency confirmed the inhibitory effect of cervical VagX on AngII-induced SSNA (n_{mice}=5; paired samples Student's t-test, t(4)=8.524, ***P<0.001). (c) Conversely, no effect of cervical VagX on the mean amplitude gain of spikes was observed, suggesting that this pattern of SSNA was regulated by pathways different from the vagus nerve (n_{mice}=5; paired samples Student's t-test, t(4)=−2.764, P=0.051). (d) To verify whether the effect was due to the afferent or efferent branch of the vagus nerve, a further group of AngII-infused mice underwent coeliac vagotomy (VagX) while recording SSNA. Even in this case, splenic nerve activity was completely inhibited by coeliac VagX. (e) Analysis of firing frequency confirmed the inhibitory effect of coeliac VagX on AngII-induced SSNA (n_{mice}=5; paired samples Student's t-test, t(4)=11.059, ***P<0.001). (f) Yet, no effect of coeliac VagX on the

mean amplitude gain of spikes was observed, further supporting that this pattern of SSNA was regulated by pathways different from the vagus nerve (n_{mice}=5; paired samples Student's t-test, t(4)=−1.518, P=0.204).

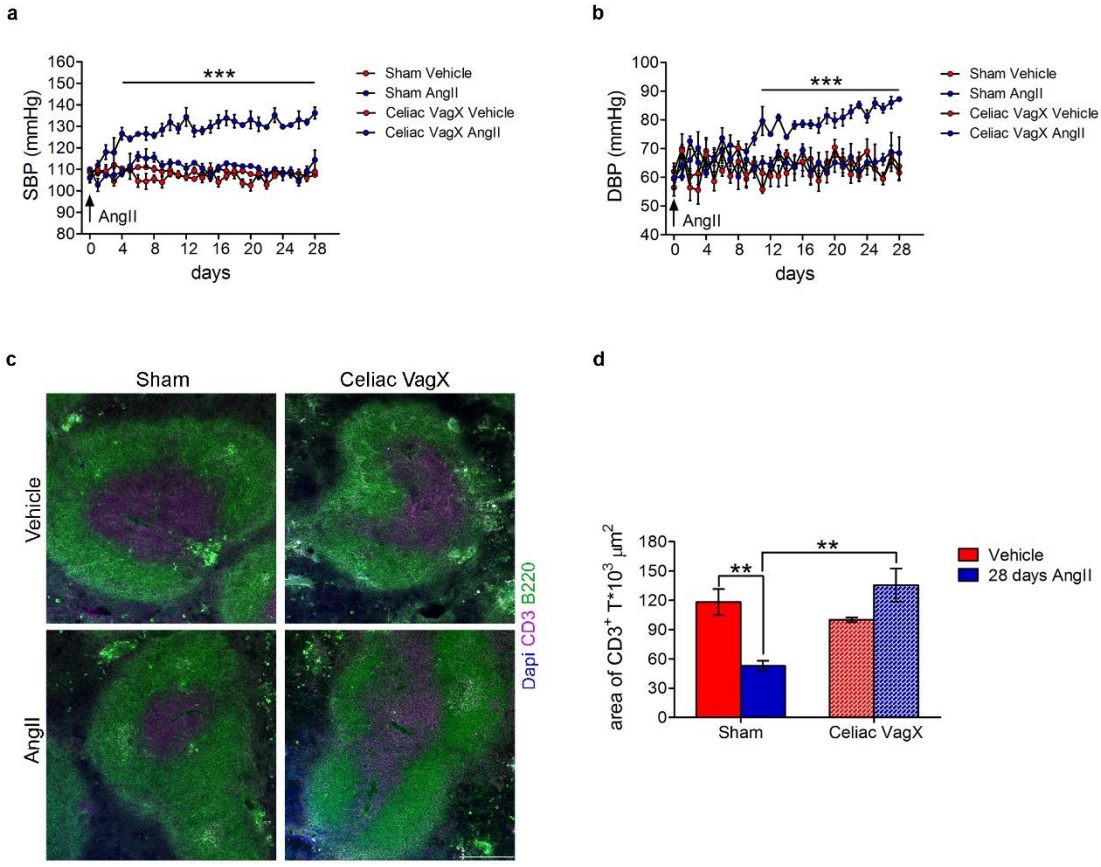

Figure 4. Coeliac vagotomy protects from AngII-induced blood pressure increase and T cell egression. a,b) Mice with left coeliac VagX did not become hypertensive in response to chronic AngII infusion (n_{mice}=5 for each group; two-way ANOVA for repeated measures; (a) systolic blood pressure SBP, F(interaction)=3.321, ***P<0.001; (b) Diastolic blood pressure DBP, F(interaction)=2.284, ***P<0.001). (c) Left coeliac VagX was also effective in inhibiting the T cell egression induced by AngII, as evidenced by the area of CD3+ cells (magenta), representing the white pulp and delimited by B220+ cells (green) delineating the red pulp (scale bar, 200 µm). (d) Graph showing the relative quantitative analysis (n_{mice}=5 for each group; two-way ANOVA, F(interaction)=20.160, **P<0.01).

Overall, these results support our proposal that, although the vagus nerve has been considered paradigmatic for parasympathetic modulation of blood pressure[28], it also activates the splenic nerve under hypertensive challenges. This previously unknown aspect of

hypertension may indicate that completely different pathophysiological conditions, such as sepsis and hypertension, can affect the same neuro-immune connection.

α7nAChR at the intersection of the vagus and splenic nerves

Mammals regulate synaptic transmission across sympathetic and parasympathetic ganglia via nicotinic acetylcholine receptors (nAChR), which can assemble in various stoichiometries and therefore have many functions[29]. One nAChR, the α7 subunit, can form homomeric pentamers that mediate excitatory postsynaptic currents. Interestingly, α7nAChR also participates in the cholinergic anti-inflammatory reflex and, though initially discovered as a modulator of macrophage function, has been shown to couple the vagus-splenic connection at the neuronal level[25,26]. Yet α7nAChR is not required for the parasympathetic modulations exerted by the vagus nerve in typical cardiovascular parameters such as heart rate[30]. To our surprise, α7nAChR KO mice infused with AngII had significantly inhibited SSNA firing frequency (Fig. 5a–d), which suggests the drive was hampered before reaching the splenic nerve. As observed in vagotomized mice, AngII infusion did not alter SSNA amplitude gain in α7nAChR KO mice (Fig. 5e). It may be that different SNA patterns can evoke different neurotransmitter responses[10]. Because the AngII-infused vagotomized and α7nAChR KO mice showed the vagus-splenic connection affects firing frequency but not amplitude gain, we asked which pattern is relevant for noradrenaline release in the spleen. Since AngII increases noradrenaline in the spleen through the activation of tyrosine hydroxylase[7], we examined this response in AngII-infused α7nAChR KO mice and found that both noradrenaline content (Supplementary Fig. 6a) and tyrosine hydroxylase staining (Supplementary Fig. 6b) were significantly inhibited as compared with WT mice. In particular, the adrenergic fibers typically innervating the marginal zone of the spleen, evidenced by the CD169 antigen, were almost absent in α7nAChR KO mice (Supplementary Fig. 6b). Further, AngII challenge in α7nAChR KO mice produced neither the increased blood pressure typically observed in WT mice (Fig. 6a,b) nor the expected T cell egression (Fig. 6c,d). Overall, these data support the existence of a vagus-splenic nerve connection that is recruited by hypertensive stimuli and mediated by α7nAChR.

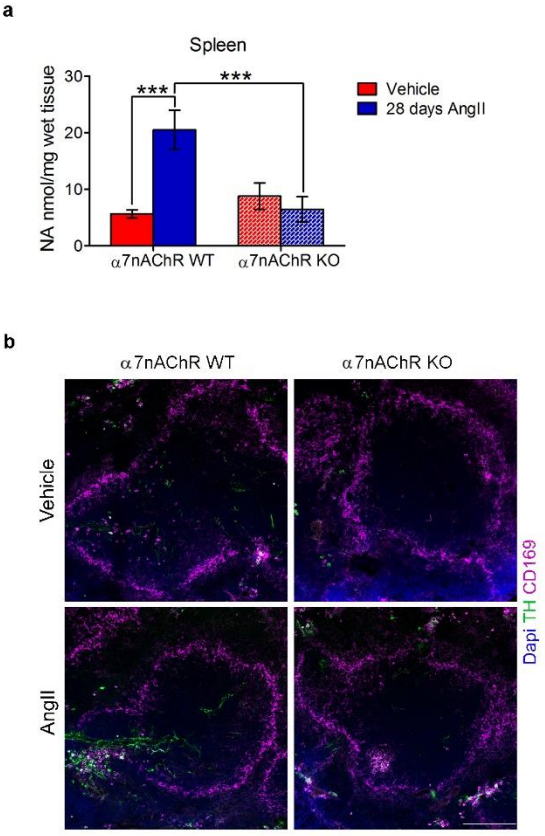

Supplementary Figure 6. AngII fails to increase noradrenaline in the spleen in α7nAChR KO. (**a**) Analysis of noradrenaline content in the spleen further indicates that AngII fails to synthetize the neurotransmitter in α7nAChR KO mice (n_{mice}=6 for each group; Two-way ANOVA, $F_{(interaction)}$ = 12.88, ***p<0.001). (**b**) Tyrosine hydroxylase staining (green) shows that α7nAChR KO mice are protected from the activation typically observed in the splenic marginal zone, delineated by $CD169^{-}$ cells (magenta), in WT mice upon AngII (n_{mice}=6 for each group; scale bar, 200 μm).

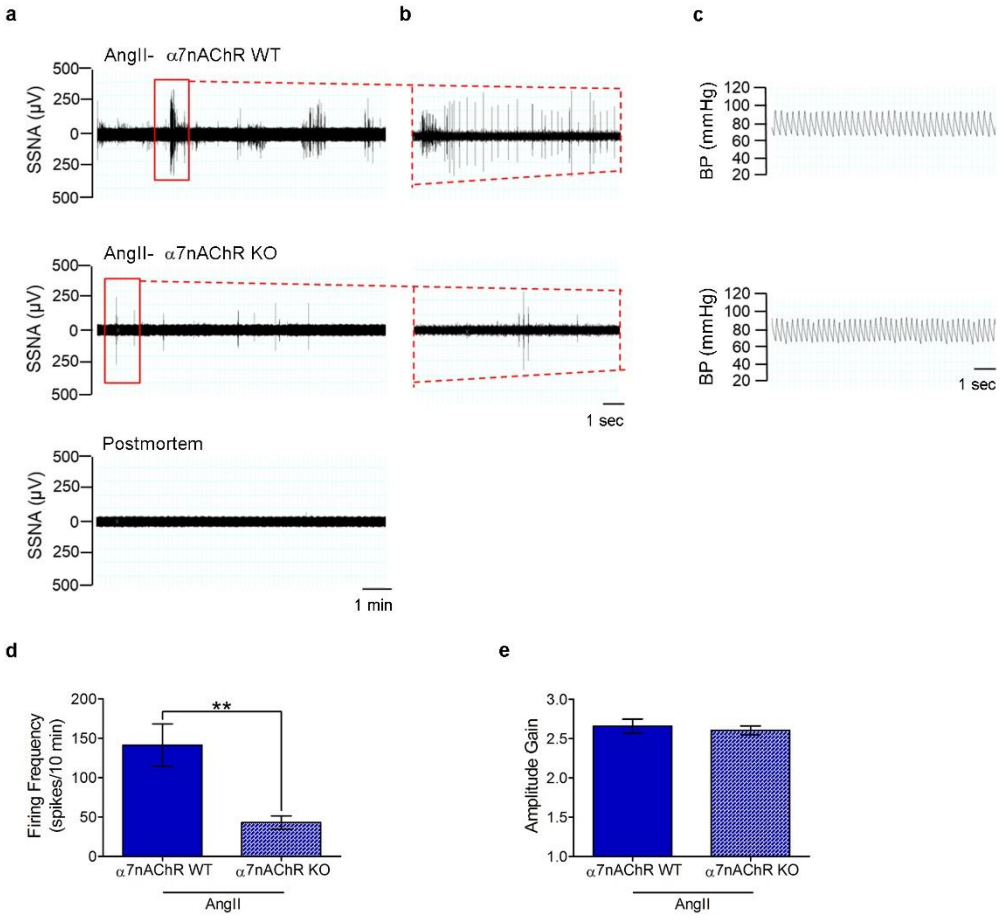

Figure 5: α7nAChR is necessary to the activation of SSNA on hypertensive challenges. (a–c) The representative raw signals of SSNA in a time bin (a) and in an enlarged particular of 10 s (b) show that α7nAChR KO mice have a reduced response to AngII infusion, as compared with WT controls. Residual SSNA during postmortem (lower panel in a) and blood pressure monitoring (c) are shown as well. (d) Analysis of firing frequency confirmed the reduced activity of α7nAChR KO mice on AngII infusion (WT and α7nAChR KO n_{mice}=7; independent samples Student's t-test, t(12)=3.493, **P<0.01). (e) Accordingly to what observed in VagX, the mean amplitude gain of spikes induced by AngII was unaffected in α7nAChR KO, showing levels comparable to that of WT mice (WT and α7nAChR KO n_{mice}=7; independent samples Student's t-test, t(12)=0.572, P=0.578).

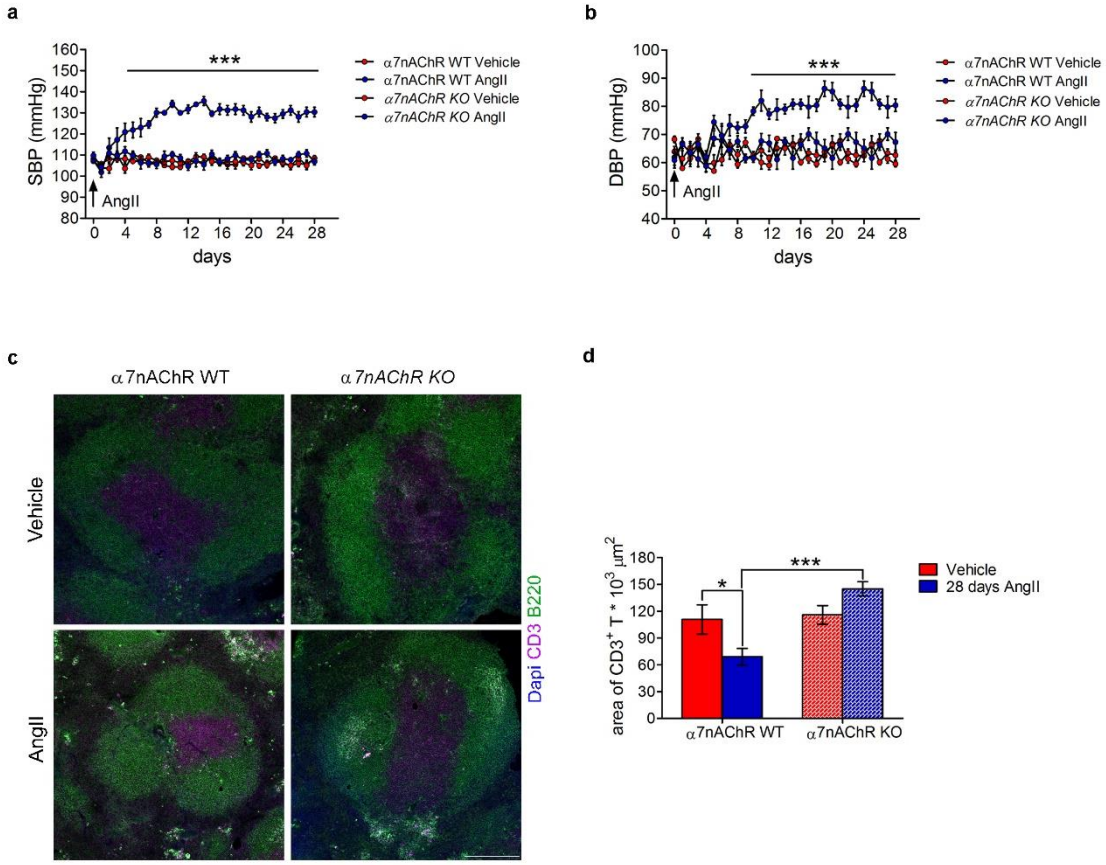

Figure 6: α7nAChR KO mice are protected from AngII-induced hypertension and T cell egression. (a,b) α7nAChR KO mice were protected from hypertension induced by chronic AngII infusion (n_{mice}=8 for each group; two-way ANOVA for repeated measures; (a) SBP, F(interaction)=5.331, ***P<0.001; (b) DBP, F(interaction)=5.087, ***P<0.001). (c) Ablation of α7nAChR was effective in blocking T cell egression on AngII, similarly to vagotomized mice, as evidenced by the area of white pulp, labelled by CD3+ cells (magenta), delimited by B220+ cells (green) of the red pulp (scale bar, 200 µm). (d) Graph showing the relative quantitative analysis (n_{mice}=7 WT vehicle; 8 WT AngII; 6 α7nAChR KO Vehicle; 6 α7nAChR KO AngII; two-way ANOVA, F(interaction)=8.939, *P<0.05 and ***P<0.001).

Splenic nerve ablation prevents immune activation on AngII

To define the relationship between SSNA and blood pressure rising in response to hypertensive stimuli, we established a procedure to denervate selectively splenic nerves (SDN) by thermoablation (Fig. 7a). Our first step was to verify that the procedure itself would not damage the artery. Ultrasound Doppler imaging revealed that SDN did not affect the normal pulse wave of the splenic artery (Fig. 7b). Moreover, microCT angiography after splenic denervation showed splenic artery integrity and consequently normal perfusion of the

spleen (Fig. 7c,d). To evaluate SDN efficacy, we injected a retrograde neurotracer into the spleen to label coeliac ganglion neurons (Fig. 8a). This procedure confirmed interrupted nerve trafficking between the central nervous system and spleen. In addition, tyrosine hydroxylase innervation was markedly reduced in the splenic arteries of SDN mice, as compared with sham (Fig. 8b), as was splenic noradrenaline (Fig. 8c). To demonstrate the selectivity of the procedure for the splenic nerve, we measured ipsilateral kidney noradrenaline content, which was comparable in SDN and sham mice (Fig. 8d), thereby affirming there were no confounding off-target SDN effects.

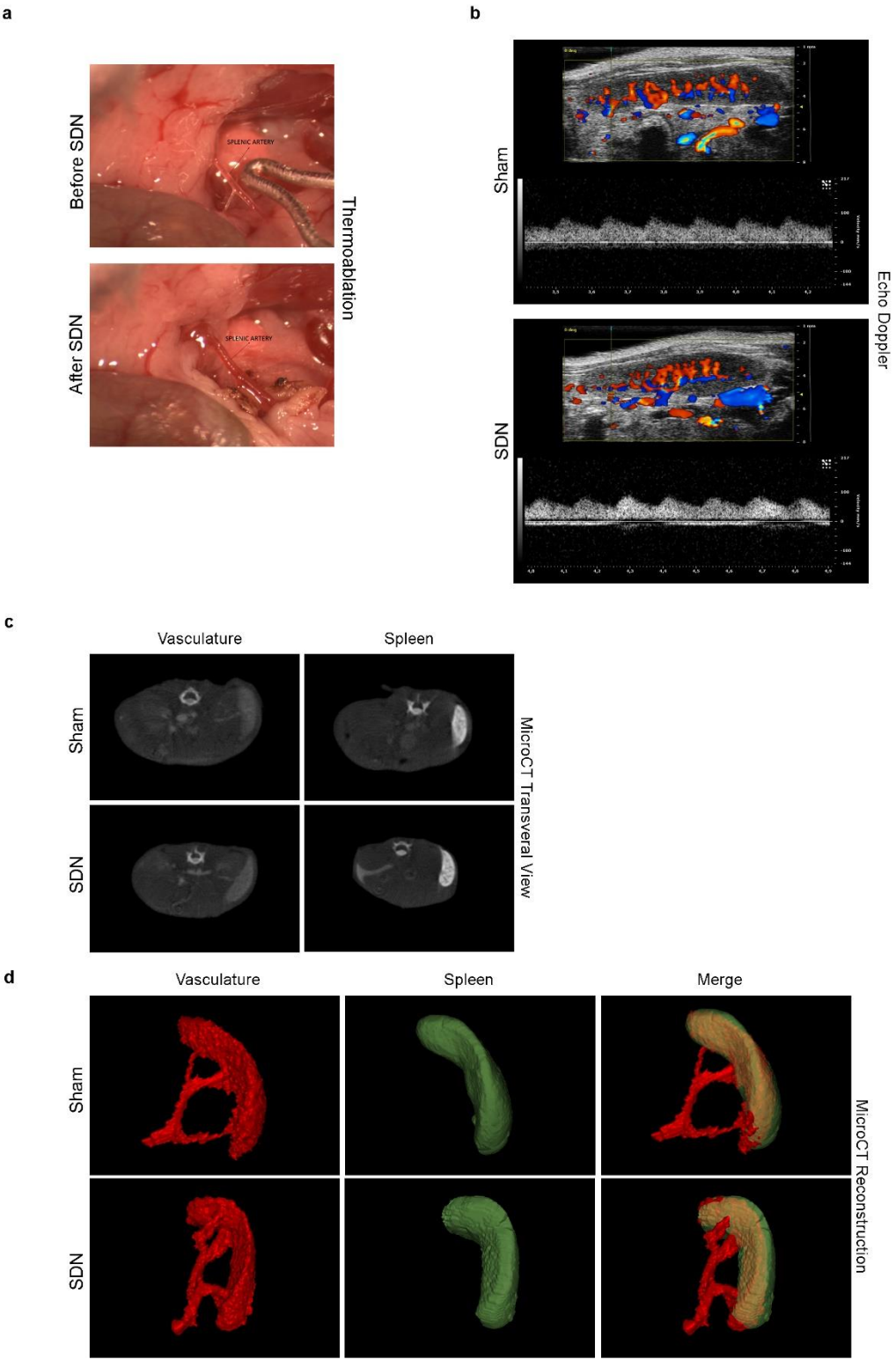

Figure 7: Establishment of a procedure for selective splenic denervation. a) Example of surgical procedure for selective SDN, showing the splenic artery before (upper panel) and after (lower panel) denervation in a representative animal. (b)

Ultrasound Doppler imaging showing a normal pulse wave of the splenic artery in splenic denervated mice, comparable to that of sham. Colour Doppler also indicate a normal perfusion of the spleen after denervation. (c) Anatomical transversal reconstruction of microCT angiography evidencing of correct uptake of the contrast agent in the spleen. (d) 3D reconstruction demonstrating integrity of splenic artery after denervation and consequent normal perfusion of the spleen.

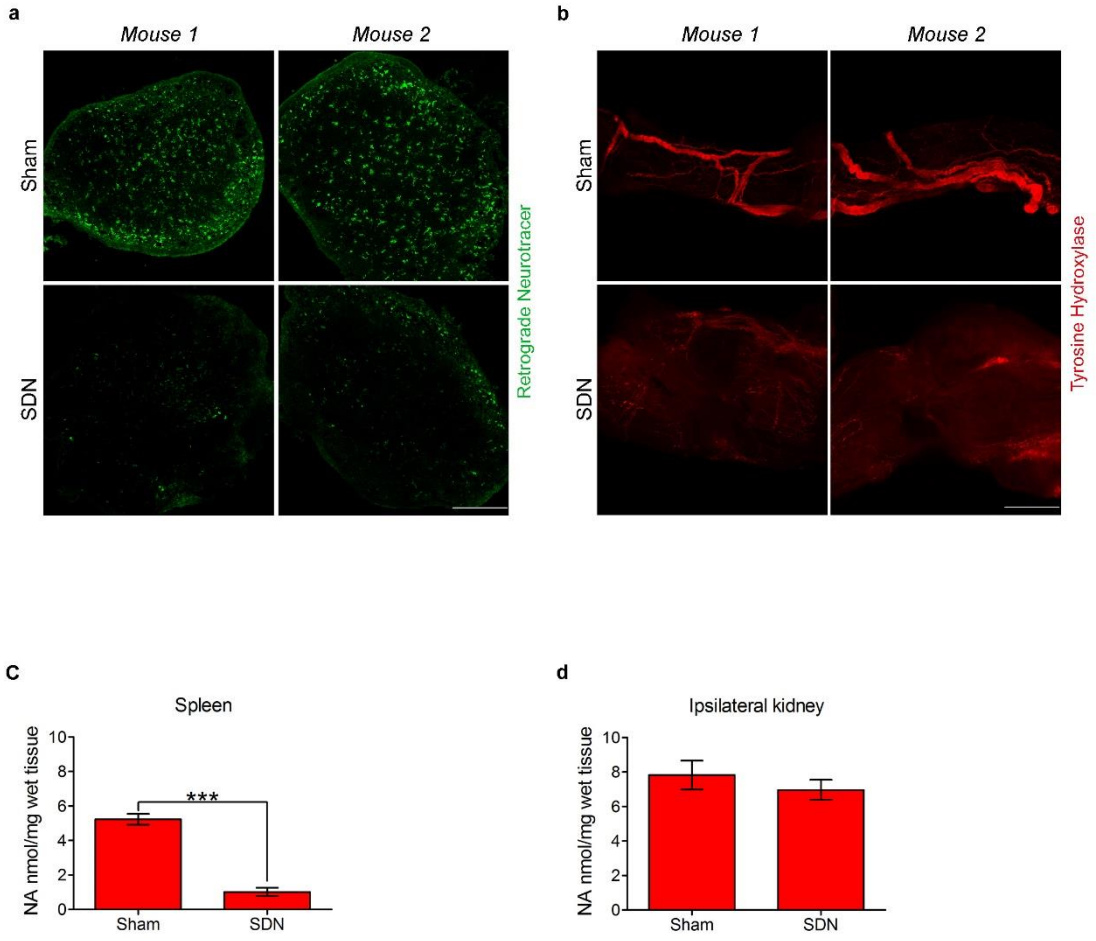

Figure 8: Selective splenic denervation blocks sympathetic nervous system in the spleen. (a) Coeliac ganglion neurons, labelled with a retrograde neurotracer injected in the splenic parenchyma, are significantly reduced in SDN mice as compared with sham controls. (n_{mice}=6 for each group; scale bar, 200 µm). (b) Significant reduction of tyrosine hydroxylase immunofluorescence in splenic artery of two representative SDN as compared with Sham mice (n_{mice}=6 for each group; scale bar, 50 µm). (c) Noradrenaline levels were significantly reduced in the spleen of SDN mice as compared with Sham mice (Sham and SDN groups n_{mice}=8; independent samples Student's t-test, t(14)=10.606, ***P<0.001). (d) Analysis of noradrenaline content in the ipsilateral kidney was unaltered in SDN mice as compared with Sham, revealing no off-target effect of the procedure (Sham and SDN groups n_{mice}=8; independent samples Student's t-test, t(14)=0.853, P=0.408).

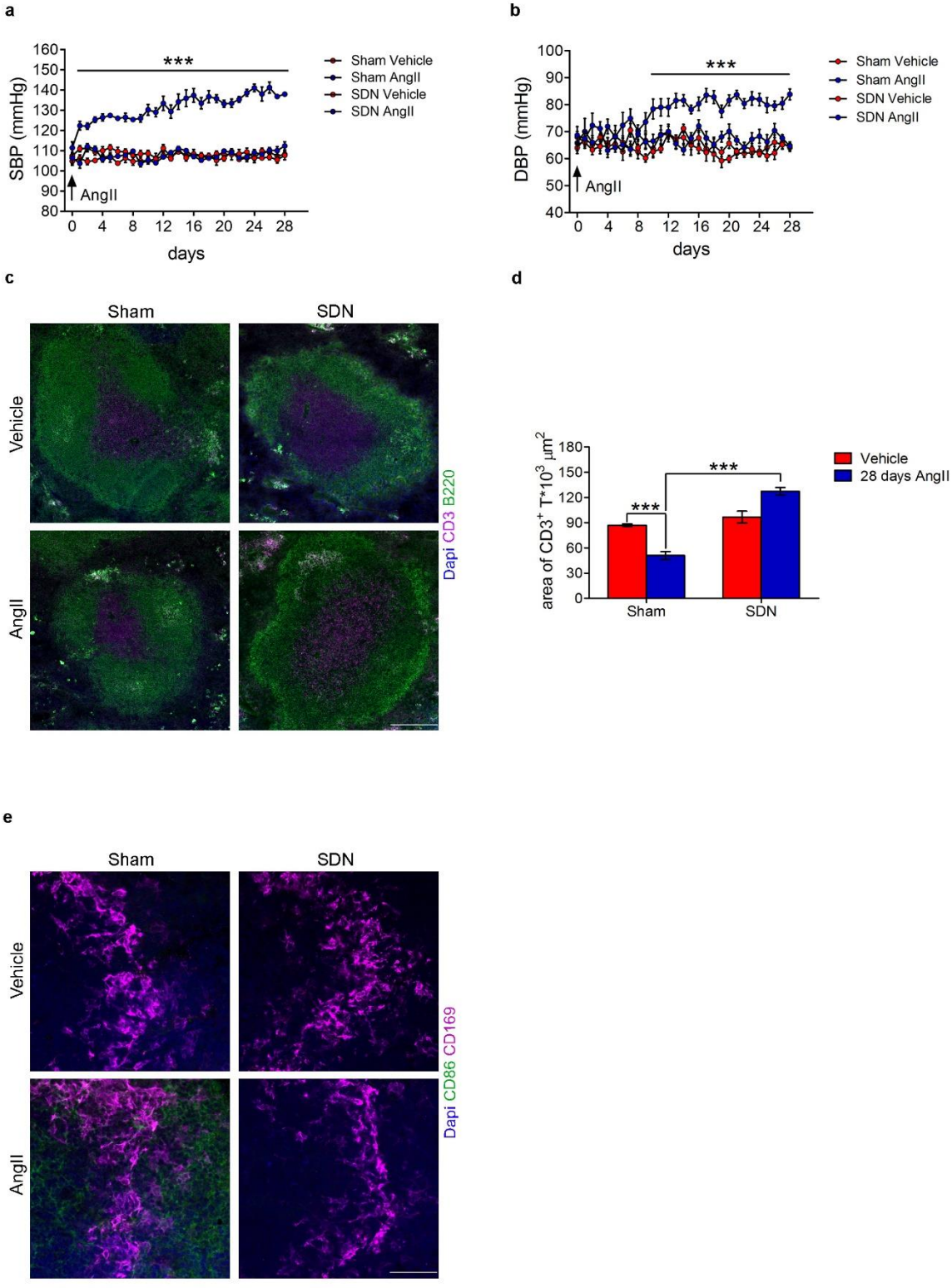

Figure 9: Splenic denervation protects from hypertension and T cell egression from spleen. (a,b) Mice with splenic denervation were protected from AngII-induced hypertension, as compared with Sham mice and SDN mice with vehicle alone (Sham-vehicle, Sham-AngII and SDN-vehicle n_{mice}=10; SDN-AngII n_{mice}=11; two-way ANOVA for repeated measures; (a) SBP, F(interaction)=6.723, ***P<0.001; (b)

DBP, F(interaction)=3.070, ***P<0.001). (c) Mice with splenic denervation are protected from the T cell egression induced by AngII, as evidenced by the area of CD3+ cells (magenta), recognizing white pulp and delimited by B220+ cells (green) delineating red pulp (n_{mice}=5 for each group; scale bar, 200 µm). (d) Graph showing the relative quantitative analysis (n_{mice}=5 for each group; two-way ANOVA, F(interaction)=46.384, ***P<0.001). (e) AngII fails to induce co-stimulation of T cells in mice with splenic denervation, as evidenced by reduced CD86+ cells (green) expression in the marginal zone of the spleen, labelled by CD169+ cells (magenta) (n_{mice}=5 for each group; scale bar, 50 µm).

Next, we infused SDN and sham mice with AngII for 28 days using osmotic minipumps to elevate sympathetic nervous system activation in the spleen, as shown by increased tyrosine hydroxylase staining (Supplementary Fig. 7a). SDN mice were protected from elevated sympathetic nervous system activity in the marginal zone of the spleen, delineated by the CD169 antigen (Supplementary Fig. 7a). More importantly, SDN mice were significantly protected from the increased blood pressure induced by chronic AngII that is typically observed in sham mice (Fig. 9a,b; Supplementary Fig. 7b,c). Similar results were obtained with both radiotelemetry (Supplementary Fig. 7b,c) and tail-cuff measurements (Fig. 9a,b). We then asked whether this effect could be due to a modulating function of SSNA on splenic T cells, which are known to be activated by hypertensive challenges, before deployment toward target organs[5,6,7]. SDN hampered AngII-induced T cell egression from the splenic reservoir, as shown by the total CD3+ T cell content and area in the white pulp (Fig. 9c,d). Indeed, AngII infusion did not reduce T cell content in mice with SDN but did in sham mice (Fig. 9c,d). We also evaluated whether the lack of T cell egression could be caused by failed T cell co-stimulation activation in the absence of an intact splenic nerve. Mice with SDN were protected from AngII-induced CD86 expression (Fig. 9e), the typical hallmark of T cell co-stimulation and hence a key indicator of full activation for target organ colonization in hypertension[6,7]. We next assessed T cell infiltration in target organs by flow cytometry and found that AngII-SDN mice were significantly protected from CD8+ T cell infiltration in the aorta (Fig. 10a) and kidneys (Fig. 10b,c) in terms of both total cells and the number of cells primed with markers for homing (CD8+ CD44+ cells) and activation (CD8+ CD69+ cells). Similar results were found for CD4+ T cell infiltrates (Fig. 10a–c). These data were also confirmed by immunohistochemical analyses of the aorta (Supplementary Fig. 8a–d) and kidneys (Supplementary Fig. 9a–d).

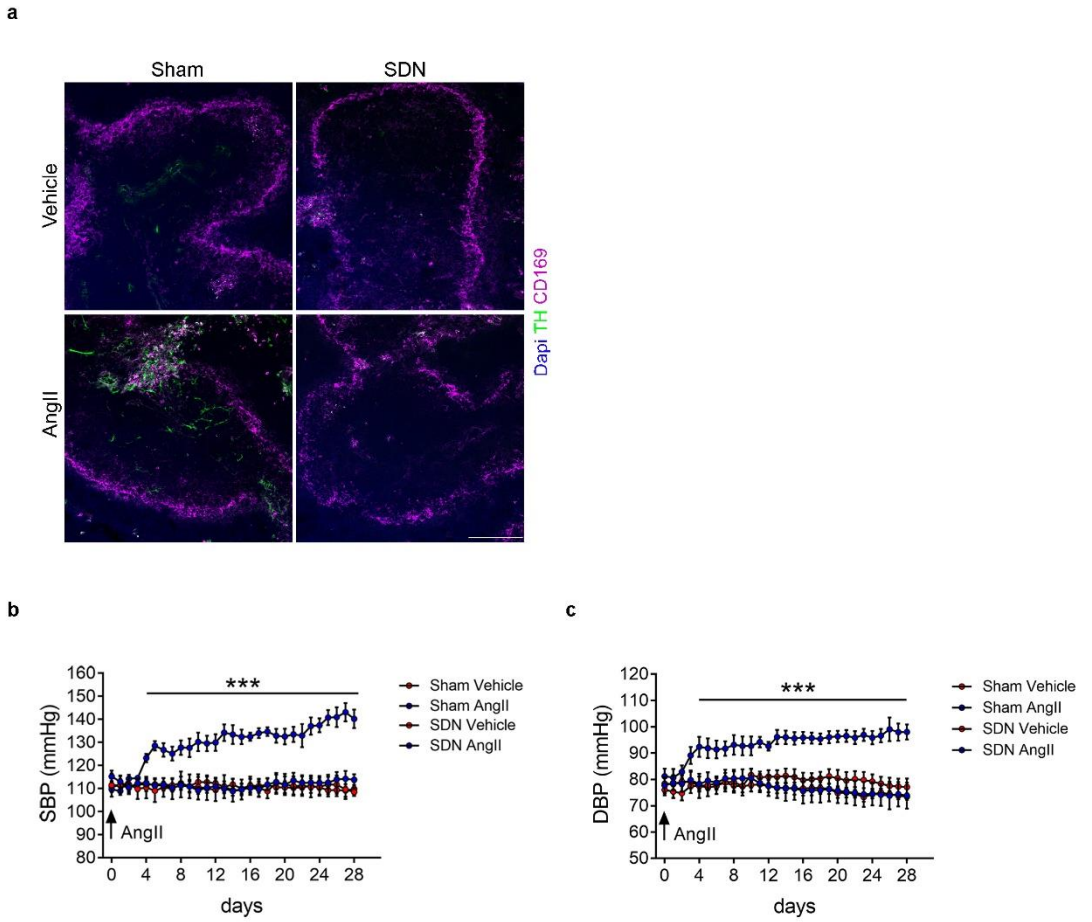

Supplementary Figure 7. Splenic denervation protects from the activation of noradrenaline synthesis and blood pressure raising induced by AngII. (**a**) A representative immunofluorescence of tyrosine hydroxylase staining (green) and CD169^{+} cells (magenta), delineating the splenic marginal zone, shows the loss of sympathetic fibers in mice subjected to splenic denervation as compared to Sham (n_{mice}=6 for each group; scale bar, 200 μm). (**b**,**c**) Radiotelemetric blood pressure measurement further indicating that splenic denervation protects mice from AngII induced hypertension (n_{mice}=6 for each group; Two-way ANOVA, (**b**) Systolic Blood Pressure SBP $F_{(interaction)}$ = 11.436, ***p<0.001; (**c**) Diastolic Blood Pressure DBP $F_{(interaction)}$ = 7.217, **p<0.01 and ***p<0.001).

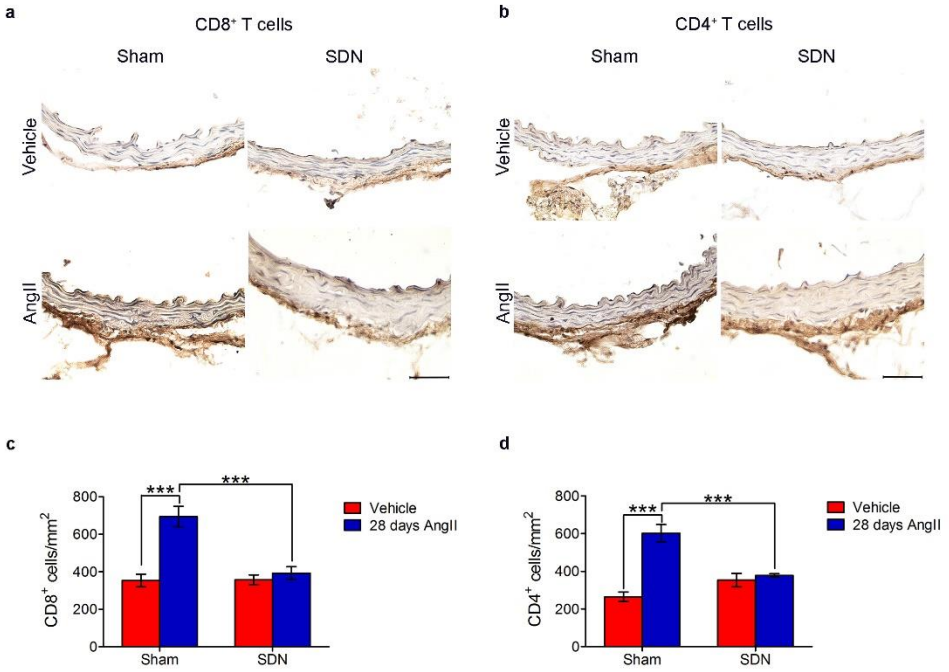

Supplementary Figure 8. Splenic denervation protects from the T cells infiltration typically observed in aortas of mice infused with AngII for 28 days, as revealed by immunohistochemistry. (a-d) Representative immunohistochemistry (**a,b**) and quantitative analysis (**c,d**) of $CD8^+$ and CD4 T cells in SDN and sham mice infused with AngII or Vehicle for 28 days (n_{mice}=6 for each group; Two-way ANOVA, CD8 $F_{(interaction)}$ = 15.40, ***p<0.001; CD4 $F_{(interaction)}$ = 23.79, ***p<0.001). Scale bar, 50 μ m.

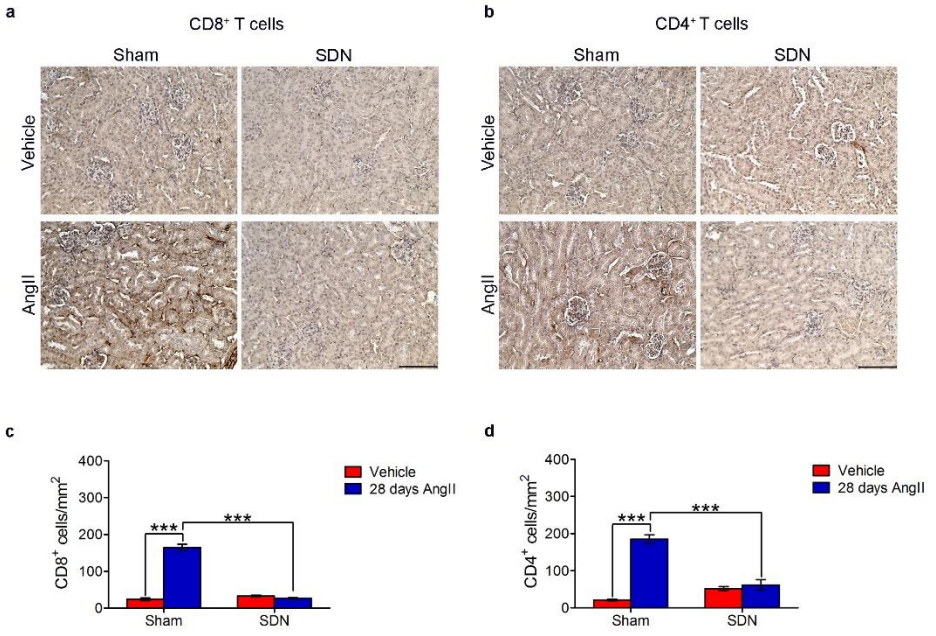

Supplementary Figure 9. Splenic denervation protected kidneys from infiltration of T cells induced by chronic AngII, as revealed by immunohistochemistry. (a-d) Representative immunohistochemistry (**a,b**) and quantitative analysis (**c,d**) of $CD8^+$ and $CD4^+$ T cells in SDN and sham mice infused with AngII or Vehicle for 28 days (n_{mice}=6 for each group; Two-way ANOVA, CD8 $F_{(interaction)}$ = 225.4, ***p<0.001; CD4 $F_{(interaction)}$ = 65.01, ***p<0.001). Scale bar, 100 μm.

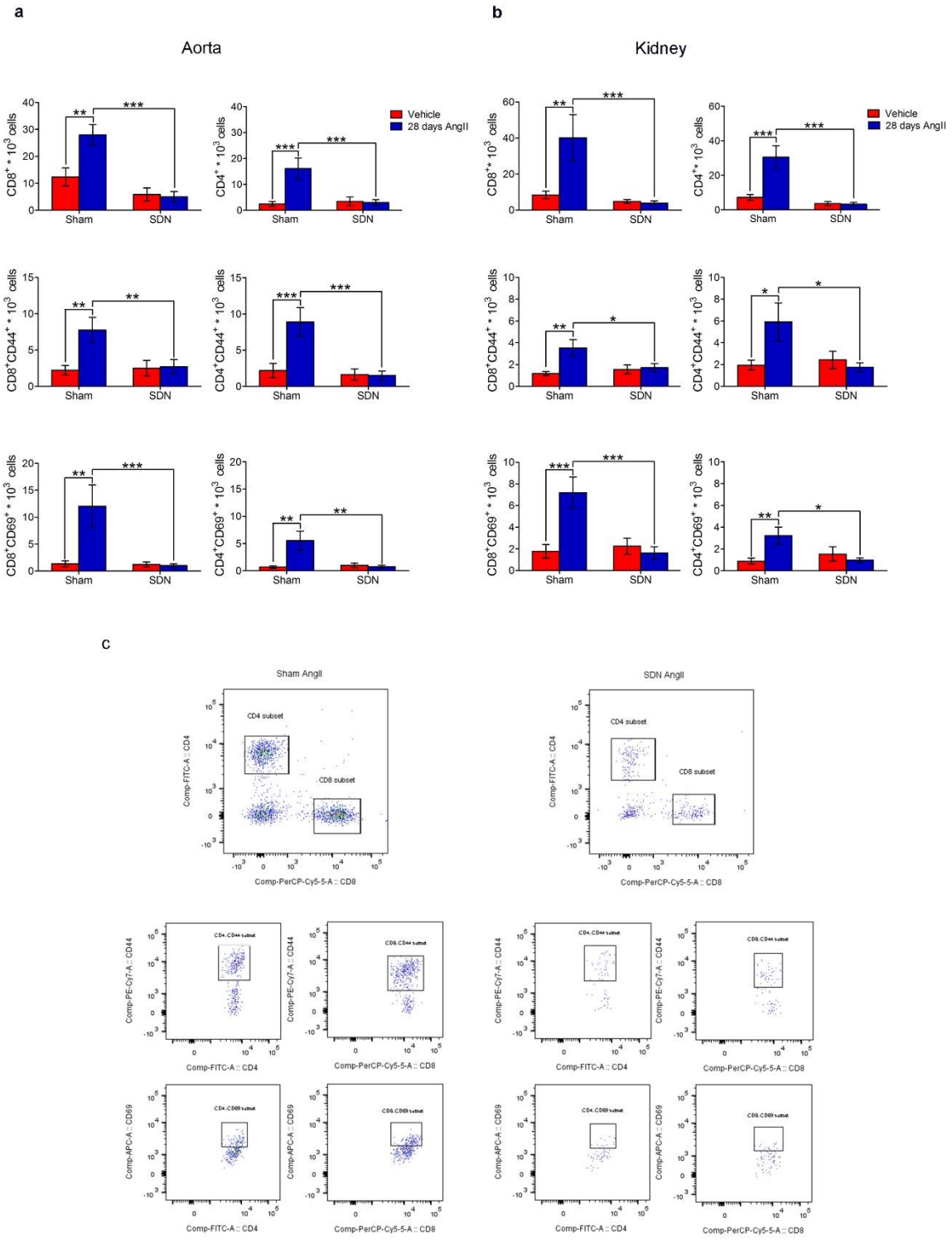

Figure 10: Splenic denervation protects from the T cells infiltration in target organs of hypertension. (a,b) Flow cytometry analysis shows that SDN mice were protected from the AngII-induced increase of total CD8+ and CD4+ T cells (upper panels) in aorta (a) and (b) kidneys. SDN mice displayed also a reduced amount of cells positive for homing (CD44) and activation (CD69) antigens (middle and lower panels, respectively) (n_{mice}=9 for each group). Significance of two-way ANOVA was

as follow for aortas: CD8 F(interaction)=7.922, CD8-CD44 F(interaction)=5.071, CD8-CD69 F(interaction)=7.344, CD4 F(interaction)=9.122, CD4-CD44 F(interaction)=7.867, CD4-CD69 F(interaction)=8.432. Significance of Two-way ANOVA was as follow for kidneys: CD8 F(interaction)=13.88, CD8-CD44 F(interaction)=5.382, CD8-CD69 F(interaction)=7.202, CD4 F(interaction)=6.248, CD4-CD44 F(interaction)=3.810, CD4-CD69 F(interaction)=10.89. *P<0.05, **P<0.01 and ***P<0.001. (c) Representative plots and gating strategies are shown for kidneys.

Discussion

Our results demonstrate that hypertensive challenges exploit a cholinergic-sympathetic drive, realized through a vagus-splenic nerve connection, to activate the T cells that eventually migrate to target organs and contribute to blood pressure regulation. We show that stimuli like chronic AngII and DOCA, which are sensed by the circumventricular organs in the brain to induce hypertension[19,23], activate potent splenic nerve discharge. We also report that SSNA depends on an intact vagus nerve efferent that terminates in the coeliac plexus ganglia where the catecholaminergic fibres of the splenic nerve originate. We further demonstrated that the vagal-coeliac-splenic nerve connection regulating blood pressure is mediated by α7nAChR, similar to dynamics previously described in endotoxemia[26]. Taken together, our findings—particularly our selective denervation of the splenic nerve—have important translational implications. Mice with splenic denervation were protected from hypertension through impeded T cell activation, egression from the spleen and consequent infiltration of target organs. These results provide a rationale for investigating novel therapeutic strategies based on splenic denervation to treat hypertension.

Historically recognized as a crucial player in hypertension, the sympathetic overdrive promotes the initial blood pressure surge in the early clinical stages of the disease and helps maintain elevated blood pressure levels[3,10]. Moreover, constant adrenergic overactivation is known to contribute, over time, to end-organ damage caused by chronic hypertension and metabolic abnormalities often observed in hypertensive patients. Researchers have sought to understand the mechanisms and effects of renal sympathetic nerves in hypertension[31]. Indeed, it is now widely accepted that, under hypertensive conditions, this system changes in pathological ways that contribute to alterations in sodium reabsorption and thus negatively influence blood pressure control[3,10,31]. Yet the results of clinical trials on renal denervation remain controversial[11,12,13], lending support to the hypothesis that there may be other mechanisms contributing to the impact of constant sympathetic overactivation in hypertension. Hence, we sought to pursue selective splenic denervation to decipher the immune system's role in hypertension. Although a simple neurectomy could in principle prove

the same concepts and provide results, selective denervation obtained by thermoablation has clinical potential for patients for whom the renal denervation has failed. Our results strongly suggest splenic denervation may be a useful tool in treating resistant hypertension in humans.

Abundant research has confirmed that the immune system plays a key role in hypertension. Yet the process by which a hypertensive challenge signals the immune system has remained largely unclear. Intriguingly, even as researchers in the field of hypertension began dissecting the role of the immune system, immunologists of the same period discovered that neural circuits can modulate immune cells[15,32]. Meanwhile, decades of studies focusing on the neurophysiological basis and broader effects of the inflammatory reflex converged on the spleen. Action potentials are transmitted from the vagus nerve to the coeliac ganglion, where the splenic nerve originates, and activated adrenergic splenic neurons can regulate a specific T cell subset in splenic white pulp. In the spleen, we now know, neural signals deal with immunity directly[33,34]. We are beginning to understand the complex relationship between the nervous system and immunity.

As researchers continue to decipher these connections, nervous circuits' largely undiscussed role in blood pressure regulation[10] will become increasingly important. On the basis of our results, it is tempting to speculate that sympathetic overactivity in hypertension has effects beyond the kidney and baroreflexes. The novel concept that the autonomic nervous system can have long-term effects on cardiovascular pathologies through immune system regulation requires us to significantly rethink the role of the autonomic nervous system[14]. Interestingly, it is well known that immune organs, and particularly the spleen, are directly innervated by the sympathetic nervous system[7,35]. In addition, the autonomic system may be a powerful regulator of immunity: although AngII has been shown to be responsible for a variety of actions that may contribute to the development of hypertension, several milestone papers demonstrate that AngII also activates the peripheral sympathetic nervous system and affects immune responses[19]. Intracerebral ventricular AngII infusion increases central sympathetic nerve activation and enhances the immune response in the periphery[36]. These findings are particularly important because they demonstrate that AngII-induced effects on both hypertension and immune system activation are not caused by direct AngII influence on the vasculature and immune cells, thus suggesting that central signals may be integrated by the immune system to drive hypertension.

We believe the results presented in this paper are significant because they reveal, for the first time, a previously unknown sympathetic pathway in hypertension. The brain-to-spleen connection's realization through a cholinergic-sympathetic nervous drive resembles the

cholinergic anti-inflammatory pathway that is protective when activated by electrically stimulating the vagus efferent during endotoxemia[24,25,26,27]. So far, this pathway has been primarily considered a way for the nervous system to modulate immune response to bacterial toxins. More specifically, vagus stimulation during septic shock determines the coupling of cholinergic pre-ganglionic neurons and postganglionic sympathetic nerves, linkages that are ultimately responsible for attenuating splenic TNFα production[24,25,26,27].

α7nAChR has been well characterized as the molecular mediator of the cholinergic anti-inflammatory pathway and therefore integral to the vagus nerve/sympathetic drive in the splenic district[26,34]. Indeed, α7nAChR can be found in several tissues, including the brain, ganglia, immune cells and so on. Our experiments showed that α7nAChR KO mice are protected from AngII-induced hypertension. Because α7nAChR is a demonstrable mediator of the cholinergic anti-inflammatory pathway expressed in cytokine-producing splenic macrophages[25,34] but also integrates the sympathetic and parasympathetic systems in presynaptic neurons of the splenic nerve[26], we sought to understand where α7nAChR acts in hypertension. That α7nAChR KO mice had markedly inhibited AngII-elicited SSNA supported the idea that α7nAChR plays a role in mediating autonomic integration among parasympathetic and sympathetic drives in the coeliac ganglion (upstream from the splenic sympathetic drive). Interestingly, vagus nerve stimulation was recently shown to mediate protection from kidney ischemia-reperfusion injury through α7nAChR in splenocytes[37]. Lastly, our findings highlight the possibility that cholinergic anti-inflammatory pathway activation during endotoxemia may be also hemodynamic and therefore relevant to fighting the hypotensive shock that is one of the fatal complications of sepsis.

Methods

Animals and drugs

All animal handling and experimental procedures were performed according to European Community guidelines (EC Council Directive 2010/63) and the Italian legislation on animal experimentation (Decreto Legislativo D.Lgs 26/2014). All efforts were made to minimize suffering, and the principles of Replacement, Reduction and Refinement (that is, the ‘three Rs’) were applied to all experiments.

C57Bl/6J male mice, aged 8-12 weeks, were purchased from Jackson Laboratory and used in all experiments. Chrna7 (α7nAChR) knockout and WT littermates (stock number 003232, Jackson Laboratory) were used where indicated. Mice were housed in an air-conditioned

room (temperature 21±1 °C, relative humidity 60±10%), with lights on from 06:00 to 18:00, and had sawdust as bedding, pellet food and tap water ad libitum. After surgical procedures, mice were housed in recovery boxes (temperature 37 °C) and carefully monitored for several days.

In acute treatments administered during electrophysiological recordings, mice received Sodium Nitroprusside (SNP; Sigma Aldrich), Phenylephrine (Phe; Sigma Aldrich) and Hexamethonium bromide (Sigma Aldrich) at the dosage indicated in the appropriate section.

A cohort of mice received 0.5 mg kg^{-1} day^{-1} of AngiotensinII (AngII; Sigma Aldrich) or Vehicle (NaCl 0.9%), delivered subcutaneously with osmotic minipumps (model 2004, ALZET)[7]. Another group of mice underwent subcutaneous implantation of a 50 mg pellet of DOCA or placebo as control (Innovative Research of America) without uninephrectomy[23]. Mice were maintained on standard chow with ad libitum access to tap water and 0.15 mol l^{-1} (0.9%) NaCl.

Electrophysiological recording

In the first set of experiments, SSNA was recorded in mice at maximum blood pressure response to either sodium nitroprusside or phenylephrine, and in the next set of experiments, SSNA was recorded three days after receiving either AngII or DOCA-salt. Mice infused with vehicle or implanted with a placebo pellet were used as respective controls. Mice were anaesthetized with 5% isoflurane and subsequently maintained with 1.5–2% (supplemented with 1 l min^{-1} oxygen). Blood pressure was monitored during the entire experiment with a single-pressure catheter (Millar, SPR-100) inserted in the left femoral artery and connected to a pressure transducer (Millar, MPVS ULTRA)[7]. Body temperature was maintained between 37 and 38 °C by a homoeothermic blanket.

An abdominal incision was made and the intestinal tract was carefully moved aside to expose the splenic artery. First, the splenic artery was isolated, and then the splenic nerve was carefully separated from surrounding tissue. A bipolar stainless steel electrode (MLA1214 Spring Clip Electrodes, ADInstruments) was adjusted to the nerve size and gently placed on the splenic nerve, according to previously described procedures[20,21,22,38]. The ground wire was plugged into mouse soft tissues. When optimum recording was obtained, the electrode was covered with silicone gel. SSNA was recorded from the implanted electrode continuously during the next 2 h, as was arterial blood pressure. Mice were then killed by isofluorane overdose, and SSNA was recorded for a further 30 minutes to estimate postmortem residual activity.

The splenic nervous signal was amplified (gain × 10,000) and then sampled at 4 kHz with a digital amplifier (Animal Bio Amp; ADInstruments). The raw signal was filtered at 300–1,000 Hz and expressed as μV. Background noise estimates for the nerve activity trace were based on postmortem recording. Raw splenic nerve activity and blood pressure signals were monitored using a PC that was online during the entire recording. Operators were blinded to the experimental group during recording.

Data were collected using a Power Lab data acquisition system and analyzed with Lab Chart 7 (Spike Analysis Module). Typically, a sympathetic burst was identified as a signal above the threshold determined by the background noise of the postmortem recording. In acute experiments, SSNA counting was measured using a bin time of 5 min at the plateau of blood pressure response after a bolus of sodium nitroprusside (2.5μg g^{-1} of body weight in a volume of 25 μl of saline followed by 50 μl of saline) or phenylephrine (20 μg g^{-1} of body weight in a volume of 25 μl of saline followed by 50μl of saline)[20]. Background noise was recorded after ganglionic blockade with hexamethonium[20] (50 μg g^{-1} of body weight in 25μl) and during postmortem. In chronic experiments, SSNA counting was performed using a bin time of 10 min and collected every 20 min. Firing frequency was measured as the mean value of total number of spikes in a time bin. The amplitude gain was calculated as the ratio between mean spike amplitude and spike identification threshold in a time bin.

Vagotomy

Surgical cervical unilateral vagotomy was performed via a cervical midline incision that exposed the left vagus trunk, which was cut with forceps. Coeliac vagotomy was performed with the same procedure, cutting the distal end of the coeliac branch of the vagus nerve. In a first set of experiments, both procedures were executed while recording SSNA. Vagus nerve was exposed while preparing the mouse for the electrophysiological recording. After the acquisition of two SSNA time bins, the cervical or coeliac vagus nerve was transected, while SSNA recording continued for at least two additionally time bins. In a second group of mice, coeliac vagotomy was performed and AngII minipumps implanted subcutaneously for chronic experiments.

Splenic denervation

After anaesthesia with isoflurane (2–5 Vol%), supplemented with 1 l min^{-1} oxygen, the mouse abdominal cavity was opened and the splenic artery was carefully exposed. The selective SDN was performed by thermoablation applied with a thermal cautery (GEIGER Medical

Technologies). The cautery was gently placed on the splenic artery for 5–6 s until the splenic artery was dilated. In sham-operated mice, the abdomen was opened and the splenic artery was exposed, but thermoablation was not performed.

Neurotracer injection

The efficacy of splenic nerve ablation was evaluated by neuronal labelling, obtained by retrograde transport, in coeliac ganglion. Mice were anaesthetized with isoflurane (2–5 Vol%), the spleen was exposed through a left flank incision and 10 injections of 2 μl hydroxystilbamidine, methanesulfonate 2% (Molecular Probes, H22845) were injected into the parenchyma[7]. Mice were allowed to recover, and seven days later they were deeply anaesthetized so that coeliac ganglia from each side could be collected.

Blood pressure measurements

Arterial blood pressure was monitored by radiotelemetry where indicated. HD-X11 pressure transmitters (Data Sciences International) were implanted in mice anaesthetized with isofluorane. The pressure-sensing catheter was inserted into the aortic arch, and the transmitter body was placed in a subcutaneous pouch on the back. Following surgery, the mice were allowed to recover for at least 1 week. Radio signals from the implanted transmitter were captured by the Physiotel RPC-1 receiver (Data Sciences International), and the data were stored online using the Dataquest Ponemah 4.9 data acquisition system (Data Sciences International) according to standardized procedures[7,39,40]. BP was recorded daily for 2 h (10am-12pm) to monitor the effects of AngII.

Noninvasive blood pressure measurement was performed by tail-cuff plethysmography (BP-2000 Series II, Visitech Systems) in conscious mice daily for 2 hours (10 am–12 pm)[7,39,40]. Operators were blinded to the experimental group during blood pressure monitoring.

In vivo imaging

Ultrasound analysis was performed with Vevo 2100 (VisualSonics, Toronto, Canada) equipped with 40MHz transducer, as previously described[7]. Mice were anaesthetized with isoflurane anaesthesia system (5 Vol% induction, 1.5 Vol% maintenance supplemented with 1 l min^{-1} oxygen) and taped to a warmed bed, positioned on the right side. The spleen area was shaved, and the probe was positioned under the chest to get a longitudinal view of the spleen. To visualize splenic artery perfusion and function after splenic denervation, PW

Doppler was applied in order to measure peak flow velocity. Colour Doppler was applied to images of the spleen to verify organ perfusion after splenic denervation.

MicroCT scanning was performed with SKYSCAN 1178 (SKYSCAN, Kontich, Belgium), as previously described[7]. The tube parameters were set to 50 kV and 615 μA, exposure 480 ms, with a rotation step of 0.360°. Mice were anaesthetized with ketamine-xylazine and positioned on the bed. Two different scans were performed: the first scan occurred immediately after contrast agent injection (ExiTron nano 12,000, 100 μl per mouse) to determine vascular perfusion; after 24 h, the second scan was performed to obtain a spleen tissue image using contrast agent accumulation in the spleen. Spleen reconstruction was performed with 3D Slicer[41]. In both scans, the image was cropped to the spleen region, then the images were co-registered with an affine transformation. The co-registered images were labelled and 3D rendered to highlight the vascularization in the first scan (shown in red) and contrast tissue absorption (shown in green) in the second scan.

Tissue isolation

At the end of each experiment, tissues were isolated for subsequent analyses. The splenic artery was isolated and fixed with 4% paraformaldehyde (PFA). Spleen and aorta were collected and embedded in OCT for cryo-sectioning. Kidneys were explanted and embedded in paraffin for immunohistochemistry. Coeliac ganglion was post-fixed in Zamboni's Fixative and embedded in OCT for cryo-sectioning. For biochemical analyses, spleen and kidneys were explanted and flash-frozen in liquid nitrogen.

Flow cytometry

After mice were exsanguinated, both kidney and aorta were collected. Kidney cell suspension was obtained by mechanically disrupting two decapsulated kidneys in 10 ml of RPMI 1640 medium (GIBCO, Invitrogen) supplemented with 5% FBS, which was then passed through a 70 μm sterile filter (Falcon, BD). The resulting cell suspension was centrifuged at 300g for 10 min to pellet the cells. To isolate leukocytes from cell suspension, the pellet was suspended in 36% Percoll (Sigma), gently overlaid onto 72% Percoll and centrifuged at 1,000g for 30 min at RT. Cells were isolated from Percoll interface and washed twice in medium at 300g for 10 min at 4 °C. Aorta cell suspension was obtained by mechanically disrupting the tissue and digesting the suspension in Digestion Cocktail (450 U ml^{-1} Collagenase I, 125 U ml^{-1} Collagense XI, 60 U ml^{-1} Hyaluronidase I-S) for 40 min at 37 °C with gentle vortexing. Cell

suspension was then passed through a 70 μm sterile filter (Falcon, BD), and the resulting cell suspension was centrifuged at 300g for 5 min to pellet the cells.

Lymphocytes from both organs' leukocytes were enriched with Mouse T Lymphocyte Enrichment Set-DM (BD IMag), and the number of the cells was assessed using trypan blue and an automated counter (Countess, Life Technologies). Total kidney and aorta lymphocytes were analyzed with flow cytometry. First, samples were pre-incubated with anti CD-16/32 Fc receptor and then incubated with various combinations of mAbs for immunofluorescence staining using BD FACSCanto (BD Biosciences). The fluorochrome-conjugated mAbs to mouse antigens used for flow cytometry analysis were as follows: PerCP-Cy5.5 anti-CD8a (53-6.7), FITC anti-CD4 (RM4-5), APC anti-CD69 (H1.2F3), APC-Cy7 anti-CD45 (30-F11), PE-Cy7 anti-CD44 (IM7) (1:100; BD PharMingen). The data were analyzed using FlowJo Software (V 10.0.8).

Immunofluorescence analysis

Splenic arteries used for immunofluorescence analysis were fixed with 4% PFA, passed in PBS for incubation with antibodies and then coverslipped with anti-fading medium (DABCO, Fluka). For coeliac ganglion and spleen, 25 μm sections were obtained with cryostat microtome. Coeliac ganglions were directly mounted and coverslipped for analysis of neurons labelled with retrograde fluorescent neurotracer. Slides from the spleen were post-fixed in PFA (4%) for 15 min and processed for staining.

The following primary antibodies were used: Sheep anti-tyrosine hydroxylase (1:800; AB1542, Millipore); Rat anti-CD169 (1:200; MCA884, Serotec); Hamster anti-CD3 (1:100; MCA269OT, Serotec); Rat anti-CD45R/B220 (1:50; 550286, BD Pharmigen); Rabbit anti-CD86 (1:100; NB110-55488, Novus Biologicals). Sections were incubated with their respective secondary antibodies conjugated to Alexa Fluor 488 or Cy3 (1:200; Jackson Immunoresearch). Slides were then coverslipped with DAPI-containing medium (Vector).

All coverslipped, mounted tissue sections were scanned using a Zeiss 780 confocal laser-scanning microscope, as previously described[7]. A 405 Diode laser was used to excite DAPI; a 488 nm argon laser to excite Alexa Fluor 488 and a 543 HeNe to excite Cy3. Quantitative analyses were determined using Image J software (NIH).

Immunohistochemistry analysis

Kidney sections were deparaffinized and rehydrated before undergoing antigen retrieval. Aortas, embedded in OCT, were post-fixed with PFA (4%) for 15 minutes. Slides were processed with the primary antibodies anti-CD8 (1:50; 550286, BD PharMingen) and anti-CD4 (1:50; 550280, BD PharMingen). Samples were incubated with biotinylated secondary antibodies (1:200; Vector) and then processed with DAB (Vector). Hematoxylin (Sigma Aldrich) was used for counterstaining. The number of CD8+ and CD4+ cells per μm^2 was determined using the Image J software Cell Counter plugin analysis tool (NIH). All images were captured using a DMI3000B Leica optical microscope provided by Leica Cameras (Leica Microsystems) and processed with the Leica Application Suite (LAS V3.3).

ELISA for noradrenaline assay

Noradrenaline levels were measured in duplicate for each spleen and kidney sample. Samples were extracted with a buffer containing 0.1 HCl and 1 mM EDTA and assayed using a high-sensitivity ELISA kit (RE59261, IBL International), following the manufacturer's instructions. Results are expressed as nmol mg^{-1} of wet tissue.

Statistical analysis

All the experiments were replicated within the laboratory. Sample size was pre-estimated from the previously published research and from pilot experiments performed in the laboratory. Data are presented as mean±s.e.m. Data distribution was assessed with the Shapiro–Wilk normality test and D'Agostino Pearson test, and assumption of homogeneity of variance was tested using Levene's test of equality of variances. For amplitude gain analysis, unequal variance between groups was observed in a minority of cases, and a Welch correction was performed for all comparisons. Statistical significance was assessed with the appropriate test according to each experimental design, as detailed in figure legends. After confirming that all data had normal distributions, we applied Student t-test for either independent samples or paired samples, according to the experimental design and as specified in the figure legends. Multiple group analysis was performed with two-way ANOVA followed by Bonferroni's post hoc. Analysis for repeated measures was applied when required by the experimental setting. $P<0.05$ was considered significant. Statistical analyses were performed with SPSS 23.0 (IBM Software) and graphs were made with GraphPad Software PRISM5.

References

1. Chobanian, A. V. Time to reassess blood-pressure goals. N. Engl. J. Med. 373, 2093–2095 (2015).

2. Chobanian, A. V. Shattuck lecture. the hypertension paradox—more uncontrolled disease despite improved therapy. N. Engl. J. Med. 361, 878–887 (2009).

3. Coffman, T. M. Under pressure: the search for the essential mechanisms of hypertension. Nat. Med. 17, 1402–1409 (2011).

4. Harrison, D. G. The mosaic theory revisited common molecular mechanisms coordinating diverse organ and cellular events in hypertension. J. Am. Soc. Hypertens. 7, 68–74 (2013).

5. Guzik, T. J. et al. Role of the T cell in the genesis of angiotensin II induced hypertension and vascular dysfunction. J. Exp. Med. 204, 2449–2460 (2007).

6. Vinh, A. et al. Inhibition and genetic ablation of the B7/CD28 T-cell costimulation axis prevents experimental hypertension. Circulation 122, 2529–2537 (2010).

7. Carnevale, D. et al. The angiogenic factor PlGF mediates a neuroimmune interaction in the spleen to allow the onset of hypertension. Immunity 41, 737–752 (2014).

8. McMaster, W. G., Kirabo, A., Madhur, M. S. & Harrison, D. G. Inflammation, immunity, and hypertensive end-organ damage. Circ. Res. 116, 1022–1033 (2015).

9. Zhang, J. & Crowley, S. D. Role of T lymphocytes in hypertension. Curr. Opin. Pharmacol. 21, 14–19 (2015).

10. Malpas, S. C. Sympathetic nervous system overactivity and its role in the development of cardiovascular disease. Physiol. Rev. 90, 513–557 (2010).

11. Symplicity HTN-2 Investigators. et al. Renal sympathetic denervation in patients with treatment-resistant hypertension (the symplicity HTN-2 trial): a randomised controlled trial. Lancet 376, 1903–1909 (2010).

12. Esler, M. D. et al. Catheter-based renal denervation for treatment of patients with treatment-resistant hypertension: 36 month results from the SYMPLICITY HTN-2 randomized clinical trial. Eur. Heart. J. 35, 1752–1759 (2014).

13. Bhatt, D. L. et al. A controlled trial of renal denervation for resistant hypertension. N. Engl. J. Med. 370, 1393–1401 (2014).

14. Abboud, F. M., Harwani, S. C. & Chapleau, M. W. Autonomic neural regulation of the immune system: implications for hypertension and cardiovascular disease. Hypertension 59, 755–762 (2012).

15. Andersson, U. & Tracey, K. J. Neural reflexes in inflammation and immunity. J.Exp. Med. 209, 1057–1068 (2012).

16. Ordovas-Montanes, J. et al. The regulation of immunological processes by peripheral neurons in homeostasis and disease. Trends Immunol. 36, 578–604 (2015).

17. Nahrendorf, M. & Swirski, F. K. Innate immune cells in ischaemic heart disease: does myocardial infarction beget myocardial infarction? Eur. Heart. J. 37, 868–872 (2016).

18. King, A. J., Osborn, J. W. & Fink, G. D. Splanchnic circulation is a critical neural target in angiotensin II salt hypertension in rats. Hypertension 50, 547–556 (2007).

19. Marvar, P. J. et al. Central and peripheral mechanisms of T-lymphocyte activation and vascular inflammation produced by angiotensin II-induced hypertension. Circ. Res. 107, 263–270 (2010).

20. Hamza, S. M. & Hall, J. E. Direct recording of renal sympathetic nerve activity in unrestrained, conscious mice. Hypertension 60, 856–864 (2012).

21. Stocker, S. D. & Muntzel, M. S. Recording sympathetic nerve activity chronically in rats: surgery techniques, assessment of nerve activity, and quantification. Am. J. Physiol. Heart. Circ. Physiol. 305, 1407–1416 (2013).

22. Guild, S. J. et al. Quantifying sympathetic nerve activity: problems, pitfalls and the need for standardization. Exp. Physiol. 95, 41–50 (2010).

23. Hilzendeger, A. M. et al. Angiotensin type 1a receptors in the subfornical organ are required for deoxycorticosterone acetate-salt hypertension. Hypertension 61, 716–722 (2013).

24. Huston, J. M. et al. Splenectomy inactivates the cholinergic antiinflammatory pathway during lethal endotoxemia and polymicrobial sepsis. J. Exp. Med. 7, 1623–1628 (2006).

25. Rosas-Ballina, M. et al. Splenic nerve is required for cholinergic antiinflammatory pathway control of TNF in endotoxemia. Proc. Natl Acad. Sci. USA 105, 11008–11013 (2008).

26. Vida, G., Peña, G., Deitch, E. A. & Ulloa, L. α7-cholinergic receptor mediates vagal induction of splenic norepinephrine. J. Immunol. 186, 4340–4346 (2011).

27. Borovikova, L. V. et al. Vagus nerve stimulation attenuates the systemic inflammatory response to endotoxin. Nature 405, 458–462 (2000).

28. Guo, G. B., Thames, M. D. & Abboud, F. M. Differential baroreflex control of heart rate and vascular resistance in rabbits. Relative role of carotid, aortic, and cardiopulmonary baroreceptors. Circ. Res. 50, 554–565 (1982).

29. Stokes, C., Treinin, M. & Papke, R. L. Looking below the surface of nicotinic acetylcholine receptors. Trends Pharmacol. Sci. 36, 514–523 (2015).

30. Deck, J. et al. α7-Nicotinic acetylcholine receptor subunit is not required for parasympathetic control of the heart in the mouse. Physiol. Genomics 22, 86–92 (2005).

31. DiBona, G. F. & Kopp, U. C. Neural control of renal function. Physiol. Rev. 77, 75–197 (1997).

32. Rosas-Ballina, M. & Tracey, K. J. The neurology of the immune system: neural reflexes regulate immunity. Neuron 64, 28–32 (2009).

33. Peña, G. et al. Cholinergic regulatory lymphocytes re-establish neuromodulation of innate immune responses in sepsis. J. Immunol. 2, 718–725 (2011).

34. Rosas-Ballina, M. et al. Acetylcholine-synthesizing T cells relay neural signals in a vagus nerve circuit. Science 334, 98–101 (2011).

35. Nance, D. M. & Sanders, V. M. Autonomic innervation and regulation of the immune system. Brain Behav. Immun. 21, 736–745 (2007).

36. Ganta, C. K. et al. Central angiotensin II-enhanced splenic cytokine gene expression is mediated by the sympathetic nervous system. Am. J. Physiol. Heart. Circ. Physiol 289, 1683–1691 (2005).

37. Inoue, T. et al. Vagus nerve stimulation mediates protection from kidney ischemia-reperfusion injury through α7nAChR+ splenocytes. J. Clin. Invest. 126, 1939–1952 (2016).

38. Rahmouni, K., Haynes, W. G., Morgan, D. A. & Mark, A. L. Role of melanocortin-4 receptors in mediating renal sympathoactivation to leptin and insulin. J. Neurosci. 23, 5998–6004 (2003).

39. Brancaccio, M. et al. Melusin, a muscle-specific integrin beta1-interacting protein, is required to prevent cardiac failure in response to chronic pressure overload. Nat. Med 9, 68–75 (2003).

40. Zacchigna, L. et al. Emilin1 links TGF-beta maturation to blood pressure homeostasis. Cell 124, 929–942 (2006).

41. Fedorov, A. et al. 3D Slicer as an Image Computing Platform for the Quantitative Imaging Network. Magn. Reson. Imaging 9, 1323–1341 (2012).

8. **Deoxycorticosterone acetate-salt hypertension activates placental growth factor in the spleen to couple sympathetic drive and immune system activation.**

Perrotta M, Lori A, Carnevale L, Fardella S, Cifelli G, Iacobucci R, Mastroiacovo F, Iodice D, Pallante F, Storto M, Lembo G, Carnevale D.

This work was published in Cardiov Res. 8 January 2018. *DOI: 10.1093/cvr/cvy001*

Abstract

Aims. Chronic increase of mineralocorticoids obtained by administration of Deoxycorticosterone acetate (DOCA) results in salt dependent hypertension in animals. Despite the lack of a generalized sympathoexcitation, DOCA-salt hypertension has been also associated to overdrive of peripheral nervous system in organs typically targeted by blood pressure (BP), as kidneys and vasculature. Aim of this study was to explore whether DOCA-salt recruits immune system by overactivating sympathetic nervous system in lymphoid organs and whether this is relevant for hypertension.

Methods and results. To evaluate the role of the neurosplenic sympathetic drive in DOCA-salt hypertension, we challenged splenectomized mice or mice with left coeliac ganglionectomy with DOCA-salt, observing that they were both unable to increase BP. We next evaluated by immunofluorescence and ELISA the levels of PlGF upon DOCA-salt challenge, which significantly increased the growth factor expression but only in the presence of an intact neurosplenic sympathetic drive. When PlGF KO mice were subjected to DOCA-salt, they were significantly protected from the increased BP observed in WT mice under same experimental conditions. In addition, absence of PlGF hampered DOCA-salt mediated T cells co-stimulation and their consequent deployment toward kidneys where they infiltrated tissue and provoked end-organ damage.

Conclusion. Overall our study demonstrates that DOCA-salt requires an intact sympathetic drive to the spleen for priming of immunity and consequent BP increase. The coupling of nervous system and immune cells activation in the splenic marginal zone is established through a sympathetic-mediated PlGF release, suggesting that this pathway could be a valid therapeutic target for hypertension.

1. Introduction

Deoxycorticosterone acetate (DOCA)-salt hypertensive challenge in mice resembles a condition of salt sensitivity, observed in some hypertensive patients and often leading to increased susceptibility to higher BP[1]. Although polydipsia and increased metabolic rate induced by DOCA-salt were considered as major culprits of the resulting hypertensive phenotype, a large body of researches focused the attention on the brain-mediated effects of DOCA-salt[2,3]. It has been reported that the DOCA-salt model, optimal to reproduce low circulating levels of renin–angiotensin system (RAS) activity[4], determines instead a concomitant elevation of brain RAS activity[5-7], thus suggesting the existence of a brain-mediated overactivation of peripheral sympathetic tone. On a different note, it has been reported that DOCA-salt hypertension depends on the activation of adaptive immunity, in a way similar to that observed for angiotensin (AngII)[8]. Thus, despite different in the etiology, AngII and DOCA-salt need mobilization of activated T cells, directed toward target organs of hypertension, particularly to kidneys[9]. While lots of studies focused on immune mechanisms activated during DOCA-salt challenge and participating in the establishment of hypertensive disease[9-12], less is known about how the neurogenic effect of DOCA-salt connects to priming of immunity. In a previous study we found that the angiogenic Placental Growth Factor (PlGF), belonging to vascular endothelial growth factors family (VEGFs), mediates the neuroimmune coupling established in the spleen upon chronic AngII, playing a central role in the increase of BP[13]. It has been described that the activation of RAS activity in the brain exerted by AngII and acting through the AngII type 1 receptors (AT1Rs)[14], was similarly activated by DOCA-salt challenge[7, 15]. In particular it has been shown that, despite lesions of the Subfornical Organ (SFO), a circumventricular organ acting as a sensory brain structure, were not able to prevent DOCA-salt effects on BP[16], a highly selective deletion of AT1aRs in this area attenuated fluid intake and blunted the hypertensive response[7]. Overall these data support the concept that the two hypertensive challenges, despite different in their nature, recruit a common pathway in the brain, which in turn recruit the hypertensive disease. In the most classical meaning, the activation of this pathway in the brain mediates the typical overactivation of the sympathetic nervous system (SNS) in peripheral districts typically controlling BP levels, like kidneys an vasculature[17]. More recently, we also showed that both AngII and DOCA-salt enhanced the sympathetic activity of the splenic nerve (SSNA) through a brain-vagus-splenic circuit[18]. However, it is still unknown whether the two hypertensive hits, with different peripheral mechanisms of action, share common neuroimmune mechanisms in the onset of hypertension. Here we tested the hypothesis that PlGF could mediate DOCA-salt hypertension by coupling nervous and immune systems in the spleen.

2. Methods

2.1 Mice

All the experimental procedures were performed according to European Communities guidelines and the Italian legislation on animal experimentation (Decreto L.vo 26/14). The protocol was approved by the Italian Ministry of Health and by our Institutional Committee. PlGF knock-out (KO) mice were backcrossed for 11 generations in C57Bl/6J mice from the original strain in 50% 129Sv/50% Swiss mice[19]. Wild-type (WT) mice with the same genetic background (C57Bl/6J) were obtained from the KO colony and used as the appropriate control strain. Where indicated, C57Bl/6J mice were used and directly acquired from Charles River. Under anesthesia with isoflurane (2–5 Vol% for induction and 1,5-2 Vol% for maintenance), supplemented with 1 L/min oxygen, PlGF KO and WT control mice or C57Bl/6J mice of 8-12 weeks were subcutaneously implanted with 50 mg of DOCA pellet with a release time of 21 days (Innovative Research of America), as previously described[18.] Control groups of both genotypes received the appropriate placebo pellet (Innovative Research of America). Mice with DOCA were maintained with tap water plus 0.15 mol/L (0.9%) NaCl (DOCA-salt), whereas mice with placebo received tap water alone. All mice were then fed with standard chow diet ad libitum.

2.2 Blood Pressure measurements

Arterial BP was measured by tail cuff and radiotelemetry, accordingly to previously described procedures[13, 18, 20]. Tail cuff plethysmography (BP-2000 Series II, Visitech Systems) was used to daily measure BP, between 8 am and 1 pm. For continuous BP monitoring with radiotelemetry, mice were anesthetized with ketamine (90 mg/kg) and xylazine (10 mg/kg) i.p. and implanted with the pressure sensing catheter of a HD-X11 transmitter, inserted into the aortic arch (Data Sciences International), with the device placed in a subcutaneous pouch on the back of the mouse. After surgery, mice were individually kept in recovery cages (temperature 37 °C). Monitoring of BP started 1 week after surgery and data were recorded for 5 minutes every hour. The basal BP levels were registered for 3 days. Subsequently mice were treated with DOCA-salt or placebo, accordingly to the experimental groups, and BP was monitored for the following 21 days. Radio signals were transmitted to the Physiotel RPC-1 receiver and data were acquired online by the Dataquest Ponemah 4.9 data acquisition system (Data Sciences International). Operators were blinded to the experimental groups during BP measurements.

2.3 Splenectomy and Left Coeliac Ganglionectomy

C57Bl/6J mice were anesthetized with isoflurane (2–5 Vol% for induction and 1,5-2 Vol% for maintenance), supplemented with 1 L/min oxygen, to perform splenectomy or coeliac ganglionectomy (CGX) as previously described[13]. In brief, for splenectomy, the abdominal cavity of mice was opened and splenic vessels were cauterized, before careful removal of the spleen. Sham mice underwent the same surgical procedure to open the abdomen, but without removing the spleen. After surgery mice were individually placed in thermal cages for a recovery period, and then were implanted with DOCA-salt or placebo pellets.

For CGX execution, mice underwent a midline laparotomy and, after the isolation of both aorta and coeliac artery, the left coeliac ganglion was gently removed. In the group of sham mice, both aorta and left coeliac artery were isolated and then the left coeliac ganglion was exposed but without removing it. After surgery, mice were individually placed in thermal cages for the process of recovery, after which mice were implanted with DOCA-salt or placebo pellets. The rate of mortality observed for both procedures ranged from 5% to 10% at maximum and was observable only during or immediately after surgery. In the post-operative period, mice were daily monitored to observe the eventual onset of adverse events, and if this was the case mice were sacrificed.

2.4 Metabolic cages

During the last week of DOCA-salt or placebo protocol, PlGF KO and WT mice were individually housed in metabolic cages (Tecniplast), allowing acclimatization before starting with sampling of urine and plasma. Body weight was measured before and after metabolic cage entry. Mice had free access to tap water added with 0.9% NaCl for DOCA-salt group whereas the placebo group of mice was maintained with tap water alone. Urine and plasma samples were used for assessment of analytes of interests with a clinical analyzer, accordingly to standard protocols.

2.5 Immunofluorescence and immunohistochemistry

For immunofluorescence analysis, the spleen was collected and embedded in OCT. The following primary antibodies were used as previously described13, 18 27 : rat anti-CD169 (1:200; MCA884, Serotec) to identify metallophilic marginal zone macrophages; rat anti-ER-TR7 (1:200; Acris) for fibroblast reticular cells; hamster anti-CD3 (1:100; MCA269OT,

Serotec), labeling T cells; rat anti-CD45R/B220 (1:50; 550286, BD Pharmigen) to mark splenic B cells; rabbit anti-CD86 (1:100; NB110-55488, Novus Biologicals) for identifying mature antigen presenting cells (APC). Sections were incubated with the appropriate secondary antibodies conjugated to Alexa Fluor 488 (excitation wavelength 488 nm, emission wavelength 517 nm) or Cy3 (excitation wavelength 543 nm, emission wavelength 588 nm) (1:200; Jackson Immunoresearch). Slides were then coverslipped with a mounting medium containing DAPI (excitation wavelength 405, emission wavelength 453) (Vector laboratories). Tissue sections were scanned using a Zeiss 780 confocal laser scanning microscope. A 405 Diode laser was used to excite DAPI; a 488 nm argon laser to excite Alexa Fluor 488 and a 543 HeNe to excite Cy3. Quantitative analysis of white pulp area of the spleen was determined using Image J software (NIH), as previously described[18].

For renal damage assessment, kidneys were explanted and embedded in paraffin for immunohistochemistry. Sections of 4 μm were deparaffinized and rehydrated before undergoing antigen retrieval. Slides were processed with the primary antibodies anti-CD8 (1:50; 550286, BD Pharmingen) and anti-CD4 (1:50; 550280, BD Pharmingen) and then incubated with biotinylated secondary antibodies (1:200; Vector laboratories) and processed with DAB (Vector laboratories). Hematoxylin (Sigma Aldrich) was used for nuclei counterstaining. The number of CD8+ and CD4+ cells per μm^2 was determined using the Image J software Cell Counter plugin analysis tool (NIH), as previously described[13,18]. Analyses of renal damage were performed in tissue sections stained with Picrosirius Red, Masson's Trichrome and periodic acid–Schiff (PAS). Images of kidney sections were used to calculate the size of renal corpuscle, glomerular area and Bowman's capsule, and the percentage of renal fibrosis, all by using Image J software (NIH).

All images were captured using a DMI3000B Leica optical microscope provided by Leica Cameras (Leica Microsystems) and processed with the Leica Application Suite (LAS V3.3).

2.6 ELISA for determination of metabolites

PlGF protein levels were determined by a high sensitivity ELISA kit (R&D Systems), as previously described[13]. Flash frozen splenic tissues were extracted with a buffer containing PBS and protease inhibitor cocktail (Sigma Aldrich). Results were expressed as pg of PlGF for mg of wet tissue. Noradrenaline levels were measured by a high sensitivity ELISA kit (IBL International), as previously described[18]. Flash frozen splenic and renal tissues were extracted with a buffer containing 0.1N HCl and 1mM EDTA. Results were expressed as nmol of noradrenaline for mg of wet tissue.

2.7 Flow cytometry

After mice were exsanguinated, both kidneys were collected. Cell suspensions were obtained by mechanically disrupting two decapsulated kidneys in 10 ml of RPMI 1640 medium (GIBCO, 13 Invitrogen) supplemented with 5% FBS, which was then passed through a 70 µm sterile filter (Falcon, BD Biosciences). The resulting cell suspension was centrifuged at 300g for 10 min to pellet the cells.

To isolate leukocytes, the pellet was processed as previously described[13,18] and lymphocytes were enriched from total cell suspension with Mouse T Lymphocyte Enrichment Set-DM (IMag BD Bioscience), and the number of the cells was assessed using trypan blue and an automated counter (Countess, Life Technologies). Cells were analyzed by flow cytometry staining with the following mix of antibodies: PerCP-Cy5.5 anti-CD8a (53-6.7) for identification of CD8 T cells, FITC anti-CD4 (RM4-5) for CD4 T cells, APC-Cy7 anti-CD45 (30-F11) for total leukocytes identification, APC anti-CD69 (H1.2F3), recognizing the early activation marker, and PE-Cy7 anti-CD44 (IM7) (1:100; BD Pharmingen) as an homing marker. Data were analyzed using FlowJo Software (V 10.0.8).

2.8 Statistical Analysis

Sample size was pre-estimated on the basis of previously published research and from pilot experiments. Data distribution was assessed with D'Agostino Pearson test, and assumption of homogeneity of variance was tested using Levene's Test of Equality of Variances. Statistical significance was assessed with the appropriate test according to each experimental design. In details, multiple group analysis was performed with Two-way ANOVA followed by Bonferroni's post hoc and analysis for repeated measures was applied when required by the experimental setting. Data are presented as mean ± SEM. $P<0.05$ was considered significant. Statistical analyses were performed with SPSS 23.0 (IBM Software) and graphs were made with GraphPad Software PRISM5.

3. Results

3.1 DOCA-salt hypertension recruits a sympathetic neural regulation of the spleen

The consolidated notion that hypertension induced by DOCA-salt challenge associates with T cells infiltration in the kidney[8, 9], raised the interest in the search for molecular mechanisms regulating immune system upon this hypertensive hit. Despite immune mechanisms

contributing to renal damage and BP regulation in DOCA-salt hypertension have been proposed[21], we still ignore how lymphoid organs participate in the etiology of the disease. To gain information into this issue, we challenged splenectomized mice with DOCA-salt and measured BP. Mice deprived of the splenic immune system were unable to rise BP upon the salt-sensitive hypertensive stimulus (Figure 1A and B), conversely to what is typically observed in control mice (Figure 1A and B), thus suggesting a relevant role of splenic immune cells in DOCA-salt hypertension. We previously found that splenic nerve activity is sensitive to this hypertensive hit, as reflected by increased firing activity of the nerve early after DOCA-salt administration[18]. Here we found that DOCA-salt induces a precocious increase in the expression of Tyrosine Hydroxylase (TH), the rate limiting enzyme of noradrenaline (NA) in the marginal zone (MZ) of the spleen, defined by CD169+ metallophilic macrophages (Figure 1C and D). In order to ascertain the dependence of this sympathetic input on the nervous drive passing through the coeliac ganglion, we analyzed TH expression in a further group of mice where CGX was performed before DOCA-salt administration. DOCA-salt was unable to induce TH expression in mice subjected to CGX (Figure 1C), being the % of TH stained area in the spleen significantly reduced compared to sham mice subjected to the same challenge (Figure 1 D). This result was further confirmed by the quantitative measurement of NA in the spleen, showing that DOCA-salt increased NA content and that CGX was effective in hampering its induction (see Supplementary material online, Figure S1A). In order to assess the selectivity of this procedure in denervating the spleen without affecting the renal innervation, we also measured the NA content of contralateral kidney, which resulted unaffected (see Supplementary material online, Figure S1B). To add information on the functional relevance of this pathway, we monitored BP response to DOCA salt challenge in a further group of CGX mice, as compared to the sham controls, finding that they were protected from hypertension (Figure 1E and F).

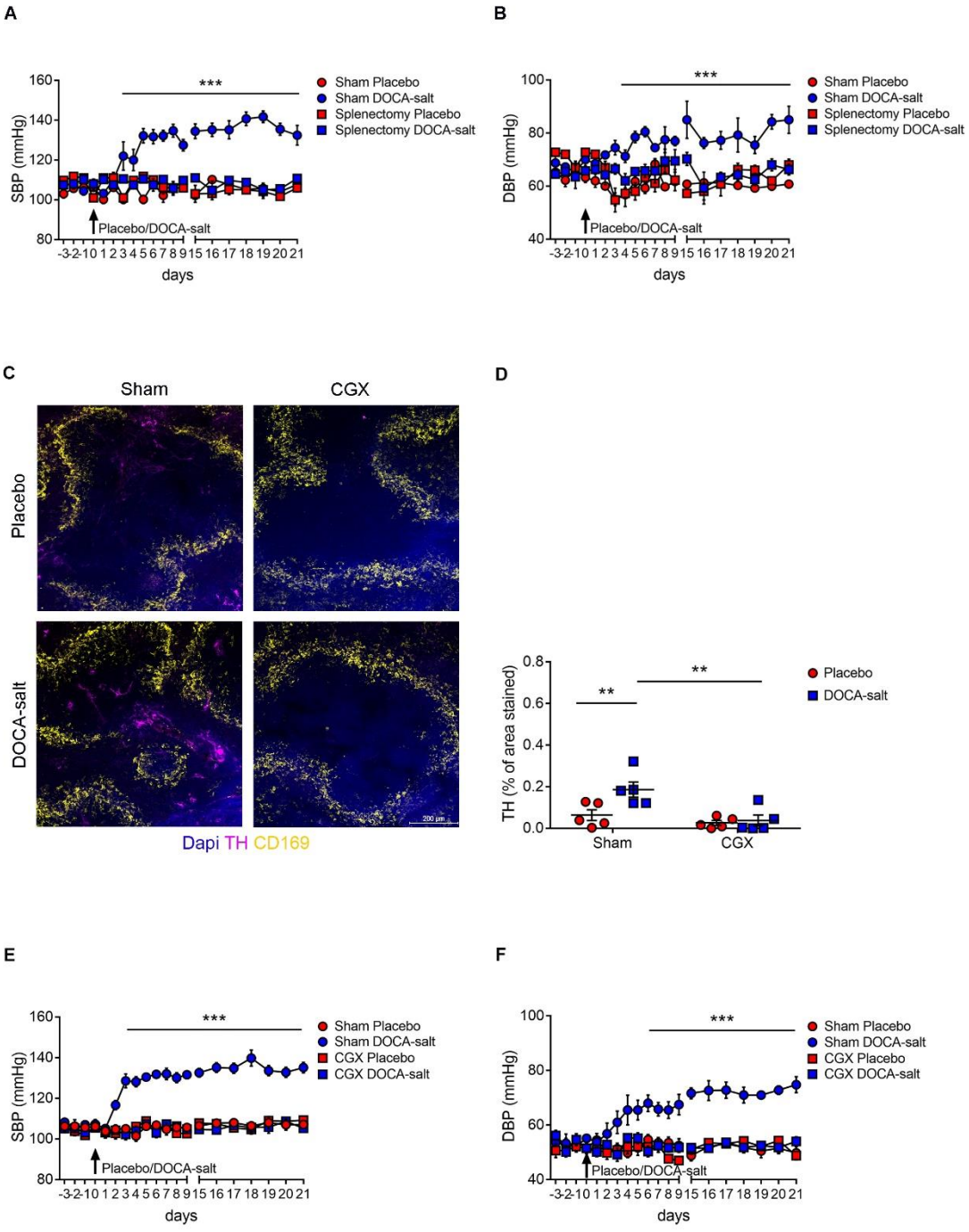

Figure 1. DOCA-salt challenge requires a neurosplenic drive to induce hypertension. (A, B) Tail cuff BP measurements to monitor the response to DOCA-salt, in sham and splenectomized mice, as compared to the placebo treated groups. Panels represent mean ± SEM values of systolic BP (SBP) (A) and diastolic BP (DBP) (B). ***p<0.001 sham DOCA-salt mice vs all the other groups (n=4 mice for each group). (C) Immunostaining of Tyrosine Hydroxylase (TH) (Cy3-conjugated secondary antibody, magenta) in the MZ of the spleen, labeled with anti-CD169 (Alexa488-conjugated secondary antibody, yellow) antibody for metallophilic macrophages, in sham and CGX mice, treated with DOCA-salt or placebo. Images represents n=5 mice for each group; scale bar 200 μm. (D) Graph showing the quantitative analysis of TH expression as % of stained area. **p<0.01. (E, F) Tail cuff BP measurements to monitor the response to DOCA-salt, in sham and CGX mice. Panels represent mean ± SEM values of SBP (E) and DBP (F). ***p<0.001 sham DOCA-salt mice vs all the other groups (n=6 mice for each group).

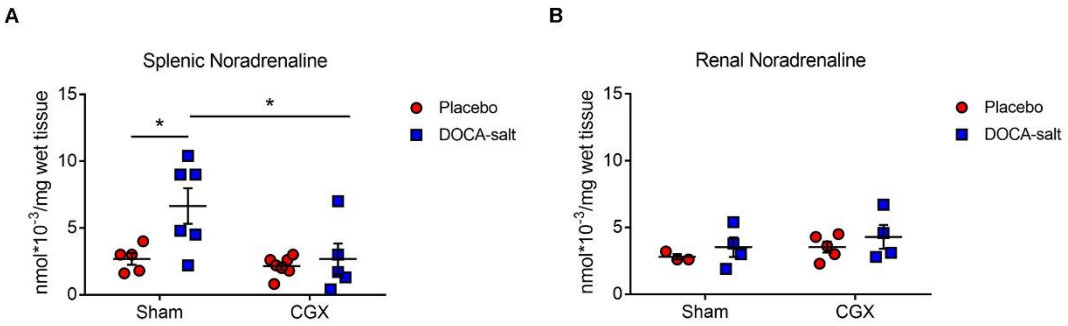

Figure S1. CGX significantly decreased the noradrenaline content in the spleen but not in the ipsilateral kidney after DOCA-salt. (A) Noradrenaline release in the spleen of Sham and CGX mice upon DOCA-salt or placebo expressed as nmol*10^{-3}/mg of wet tissue as determined by ELISA. *p<0.05 (n=5 mice for Sham placebo, n=6 for Sham DOCA-salt, n=7 for CGX placebo and n=5 for CGX DOCA-salt). (B) Noradrenaline release in the ipsilateral kidney from sham and CGX mice upon DOCA-salt or placebo, expressed as nmol*10^{-3}/mg of wet tissue as determined by ELISA (n=3 mice for Sham placebo, n=4 for Sham DOCA-salt, n=5 for CGX placebo and n=4 for CGX DOCA-salt).

3.2 PlGF is critically involved in DOCA-salt-induced hypertension

Previous studies showed that neural modulation of the spleen can have several effects in different pathophysiological contexts[13,18,22] and that the pathway activated by PlGF is crucial in immune functions involved in hypertensive responses to AngII. Thus, we sought to determine whether this pathway could be involved in mediating the response to DOCA-salt. Immunofluorescence analysis showed that DOCA-salt administration significantly induced PlGF expression in the MZ of the WT spleen, marked by the co-staining with CD169 metallophilic macrophages (Figure 2A and B) and ERT-R7 fibroblast reticular cells (see Supplemental material online, Figure S2A), as compared to the basal levels found in mice treated with placebo alone (Figure 2A and B). As expected no signal of staining positive for PlGF was found in PlGF KO mice (Figure 2A and B). To determine whether the activation of PlGF pathway was directly induced in the spleen or mediated by the increased sympathetic splenic drive activated by DOCA-salt, the % of PlGF positive area was also measured in mice subjected to CGX prior to starting the hypertensive challenge. As shown by immunofluorescence and related quantitative analysis, the sympathetic denervation of the spleen hampered PlGF expression upon DOCA-salt (Figure 2A and B). In addition, we quantitatively measured PlGF protein levels, released in the spleen after DOCA-salt challenge, confirming the finding of a sympathetic-dependent release of PlGF upon DOCA-salt (Figure 2C). We next questioned whether this pathway had an impact on the hypertensive

phenotype. Thus, we subjected PlGF KO mice and their WT controls to the 21 days protocol of DOCA-salt administration or placebo and chronically measured BP both by radiotelemetry and tail cuff. The results evidenced an indispensable role of PlGF to allow BP increase upon DOCA-salt challenge (Figure 2D and E, see Supplemental material online, Figure S2B and C). As expected, placebo had no effect on BP of both genotypes (Figure 2D and E, see Supplemental material online, Figure S2B and C).

Data obtained so far, proposed PlGF as a mediator of the neuroimmune drive recruited by DOCA-salt in the spleen. To rule out the possibility that this effect could be due to an impairment of PlGF KO in the activation of the sympathetic splenic drive, we assessed the effects of DOCA-salt on TH expression in the spleen. As shown by immunofluorescence and quantitative analysis of TH positive area in the MZ, there was no difference in the levels of up-regulation of SNS induced by DOCA-salt in PlGF KO mice as compared to WT controls (see Supplemental material online, Figure S3A and B), thus suggesting a local splenic effect of PIGF. Taken together these results support the hypothesis that PlGF is the mediator of the cross-talk established between nervous and immune systems in DOCA-salt hypertension.

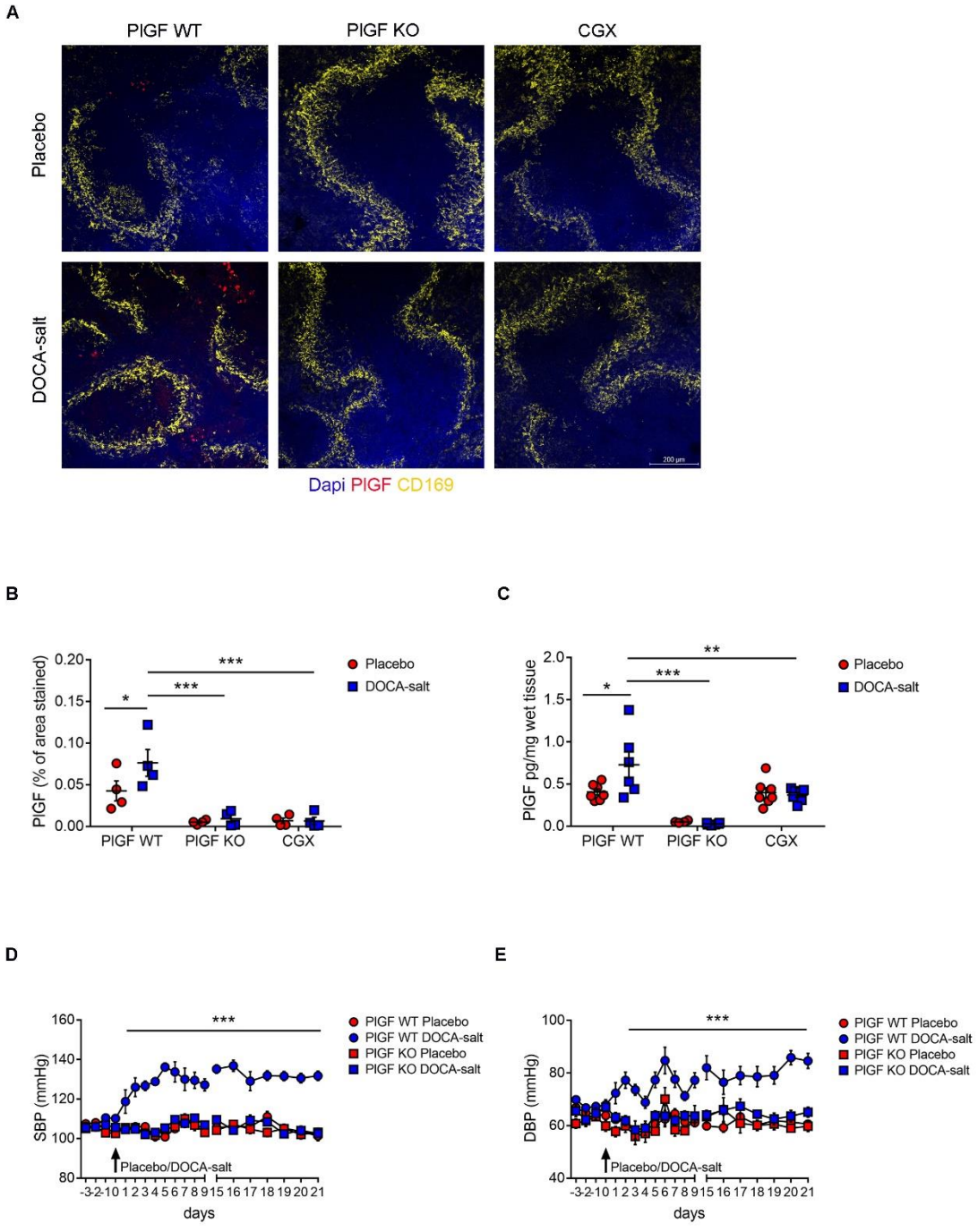

Figure 2. DOCA-salt activates noradrenergic-mediated release of PlGF in the spleen to induce BP increase. (A) Immunostaining of PlGF (Alexa488-conjugated secondary antibody, red) in splenic MZ, labeled with anti-CD169 antibody (Cy3-conjugated secondary antibody, yellow), showing the effect of DOCA-salt on PlGF levels in WT mice, with or without CGX, and in PlGF KO mice as negative control. Images are representative of n=4 mice for each group; scale bar 200 μm. (B) Graph showing the quantitative analysis of PlGF expression as % of stained area. *p<0.05 and ***p<0.001. (C) Quantitative analysis of PlGF protein levels in the spleen of mice treated with DOCA-salt with intact (sham) or denervated (CGX) sympathetic drive.

Levels of PlGF protein in PlGF KO mice are shown as controls. *p<0.05, **p<0.01 and ***p<0.001 (WT: n=7 for placebo and n=6 for DOCA-salt; PlGF KO: n=4 for placebo and n=6 for DOCA-salt; CGX: n=7 for placebo and DOCA-salt). (D, E) Tail cuff BP measurements to monitor the response of PlGF KO to DOCA-salt or placebo, as compared to WT mice. Panels represent mean ± SEM values of SBP (D) and DBP (E). ***p<0.001 DOCA-salt WT mice vs all the other groups (n=8 mice for each group).

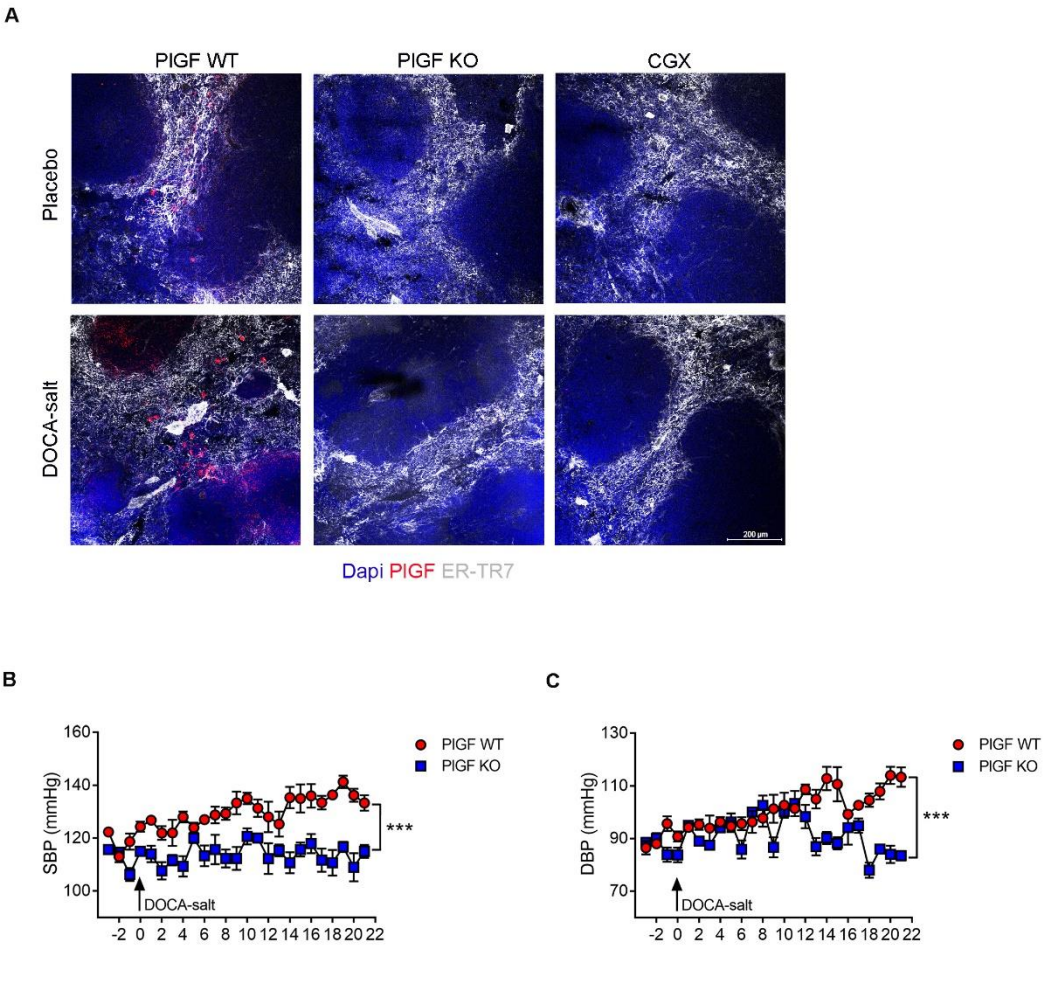

Figure S2. DOCA-salt induces PlGF through noradrenergic fibers in the stromal tissue of the spleen. (A) Immunostaining of PlGF (Alexa488-conjugated antibody, red) in the stromal zone of the spleen, labeled with anti-ER-TR7 antibody (Cy3-conjugated antibody, white), isolated from WT mice with an intact (Sham) or denervated (CGX) splenic sympathetic drive and from PlGF KO mice as negative controls. All groups were treated with DOCA-salt or placebo. Images represent n=4 mice per group; scale bar 200 µm. (B, C) Radiotelemetric monitoring of arterial blood pressure upon DOCA-salt in PlGF KO and WT mice measured for 21-days. Panels represent mean ± SEM values of systolic blood pressure (SBP) (B) and diastolic blood pressure (DBP) (C). ***p<0.001 after DOCA-salt in WT vs PlGF KO mice (n=4 mice per group).

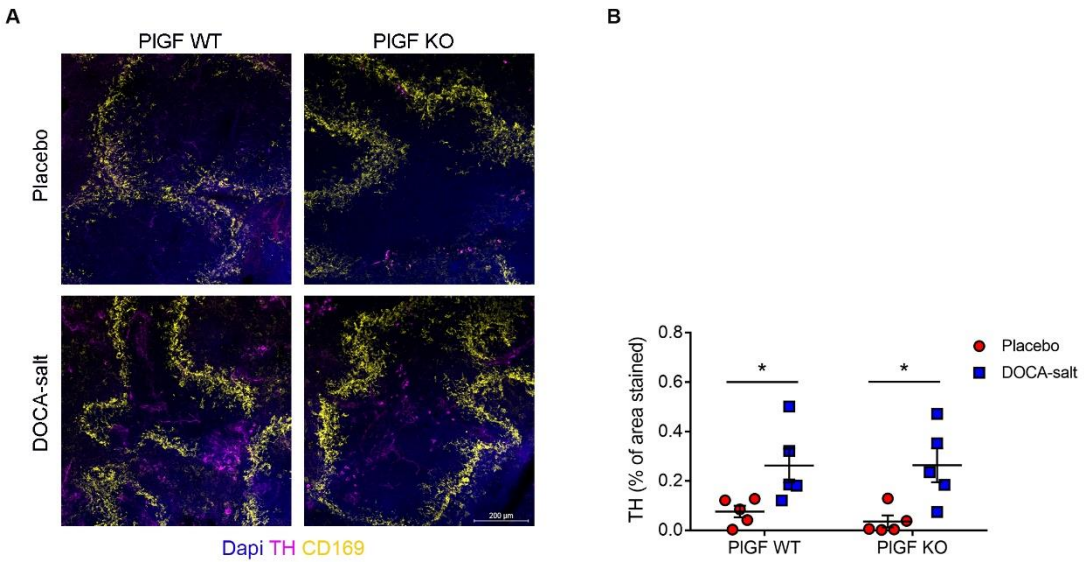

Figure S3. DOCA-salt increases the amount of Tyrosine Hydroxylase (TH) in both PlGF KO and WT mice. (A) Double staining for Tyrosine Hydroxylase (TH) (Cy3-conjugated secondary antibody, magenta) and anti-CD169 (Alexa488-conjugated secondary antibody, yellow) antibody for metallophilic macrophages of the splenic marginal zone (MZ), in PlGF KO and WTmice treated with DOCA-salt or placebo. Scale bar 200 μm. (B) The relative quantitative analysis is shown in panel B (n=5 for each group).

3.3 DOCA-salt-induced activation of co-stimulation process and deployment of T cells for consequent infiltration in target organs depends on PlGF

In order to investigate to which extent the activation of splenic PlGF mediated by DOCA-salt induced sympathetic splenic overdrive, could affect the immune response involved in damage of target organs of hypertension, we assessed the amount of T cell deploying from the spleen. We evaluated by immunofluorescence analysis the area of CD3+ T cells in the white pulp of the spleen, revealed by co-staining with B220 labeled B cells. DOCA-salt induced a significant egression of T cells in WT mice, whereas the spleens of PlGF KO mice remained unaffected, maintaining an equal amount of CD3+ T cells as compared to placebo treated mice (Figure 3A and B). On this notice, it has been previously shown that DOCA-salt activates the process of T cells co-stimulation mediated by CD86, which is one of the main critical step in the full activation of T cells and prodromal for the later deployment from lymphoid organs[8, 13, 18, 23]. Thus, we tested whether the neuroimmune modulation exerted by

DOCA-salt in the spleen and mediated by PlGF was relevant for the activation of costimulation. To this aim, we analyzed the amount of CD86 positive staining, a typical pattern of activation expressed by antigen presenting cells (APC) in the MZ and known to be regulated by DOCA[8]. Here we show that PlGF is indispensable to allow DOCA-salt induced co-stimulation on APC, being CD86 expression hampered in PlGF KO mice (Figure 3C and D) infiltration of activated immune cells in target organs, a crucial event contributing to BP increase and end-organ damage[9, 13].

Kidneys isolated from DOCA-salt treated mice were analyzed for determination of activated T cells content by flow cytometry. As shown by representative plots and quantitative analysis, WT mice subjected to DOCA-salt accumulated a significant amount of CD8 and CD4 T cells positive for markers of activation (CD69) and homing (CD44), as compared to placebo treated mice (Figure 4A-F). Conversely, kidneys isolated from PlGF KO mice were spared from infiltrating activated CD8 and CD4 T cells, showing no significant difference when compared with placebo treated mice (Figure 4A-F). We further added evidence to this result by looking at immune cells infiltrating kidneys with immunohistochemistry (see Supplemental material online, Figure S4A-D). Indeed, PlGF KO mice were protected from the significant increase of CD4+ T and CD8+ T cells observed in the renal tubules and glomeruli of WT mice challenged with DOCA-salt, as compared to mice receiving placebo alone (see Supplemental material online, Figure S4A-D).

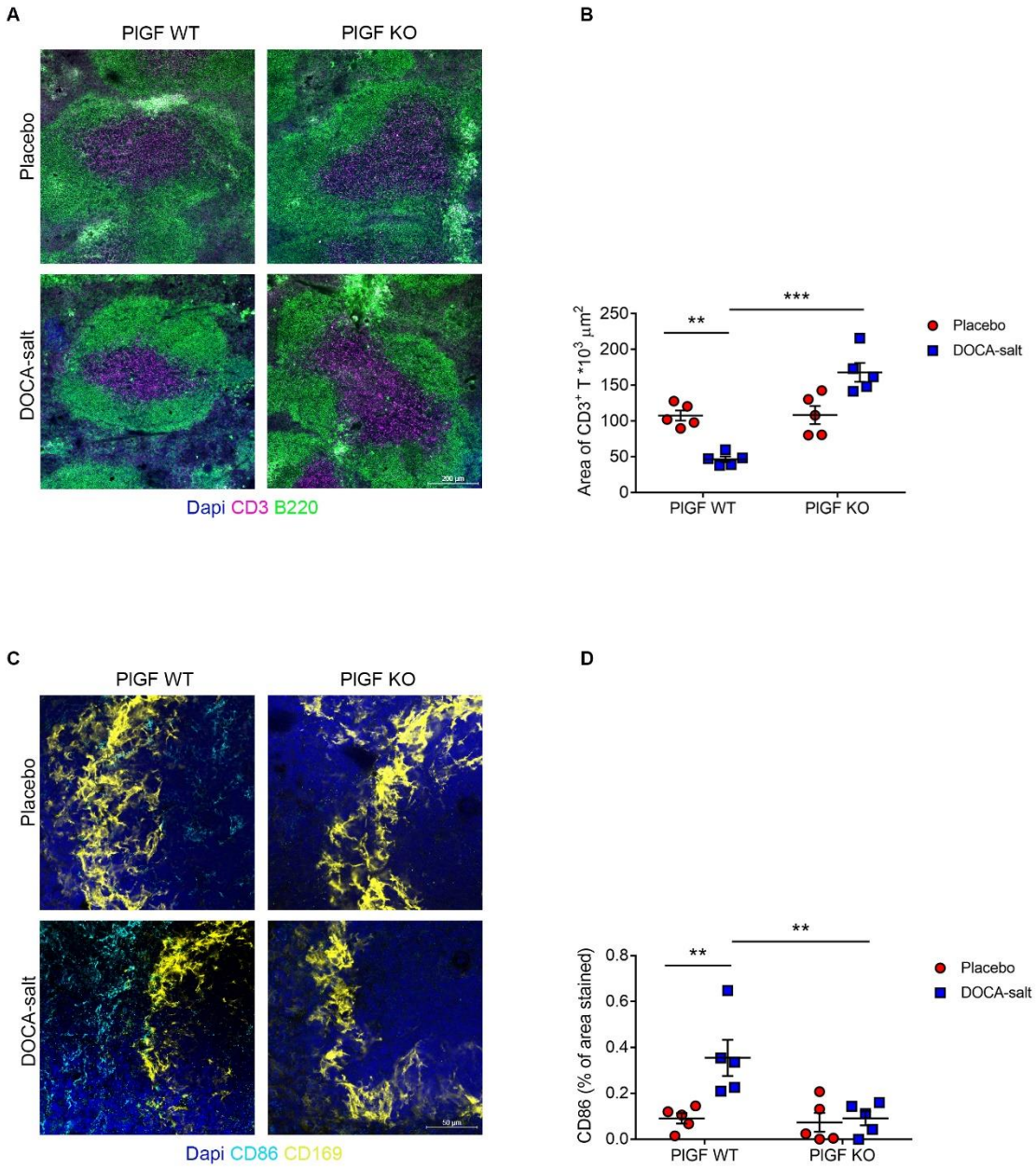

Figure 3. DOCA-salt induces T cells egression from the spleen by activating co-stimulation through PlGF. (A) Immunostaining of CD3+ T cells (Cy3-conjugated secondary antibody, magenta) in the white pulp area of the spleen and B220 (Alexa488-conjugated secondary antibody, green) for B cells labeling. (B) Quantitative analysis of the area of the spleen positive for CD3. Images represents n=5 mice for each group; scale bar 200 μm. **p<0.01 and ***p<0.001. (C) Staining of CD86 (Alexa488-conjugated secondary antibody, cyan) in the marginal zone of the spleen labeled with anti-CD169 antibody (Cy3-conjugated secondary antibody, yellow), showing cells positive for the co-stimulation molecule. Images represent n=5 mice for group; scale bar 50 μm. (D) Quantitative analysis of CD86 expressed as % of stained area. **p<0.01.

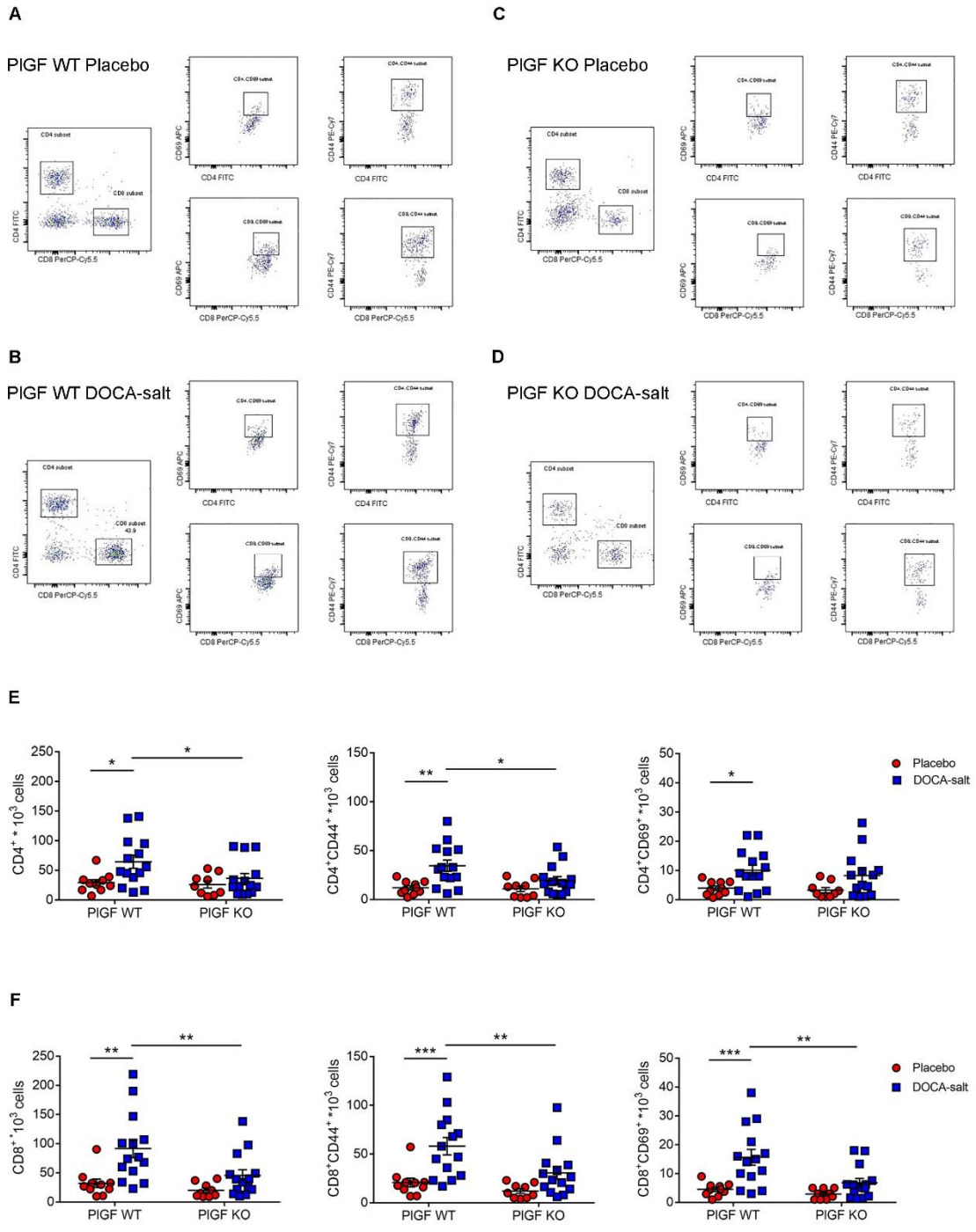

Figure 4. PlGF KO mice are protected from DOCA-salt induced infiltration of activated T cells in kidneys. (A-D) Plots of flow cytometry analysis showing CD4+ and CD8+ T cells infiltrating kidneys of PlGF KO and WT mice, treated with DOCA-salt or placebo. (E, F) Graphs showing the quantitative analysis of CD4 and CD8 T cells, positive for the homing marker CD44 and for the early activation marker CD69, in PlGF KO and WT mice, treated with DOCA-salt or placebo. ∗p<0.05, **p<0.01 and ∗∗∗p<0.001 (n=10 mice for PlGF WT placebo; n=9 mice for PlGF KO placebo; n=14 mice for PlGF WT and KO mice treated with DOCA-salt).

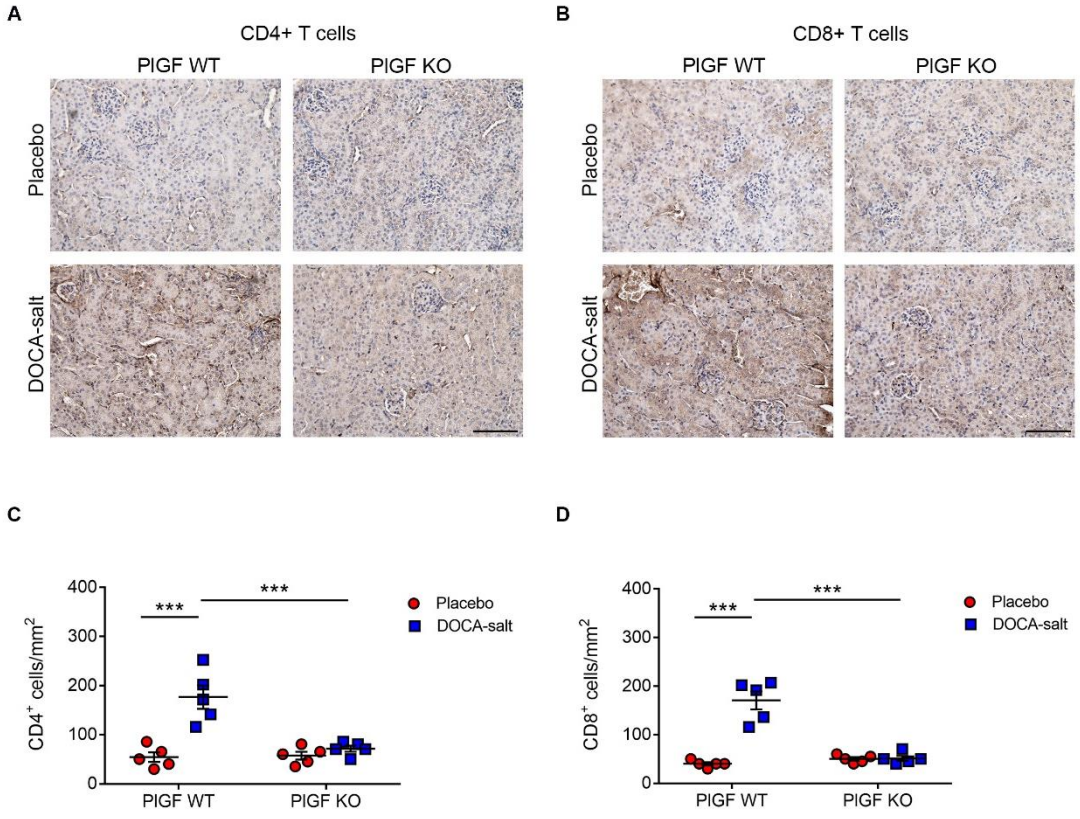

Figure S4. PlGF deficiency reduces the chronic inflammation of kidneys induced by DOCA-salt. (A, B) Immunostaining and quantitative analysis of CD4+ and CD8+ T cells in kidneys of PlGF KO and WT mice after 21 days of DOCA-salt or placebo administration. ***p<0.001 (n=5 mice for group).

3.4 PlGF KO mice are protected from DOCA-salt induced end-organ damage

To determine whether the protection from renal infiltration of activated immune cells, observed in PlGF KO upon DOCA-salt challenge resulted in protection from end-organ damage, we assessed renal fibrosis and glomerular injury. We found that upon DOCA-salt administration WT mice showed a significant amount of renal fibrosis, evidenced by staining kidneys with Picrosirius Red and Masson's Trichrome (Figure 5A-C). Instead PlGF KO mice were protected from renal fibrosis (Figure 5A-C), thus paralleling the observation that PlGF KO kidneys were spared from infiltrating activated T cells. The apposition of fibrotic tissue in WT mice treated with DOCA-salt was particularly evident in both glomeruli and tubules, thus suggesting that infiltrating T cells negatively affect tissue homeostasis, determining in the long term structural alterations that could deteriorate renal function, further contributing to the hypertensive phenotype. Accordingly, we also observed that chronic DOCA-salt challenge

provoked an enlargement of renal corpuscle size and an increase of glomerular dimensions with an irregular area, as represented by PAS staining, which was otherwise absent in PlGF KO mice (Figure 5D and E; see Supplemental material online, Figure S5A). The enlargement of Bowman's capsule size displayed by WT mice subjected to DOCA-salt was similarly reduced in PlGF KO mice (see Supplemental material online, Figure S5B), thus further supporting that the inhibition of immune system activation and recruitment to target organs obtained in the absence of PlGF was effective in preventing not only BP increase but also end-organ damage. Lastly, to provide functional data related to the above described renal injury, we assessed key parameters of renal function in PlGF KO and WT mice placed in metabolic cages at the end of DOCA-salt or placebo administration. A marked increase in urine output was observed after 21 days of DOCA-salt (Figure 6A), with a consequent reduction of urinary osmolality (Figure 6B). Despite the increase in urine output was significantly blunted in PlGF KO mice (Figure 6A), the urinary osmolality was comparable, as it was the plasma osmolality, moderately increased in both WT and PlGF KO mice (Figure 6C), thus suggesting that the stimulus induced by DOCA-salt determined an equal fluid balance in the two groups. When we measured renal function, the creatinine clearance was significantly reduced in WT mice but preserved in PlGF KO mice (Figure 6D). Similarly, PlGF KO mice were preserved from the DOCA-salt induced renal damage observed in WT mice, in terms of protein excretion, measured as total proteins to creatinine ratio. In fact, the marked increase observed in WT mice after 21 days of DOCA-salt was significantly hampered in PlGF KO mice (Figure 6E).

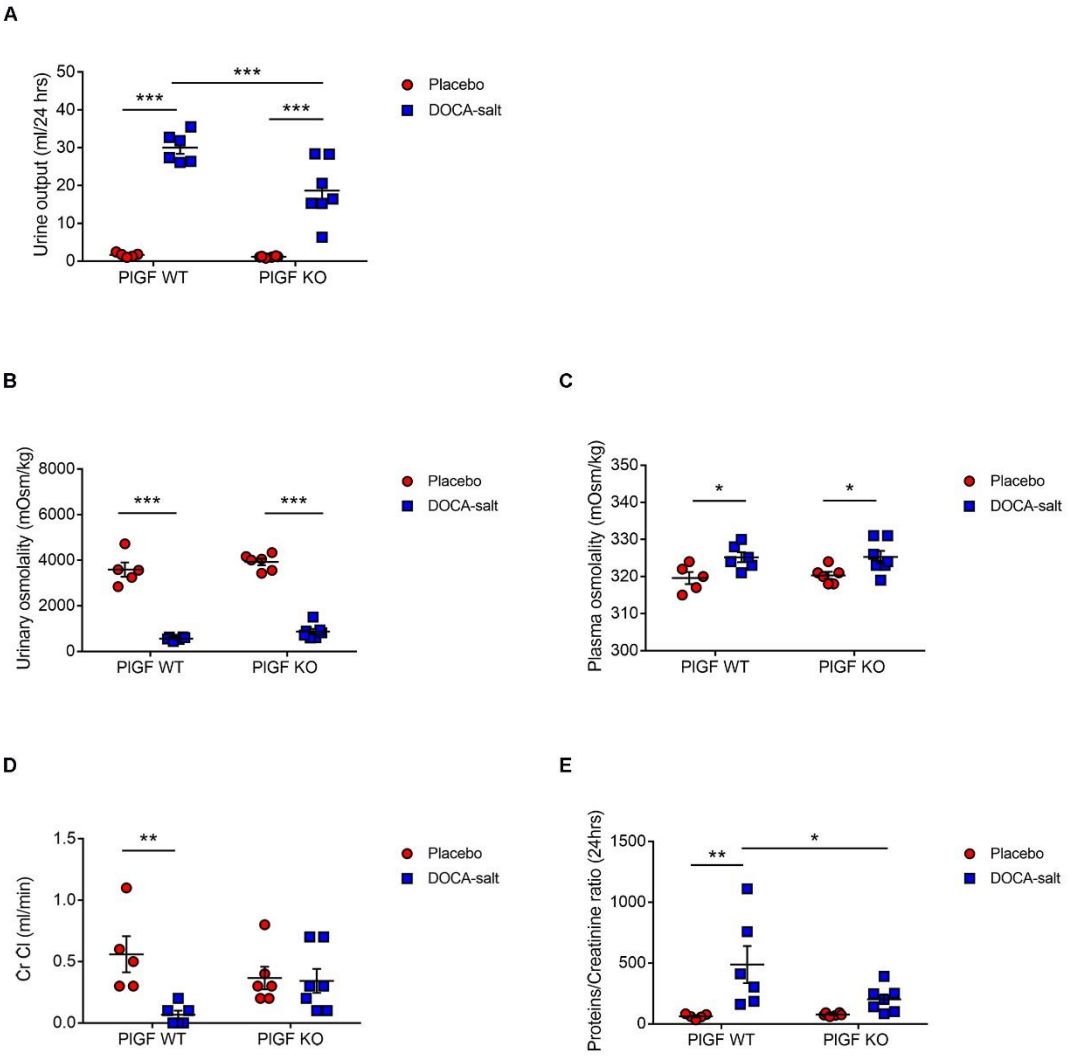

Figure 6. Renal end-organ damage induced by DOCA-salt is significantly hampered by PlGF deficiency. (A-C) Evaluation of fluid balance in PlGF KO and WT mice treated with DOCA-salt as shown by urine output (A), urine (B) and plasma (C) osmolality, measured in mice placed in metabolic cages. (D) Analysis of renal function expressed as creatinine clearance (Cr Cl) in the 24 hours in PlGF KO and WT mice after DOCA-salt or placebo treatment. (E) Protein excretion is expressed as the ratio between total urinary proteins and urinary creatinine in PlGF KO and WT mice, treated with DOCA-salt or placebo. *p<0.05, **p<0.01 and ***p<0.001 (n=5 mice for PlGF WT placebo, n=6 for PlGF WT DOCA-salt and PlGF KO placebo, n= 7 for PlGF KO DOCA-salt).

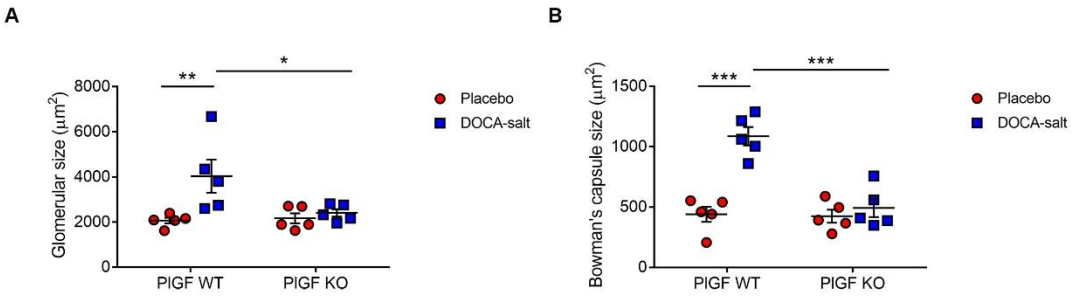

Figure S5. PlGF KO mice are protected from the renal structural damage caused by chronic DOCA-salt. (A, B) Quantitative analysis of PAS staining showing the estimated measure of the Bowman's capsule size (B), and glomerular dimensions (A), in PlGF KO and WT mice, treated with DOCA-salt or placebo. ∗<0.05, ∗∗p<0.01 and ∗∗∗p<0.001 (n=5 mice per group).

4. Discussion

The main findings of this study put in evidence that the activation of PlGF in the spleen is necessary to couple the brain-mediated effects of DOCA-salt challenge to the activation of immune cells directed toward kidneys, where they contribute to BP increase and organ damage. Summarizing our results (Figure 7), we here show that: 1) DOCA-salt challenge requires splenic immunity to drive hypertension and 2) exploits the splenic sympathetic innervation to activate T cells through PlGF release in the MZ; 3) PlGF KO mice are protected from hypertension and target organ damage.

Overall these data suggest that the brain-to-spleen neuroimmune circuit is a common pathway activated by different hypertensive hits, like AngII and DOCA-salt, to prime an immune response necessary to establish the hypertensive disease. Previous works highlighted how DOCA-salt challenge, mostly known to reproduce a condition of peripherally depressed RAS activity[4], frequently found also in hypertensive patients[24], strongly activates signaling pathways in circumventricular organs, similarly to what observed upon AngII[1, 6, 7, 14, 15, 24, 25]. It is notable that a denervation of splanchnic sympathetic innervation of the spleen, obtained through left CGX here proved to be effective in blocking BP increase in mice administered with DOCA-salt. Previous reports also showed that splanchnic innervation is crucial for AngII and DOCA-salt responses in rats[26, 27]. Additionally, a previous work by the group of Fink reported that the same model of DOCA-salt hypertension was not characterized by a generalized sympathoexcitation[28], adding evidence to the notion that AngII and DOCA-salt hypertensive hits act in a completely different way in the periphery. However, this is not

surprising as one of the main feature of the SNS is its highly heterogeneous regionality. Data presented in this work also evidence that the pathway mediating a neural modulation of immunity upon DOCA-salt hypertension, is not involved in the sensing of the stimulus, showing PlGF KO mice a similar pattern of fluid intake regulation. Whereas it becomes clear that the neuroimmune pathway mediated by splenic PlGF is downstream to sensing stations of DOCA-salt and primes immune cells lastly responsible for renal effects relevant for BP regulation and end-organ damage.

Overall, previous and present findings support the concept that a specific pattern of splanchnic SNS activity, required for the activation of immune system in the spleen, is commonly recruited by different hypertensive challenges, acting through distinct peripheral mechanisms of action.

Hypertension is indeed a complex disorder that may arouse because of a wide variety of hits to BP homeostasis[29, 30]. Some of the mechanisms involved in regulation of BP levels are very different and various experimental models of hypertension have been developed in the attempt to recapitulate this complexity. DOCA-salt and chronic AngII are among the most used approaches to model different conditions observed in the human pathology. Despite the huge work that has been done to understand the different pathophysiological mechanisms underlying hypertension in these two conditions, it emerges now that their capability to commonly recruit the brain-to-spleen circuit, a primer of adaptive immunity, previously shown to crucially participate to the hypertensive disease characterized in both models. These findings further add a piece of knowledge in the understanding of how neuroimmune reflexes participate to the modulation of cell trafficking and lymphoid architecture in different pathophysiological contexts[31]. Notably, ablation of this neurosplenic axis has no effect in basal conditions, whereas it effectively protects from hypertension and its related target organ damage. The fact that the neurosplenic axis is dispensable in physiological conditions but essential in hypertension sounds particularly important in terms of translational perspectives.

A last opportunity from the clinical point of view is suggested by the availability of antibodies targeting PlGF already under investigation in advanced therapies for cancer and macular degeneration[32-34]. The insights here proposed, reporting the activation of a common neuroimmune mechanism underlying the hypertensive disease from different causes, strongly encourage the possibility to exploit a therapeutic strategy blocking this pathway, as a novel clinical opportunity for patients resistant to all ongoing available medications. On a different notice, our results also warrant another reflection relevant for the clinical implications emerging from the proof of concept that targeting PlGF mediated pathway would protect from hypertension. There is a consistent and increasing amount of reports in the literature that

associates the use of anti-angiogenic therapies, mainly based on inhibitors of the VEGF (growth factor belonging to the same family of PlGF), with increased cardiovascular risk and, especially, induction of hypertension[35]. In principle, one would have expected that PlGF inhibition could have similar effects. Instead our previous and present data demonstrate that it is not the case, being PlGF inhibition associated with a protection from BP increase and target organ damage in experimental models of hypertension. On this basis, data acquired so far would suggest that the inhibition of PlGF in cancer would have a dual positive role: on the one hand, it would protect from tumor growth[32-34, 36, 37] and at same time hamper hypertension. Future studies will be necessary to investigate this important translational perspective.

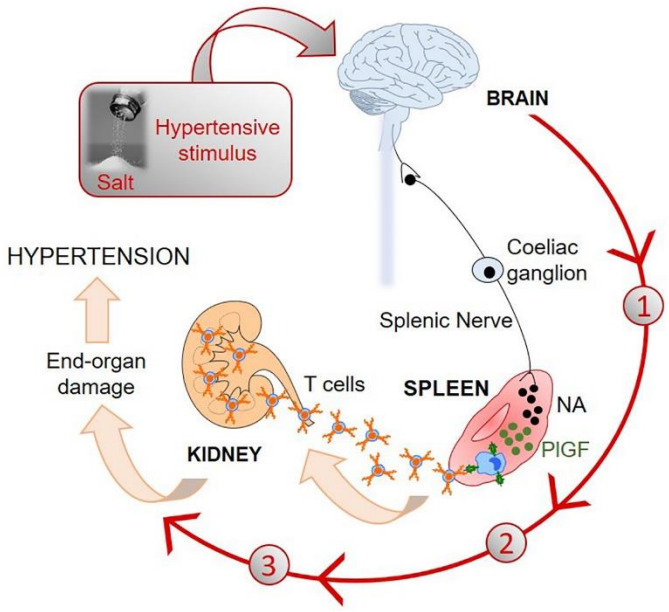

Figure 7. PlGF mediates the neural modulation exerted by the splenic sympathetic drive activated by DOCA-salt to induce hypertension. Pathophysiological circuit of neural modulation of immune system in DOCA-salt hypertension. The schematic representation recapitulates the three main steps involved in sensing and transduction of DOCA-salt neuro-immune effects. 1) DOCA-salt acts on the brain to activate the splenic sympathetic drive passing through the coeliac ganglion and reaching the spleen where 2) noradrenaline release mediates PlGF production in the MZ. In turn, PlGF production is necessary to allow T cells co-stimulation by increasing the expression of CD86 co-stimulation molecule, a permissive step for deployment of T cells from lymphoid organs. 3) Activated T cells reach kidneys where they contribute to BP increase and end-organ damage.

References

1. Basting T, Lazartigues E. DOCA-Salt Hypertension: an Update. Curr Hypertens Rep 2017;19:32.

2. Gutkind JS, Kurihara M, Saavedra JM. Increased angiotensin II receptors in brain nuclei of DOCA-salt hypertensive rats. Am J Physiol 1988;255:H646-650.

3. Berecek KH, Barron KW, Webb RL, Brody MJ. Vasopressin-central nervous system interactions in the development of DOCA hypertension. Hypertension 1982;4:131-137.

4. Gavras H, Brunner HR, Laragh JH, Vaughan ED, Jr., Koss M, Cote LJ, Gavras I. Malignant hypertension resulting from deoxycorticosterone acetate and salt excess: role of renin and sodium in vascular changes. Circ Res 1975;36:300-309.

5. Itaya Y, Suzuki H, Matsukawa S, Kondo K, Saruta T. Central renin-angiotensin system and the pathogenesis of DOCA-salt hypertension in rats. Am J Physiol 1986;251:H261-268.

6. Grobe JL, Grobe CL, Beltz TG, Westphal SG, Morgan DA, Xu D, de Lange WJ, Li H, Sakai K, Thedens DR, Cassis LA, Rahmouni K, Mark AL, Johnson AK, Sigmund CD. The brain Renin-angiotensin system controls divergent efferent mechanisms to regulate fluid and energy balance. Cell Metab 2010;12:431-442.

7. Hilzendeger AM, Cassell MD, Davis DR, Stauss HM, Mark AL, Grobe JL, Sigmund CD. Angiotensin type 1a receptors in the subfornical organ are required for deoxycorticosterone acetate-salt hypertension. Hypertension 2013;61:716-722.

8. Vinh A, Chen W, Blinder Y, Weiss D, Taylor WR, Goronzy JJ, Weyand CM, Harrison DG, Guzik TJ. Inhibition and genetic ablation of the B7/CD28 T-cell costimulation axis prevents experimental hypertension. Circulation 2010;122:2529-2537.

9. Guzik TJ, Hoch NE, Brown KA, McCann LA, Rahman A, Dikalov S, Goronzy J, Weyand C, Harrison DG. Role of the T cell in the genesis of angiotensin II induced hypertension and vascular dysfunction. J Exp Med 2007;204:2449-2460.

10. Elmarakby AA, Quigley JE, Imig JD, Pollock JS, Pollock DM. TNF-alpha inhibition reduces renal injury in DOCA-salt hypertensive rats. Am J Physiol Regul Integr Comp Physiol 2008;294:R76-83.

11. Mattson DL. Infiltrating immune cells in the kidney in salt-sensitive hypertension and renal injury. Am J Physiol Renal Physiol 2014;307:F499-508.

12. Liu Y, Rafferty TM, Rhee SW, Webber JS, Song L, Ko B, Hoover RS, He B, Mu S. CD8+ T cells stimulate Na-Cl co-transporter NCC in distal convoluted tubules leading to salt-sensitive hypertension. Nat Commun 2017;8:14037.

13. Carnevale D, Pallante F, Fardella V, Fardella S, Iacobucci R, Federici M, Cifelli G, De Lucia M, Lembo G. The angiogenic factor PlGF mediates a neuroimmune interaction in the spleen to allow the onset of hypertension. Immunity 2014;41:737-752.

14. Feng Y, Yue X, Xia H, Bindom SM, Hickman PJ, Filipeanu CM, Wu G, Lazartigues E. Angiotensin converting enzyme 2 overexpression in the subfornical organ prevents the angiotensin II-mediated pressor and drinking responses and is associated with angiotensin II type 1 receptor downregulation. Circ Res 2008;102:729-736.

15. Grobe JL, Buehrer BA, Hilzendeger AM, Liu X, Davis DR, Xu D, Sigmund CD. Angiotensinergic signaling in the brain mediates metabolic effects of deoxycorticosterone (DOCA)-salt in C57 mice. Hypertension 2011;57:600-607.

16. Osborn JW, Jacob F, Hendel M, Collister JP, Clark L, Guzman PA. Effect of subfornical organ lesion on the development of mineralocorticoid-salt hypertension. Brain Res 2006;1109:74-82.

17. Guyenet PG. The sympathetic control of blood pressure. Nat Rev Neurosci 2006;7:335-346.

18. Carnevale D, Perrotta M, Pallante F, Fardella V, Iacobucci R, Fardella S, Carnevale L, Carnevale R, De Lucia M, Cifelli G, Lembo G. A cholinergic-sympathetic pathway primes immunity in hypertension and mediates brain-to-spleen communication. Nat Commun 2016;7:13035.

19. Gigante B, Morlino G, Gentile MT, Persico MG, De Falco S. Plgf-/-eNos-/- mice show defective angiogenesis associated with increased oxidative stress in response to tissue ischemia. FASEB J 2006;20:970-972.

20. Zacchigna L, Vecchione C, Notte A, Cordenonsi M, Dupont S, Maretto S, Cifelli G, Ferrari A, Maffei A, Fabbro C, Braghetta P, Marino G, Selvetella G, Aretini A, Colonnese C, Bettarini U, Russo G, Soligo S, Adorno M, Bonaldo P, Volpin D, Piccolo S, Lembo G, Bressan GM. Emilin1 links TGF-beta maturation to blood pressure homeostasis. Cell 2006;124:929-942.

21. Itani HA, Harrison DG. Memories that last in hypertension. Am J Physiol Renal Physiol 2015;308:F1197-1199.

22. Rosas-Ballina M, Tracey KJ. The neurology of the immune system: neural reflexes regulate immunity. Neuron 2009;64:28-32.

23. Xiao L, Kirabo A, Wu J, Saleh MA, Zhu L, Wang F, Takahashi T, Loperena R, Foss JD, Mernaugh RL, Chen W, Roberts J, 2nd, Osborn JW, Itani HA, Harrison DG. Renal Denervation Prevents Immune Cell Activation and Renal Inflammation in Angiotensin II-Induced Hypertension. Circ Res 2015;117:547-557.

24. Sinnayah P, Lazartigues E, Sakai K, Sharma RV, Sigmund CD, Davisson RL. Genetic ablation of angiotensinogen in the subfornical organ of the brain prevents the central angiotensinergic pressor response. Circ Res 2006;99:1125-1131.

25. Jo F, Jo H, Hilzendeger AM, Thompson AP, Cassell MD, Rutkowski DT, Davisson RL, Grobe JL, Sigmund CD. Brain endoplasmic reticulum stress mechanistically distinguishes the saline-intake and hypertensive response to deoxycorticosterone acetate-salt. Hypertension 2015;65:1341-1348.

26. Kandlikar SS, Fink GD. Splanchnic sympathetic nerves in the development of mild DOCA-salt hypertension. Am J Physiol Heart Circ Physiol 2011;301:H1965-1973.

27. King AJ, Osborn JW, Fink GD. Splanchnic circulation is a critical neural target in angiotensin II salt hypertension in rats. Hypertension 2007;50:547-556.

28. Kandlikar SS, Fink GD. Mild DOCA-salt hypertension: sympathetic system and role of renal nerves. Am J Physiol Heart Circ Physiol 2011;300:H1781-1787.

29. Coffman TM. Under pressure: the search for the essential mechanisms of hypertension. Nat Med 2011;17:1402-1409.

30. Oh YS, Appel LJ, Galis ZS, Hafler DA, He J, Hernandez AL, Joe B, Karumanchi SA, Maric-Bilkan C, Mattson D, Mehta NN, Randolph G, Ryan M, Sandberg K, Titze J, Tolunay E, Toney GM, Harrison DG. National Heart, Lung, and Blood Institute Working Group Report on Salt in Human Health and Sickness: Building on the Current Scientific Evidence. Hypertension 2016;68:281-288.

31. Pavlov VA, Tracey KJ. Neural regulation of immunity: molecular mechanisms and clinical translation. Nat Neurosci 2017;20:156-166.

32. Van de Veire S, Stalmans I, Heindryckx F, Oura H, Tijeras-Raballand A, Schmidt T, Loges S, Albrecht I, Jonckx B, Vinckier S, Van Steenkiste C, Tugues S, Rolny C, De Mol M, Dettori D, Hainaud P, Coenegrachts L, Contreres JO, Van Bergen T, Cuervo H, Xiao WH, Le Henaff

C, Buysschaert I, Kharabi Masouleh B, Geerts A, Schomber T, Bonnin P, Lambert V, Haustraete J, Zacchigna S, Rakic JM, Jimenez W, Noel A, Giacca M, Colle I, Foidart JM, Tobelem G, Morales-Ruiz M, Vilar J, Maxwell P, Vinores SA, Carmeliet G, Dewerchin M, Claesson-Welsh L, Dupuy E, Van Vlierberghe H, Christofori G, Mazzone M, Detmar M, Collen D, Carmeliet P. Further pharmacological and genetic evidence for the efficacy of PlGF inhibition in cancer and eye disease. Cell 2010;141:178-190.

33. Bais C, Wu X, Yao J, Yang S, Crawford Y, McCutcheon K, Tan C, Kolumam G, Vernes JM, Eastham- Anderson J, Haughney P, Kowanetz M, Hagenbeek T, Kasman I, Reslan HB, Ross J, Van Bruggen N, Carano RA, Meng YJ, Hongo JA, Stephan JP, Shibuya M, Ferrara N. PlGF blockade does not inhibit angiogenesis during primary tumor growth. Cell 2010;141:166-177.

34. Snuderl M, Batista A, Kirkpatrick ND, Ruiz de Almodovar C, Riedemann L, Walsh EC, Anolik R, Huang Y, Martin JD, Kamoun W, Knevels E, Schmidt T, Farrar CT, Vakoc BJ, Mohan N, Chung E, Roberge S, Peterson T, Bais C, Zhelyazkova BH, Yip S, Hasselblatt M, Rossig C, Niemeyer E, Ferrara N, Klagsbrun M, Duda DG, Fukumura D, Xu L, Carmeliet P, Jain RK. Targeting placental growth factor/neuropilin 1 pathway inhibits growth and spread of medulloblastoma. Cell 2013;152:1065-1076.

35. Small HY, Montezano AC, Rios FJ, Savoia C, Touyz RM. Hypertension due to antiangiogenic cancer therapy with vascular endothelial growth factor inhibitors: understanding and managing a new syndrome. Can J Cardiol 2014;30:534-543.

36. Incio J, Tam J, Rahbari NN, Suboj P, McManus DT, Chin SM, Vardam TD, Batista A, Babykutty S, Jung K, Khachatryan A, Hato T, Ligibel JA, Krop IE, Puchner SB, Schlett CL, Hoffmman U, Ancukiewicz M, Shibuya M, Carmeliet P, Soares R, Duda DG, Jain RK, Fukumura D. PlGF/VEGFR-1 Signaling Promotes Macrophage Polarization and Accelerated Tumor Progression in Obesity. Clin Cancer Res 2016;22:2993-3004.

37. Rolny C, Mazzone M, Tugues S, Laoui D, Johansson I, Coulon C, Squadrito ML, Segura I, Li X, Knevels E, Costa S, Vinckier S, Dresselaer T, Akerud P, De Mol M, Salomaki H, Phillipson M, Wyns S, Larsson E, Buysschaert I, Botling J, Himmelreich U, Van Ginderachter JA, De Palma M, Dewerchin M, Claesson- Welsh L, Carmeliet P. HRG inhibits tumor growth and metastasis by inducing macrophage polarization and vessel normalization through downregulation of PlGF. Cancer Cell 2011;19:31-44.

Conclusions

Hypertension shares an intriguing feature with the innovative researches in immunology on one hand and the classical mechanisms of blood pressure regulation through nervous circuits mediated by the sympathetic nervous system on the other hand.

In this dissertation, it is highlighted the interaction between the immune system in physiological dysfunctions contributing to end-organ damage, the typical hallmark of the disease, and the sympathetic nervous system in the modulation of immune cells in the spleen in two different murine model of hypertension.

As previously discussed, the increase of arterial blood pressure in experimental model induced by different stimuli, as AngII or DOCA-salt, affects the RAS in the brain. In the first work, we show that the cholinergic-sympathetic drive in hypertension is realized through a vagus-splenic nerve connection from the brain to the spleen and it is able to activate the T cells in the spleen, then recruited in target organs of hypertension as kidney and vasculature, where they contribute to the development of hypertension. Both the hypertensive stimuli, AngII and DOCA-salt, increase the discharge of the splenic nerve that is dependent on an intact vagus nerve efferent. The coeliac branch of the vagus nerve terminates in the coeliac ganglion where the catecholaminergic fibers of the splenic nerve originate. This interaction is mediated by the α7nAChR expressed in the coeliac ganglion. Indeed, α7nAChR KO mice are protected from blood pressure increase upon chronic AngII and from egression of immune cells towards aorta and kidney. At the end, we propose an important translational implication with a completely innovative approach on the splenic nerve by the thermoablation, a selective procedure of denervation, which is protective against the raising of blood pressure levels induced by chronic AngII.

The novelty of this work is the concept that the autonomic nervous system is capable to determine long-term effects on the cardiovascular system in pathological states through the regulation of the immune system. The spleen is a secondary lymphoid organ directly and densely innervated by the sympathetic nervous system and as suggested by some milestone papers in hypertension, the AngII is responsible of a variety of actions that contribute to the development of hypertension, as well as the DOCA-salt treatment.

In the past researches conducted in my lab, it was found that the PlGF was a mediator of the effect on arterial blood pressure caused by chronic AngII. PlGF drives the interaction between the sympathetic nervous system and the immune system in the spleen in response to AngII, playing a central role in the regulation of blood pressure raising.

In the second part of this work, we hypothesize that the PlGF, coupling the nervous and the immune system in the spleen, could mediate T cells activation induced by DOCA-salt in mice and their infiltration into target organs of hypertension. In this study, we demonstrate that its expression in the spleen, where it drives immune responses, depends on the integrity of splenic sympathetic innervation acting as an interface between the sympathetic and immune system. The main result of this work is that chronic DOCA-salt enhances splenic sympathetic nerve fibers establishing a communication with immune cells in the spleen by PlGF. Upon this hypertensive stimulus, KO mice display a reduction of blood pressure levels and furthermore coeliac ganglionectomy mice exhibit decreased levels of PlGF in the marginal zone of the spleen. The coeliac ganglion appears as a central site whence the sympathetic innervation branched until the spleen and surprisingly, the removal of this central ganglion is useful to reduce significantly the PlGF levels in the spleen of this hypertensive murine model. We demonstrate that this hypertensive challenge shares with AngII a common central mechanism of action activating the brain RAS.

Hence, the lack of splenic PlGF determinate a protection from costimulation and egression of T cells from the splenic reservoir, considering PlGF as an important mediator in hypertension induced by DOCA-salt.

Given its roles in angiogenesis, PlGF has been studied as a molecular target for cancer treatment and interestingly, one of the main effect of anti-PlGF therapies concerns cardiovascular diseases. In perspective, the discovery of its molecular pathway in hypertension could have more implications: certainly, could lead to further knowledge on molecular mechanisms causing the onset of the disease in order to assess a holistic therapy for counteracting hypertension upon several challenges.

Acknowledgment

I would like to express my acknowledge to my tutor Prof. Daniela Carnevale (IRCSS Neuromed and Department of Angio-Cardio-Neurology, "Sapienza" University of Rome) who consistently steered me in the right direction whenever she thought I needed it. I would like to express my very profound gratitude to Prof. Giuseppe Lembo (IRCSS Neuromed and Department of Angio-Cardio-Neurology, "Sapienza" University of Rome) who conveyed me the fascination for this work and to guide me in the realization of my PhD programme.

I would like to thank them to give me the opportunity to carry out my PhD course in their research laboratory at IRCSS Neuromed and to suggest me valuable knowledge and useful basic advices, essential to my research formation.

I would like to thank Dr. Fabio Pallante (IRCSS Neuromed) and Dr. Lorenzo Carnevale (IRCSS Neuromed), who worked with me on the realization of an innovative electrophysiological technique for the recording of the splenic sympathetic nerve activity in mice. Without their passionate participation and inputs, this study could not have been successfully conducted.

I would like to thank all my colleagues who constantly worked with me providing me unfailing support throughout my years of PhD study.